Abstract

Title of dissertation: Mitochondrial outer membrane permeability to metabolites influences the onset of apoptosis

Wenzhi Tan, Doctor of Philosophy, 2007

Dissertation directed by: Professor Marco Colombini,

Department of Biology

Apoptosis is a process in multicellular organisms to signal and induce death of specific cells, while avoiding inflammatory reactions. It is an important way to recycle the materials of unwanted cells and maintain cell balance. The execution phase of apoptosis can be initiated by proteins released from mitochondria (such as cytochrome c). Results reported here are consistent with this release being influenced by changes in the mitochondrial outer membrane permeability to metabolites.

Phosphorothioate oligonucleotides induce cell death and block VDAC, a protein in the mitochondrial outer membrane that facilitates metabolite flow. These properties seem to be linked in that both require the phosphorothioate modification, both are enhanced by an increase in oligonucleotide length, and both are insensitive to nucleotide sequence.

VDAC reconstituted into planar phospholipid membranes is blocked by phosphorothioate oligonucleotides with a 1:1 stoichiometry. They block the pore of the channel through interacting with the inner wall of the pore. The rate of binding occurs at a 100 μs scale but the binding is usually unstable. However, some conformational change stabilizes the complex resulting in long-term complete blockage of VDAC.

In mitochondria, this blockage interferes with metabolite flow and inhibits the respiration of mitochondria. It is very specific for VDAC at sub-micromolar concentrations of phosphorothioate oligonucleotide and under these conditions there is minimal effect on enzymatic processes in the mitochondrial inner membrane.

The ability of PorB from *Neisseria meningitidis* to inhibit apoptosis by moving to the mitochondrial outer membrane, was investigated in light of VDAC's role in apoptosis. PorB is unable to alter VDAC's gating properties but does allow ATP to cross membranes. Thus it may restore metabolite flux when VDAC channels close early in apoptosis. Attempts to test this in yeast were not successful.

VDAC gating influences transmembrane Ca^{2+} flux. The closed states favor calcium permeation and the open state limits calcium flux. In mitochondria this gating could influence the rate of Ca^{2+}-dependent mitochondrial swelling and subsequent cytochrome c release.

Thus, the mitochondrial outer membrane permeability regulated by VDAC gating may play an important role in mitochondrial function and control of apoptosis.

MITOCHONDRIAL OUTER MEMBRANE PERMEABILITY TO METABOLITES
INFLUENCES THE ONSET OF APOPTOSIS

by

Wenzhi Tan

Dissertation submitted to the Faculty of the Graduate School of the
University of Maryland, College Park in partial fulfillment
of the requirements for the degree of
Doctor of Philosophy
2007

Advisory Committee:

  Professor Marco Colombini, Chair
  Professor Elizabeth Quinlan
  Professor Sergei Sukharev
  Professor Jeffery Davis
  Professor Eric Baehrecke

Preface

This dissertation describes my research on various aspects relating to the role of VDAC of the initiation of apoptosis. My work began about five years ago, when I joined Marco Colombini's lab at the University of Maryland – College Park. I first studied the possible interactions between VDAC and PorB from *Neisseria meningitidis*, and its mechanism of inhibiting cell apoptosis. Even though the project did not work well, I got experienced in many experimental techniques, such as electrophysiology, liposome studies, mitochondrial isolation and handling, etc. In addition, Dr. Colombini's wonderful and rigorous lectures instilled in me the fundamental concepts of biophysics. With those tools, our collaboration with Dr. C.A. Stein from Albert Einstein College of Medicine, on the role of phosphorothioate oligonucleotides, such as G3139, turned out to be fruitful. I also published several papers on the discovery that G3139 interacts with VDAC, which accounts for part of the mechanism by which it induces apoptosis. These studies make up the majority of my dissertation.

My dissertation contains eight chapters. The first chapter is a general background on apoptosis and the roles of VDAC, PorB, G3139, and calcium ions in this process. The second chapter contains the general methods used throughout my research.

Chapter 3 to 5 describe my research on G3139. In chapter 3, I present the correlation between G3139 induced VDAC closure and its ability to induce cell apoptosis. This work has been published in *PNAS*. This paper is a full collaboration between our lab and Dr. Stein's lab. My part of the research includes all the electrophysiological studies and the interaction with VDAC. It is presented in Fig. 3.5, 3.6, 3.8 and 3.9. Using different phosphorothioate oligonucleotides, we established the

importance of phosphorothioate modification in its ability to induce VDAC closure and cell apoptosis. The length of the oligonucleotides also plays a role in their efficacy. This research is important to understanding the mechanism by which G3139 induces apoptosis and guides its use in treating melanoma and other cancers.

Chapter 4 presents investigations on the influence of G3139 on VDAC function in intact mitochondria. This research has been published in *American Journal of Physiology – Cell Physiology*. The results shown in Fig. 4.8 were obtained by our collaborator. G3139 reduces the permeability of the outer membrane of mitochondria by closing VDAC. It has other effects but these are not significant at sub-micromolar G3139 concentrations. Thus G3139 is a very specific inhibitor and a useful tool to influence VDAC conductance and mitochondrial outer membrane permeability. This study also supports the hypothesis that restriction of the flow of metabolites through the mitochondrial outer membrane leads to the initiation of apoptosis.

Chapter 5 describes studies on the molecular mechanism of the interaction between G3139 and VDAC. This work is published in the *Biophysical Journal*. The electrophysiolgical studies indicate that G3139 blocks VDAC channels completely by binding to the inner wall of the channel in a one to one ratio. I also found that the length of the oligonucleotide required for full blockage of the channel agrees with previous studies on the length required to induce apoptosis. Together, chapters 3 to 5 provide a detailed analysis of the interaction between G3139 and VDAC and its implication on apoptotic control.

Chapters 6 and 7 present further studies with implications on the role of VDAC gating and the initiation of apoptosis. In chapter 6, I carefully measured the flux of

calcium ions through VDAC channels and found profound selectivity changes resulting from the gating of VDAC. Contrary to some statements in the literature, the closed states of VDAC, which allow very low metabolite flow, have a higher permeability to calcium ions. The increased permeability could increase the rate of mitochondrial calcium uptake and may have implications in mitochondrial swelling and cell apoptosis. The mathematical approach used to separate current carried by cations from that carried by anions is more rigorous than that commonly used and this may prove useful in future studies of channel selectivity. This work is currently under review in *Biochimica et Biophysica Acta – Biomembranes*.

Chapter 7 presents the results of experiments designed to explore the mechanism by which PorB channels, in the mitochondrial outer membrane, inhibit apoptosis. The results point to the ability of PorB to replace lost VDAC function but a test of this hypothesis was inconclusive.

A short discussion on future studies is presented in Chapter 8.

Dedication

I would like to dedicate this dissertation to my parents Chunlong Tan and Cuihong Wang, for their whole-hearted support. They stirred my interest in science since my early childhood, which made it possible for me enter that field of study. This dissertation is also dedicated to my beloved wife, Yuanyuan Tao, for her understanding and encouragement in my study and life.

Acknowledgements

It is my great honor to take this opportunity to thank my advisor, Dr. Marco Colombini, an extraordinary scientist, a dedicated researcher, a knowledgeable mentor and an excellent friend, whose expertise in experiments trains my hands, whose passion for research touches my heart, whose broad yet deep concepts in science lights my mind, whose easygoing character frees my nerve. I will be forever indebted to him for leading me into the world of biophysics and teaching me to think critically, to work efficiently and to communicate effectively. Without his generous encouragement and ever-lasting patience, it would have been impossible for me to have a fruitful research and finish this Ph.D dissertation. He has been the model, that I will take my whole life, to imitate, to keep up with, and hopefully to surpass. *Grazie, Marco!*

I also want to thank Drs. Sergei Sukharev, Elizabeth Quinlan, Jeffery Davis and Eric Baehrecke for serving as my committee members. I greatly appreciate my discussions and conversations with them, who generously provided me with ideas for my research and insights into science.

I am deeply grateful to my colleagues in the lab and the biology community I experienced in my five years of study here at Maryland. Dr. Johnny Stiban, Dr. Leah Siskind, Dr. Alex Komarov, Ms. Susan Hudak, Ms. Sarah O'Connell and Ms. Meenu Perera all are my true friends and wonderful co-workers. I am especially grateful to Johnny Stiban, who is my best friend, and Leah Siskind, whose experience greatly facilitated my research. I also want to thank Youjun Wang, who helped me a lot in my school life even before I came to Maryland. I wish them good luck in their scientific careers!

Table of contents

List of Tables

List of Figures

List of Abbreviations

ANT: adenine nucleotide translocator

GHK: Goldman-Hodgkin-Katz.

I_0: zero potential current

MOM: mitochondrial outer membrane

MIM: mitochondrial inner membrane

NAO: nonyl acridine orange

PMF: proton motive force

PTP: permeability transition pore

P/O ratio: ATP produced per mole of oxygen consumed.

V_{rev}: zero-current or reversal potential

VDAC: voltage dependent anion-selective channel

Chapter 1
General Introduction

Apoptosis (programmed cell death)

Apoptosis is a form of programmed cell death triggered by physiological or noxious signals. It was initially described on a morphological basis (Kerr *et al.*, 1972) because apoptosis differs from necrosis in that there is no inflammatory reaction. In recent years, intensive work has been done on apoptosis to elucidate this phenomenon. Now we know that apoptosis is characterized by the loss of cell attachment (Wyllie *et al.*, 1980; Ruoslahti and Reed, 1994), condensation of chromatin, fragmentation of the nucleus, ruffled and blebbed plasma membrane, cell shrinkage, and externalization of phosphotidylserine (Jacobson *et al.*, 1993; Jacobson *et al.*, 1994). These events are orchestrated and require metabolic energy. Cells are eventually divided into fragments, termed apoptotic bodies (Kerr *et al.*, 1972), and recognized and engulfed by phagocytes (Hart *et al.*, 1996) so as to avoid any inflammation.

Apoptosis can be induced in many ways, such as signal pathways, stress, calcium elevation and DNA damage. It is regulated by proteins such as Bcl-2 family proteins, NAIP (neuronal apoptosis inhibitor protein), TNF (tumor necrosis factor), etc. Many of these regulatory proteins seem to interact with mitochondria and induce or prevent the release of mitochondrial intermembrane space proteins such as cytochrome c and apoptosis-inducing factor. The initiation of apoptosis leads to the activation of a variety of enzymes through a complex cascade. These enzymes are part of the execution phase of cell death and include the caspase family of proteins, endonucleases, transglutaminase etc. Thus there is a clear pathway of apoptosis: the cytochrome c release into the cytosol and binding to APAF-1 (apoptotic protease-activating factor 1) activate caspase-9, which

has been shown to directly cleave and activate caspase-3 (Liu *et al.*, 1996; Yang *et al.*, 1997). Other caspases are also involved in this pathway. Caspases are cysteine proteases that cut other proteins at aspartic acid residues. They cleave specific cytosolic proteins and generate the morphological changes that characterize apoptosis. The release of mitochondrial intermembrane space proteins such as cytochrome c seems to be an irreversible step in apoptosis. What controls the release of these proteins is still unclear.
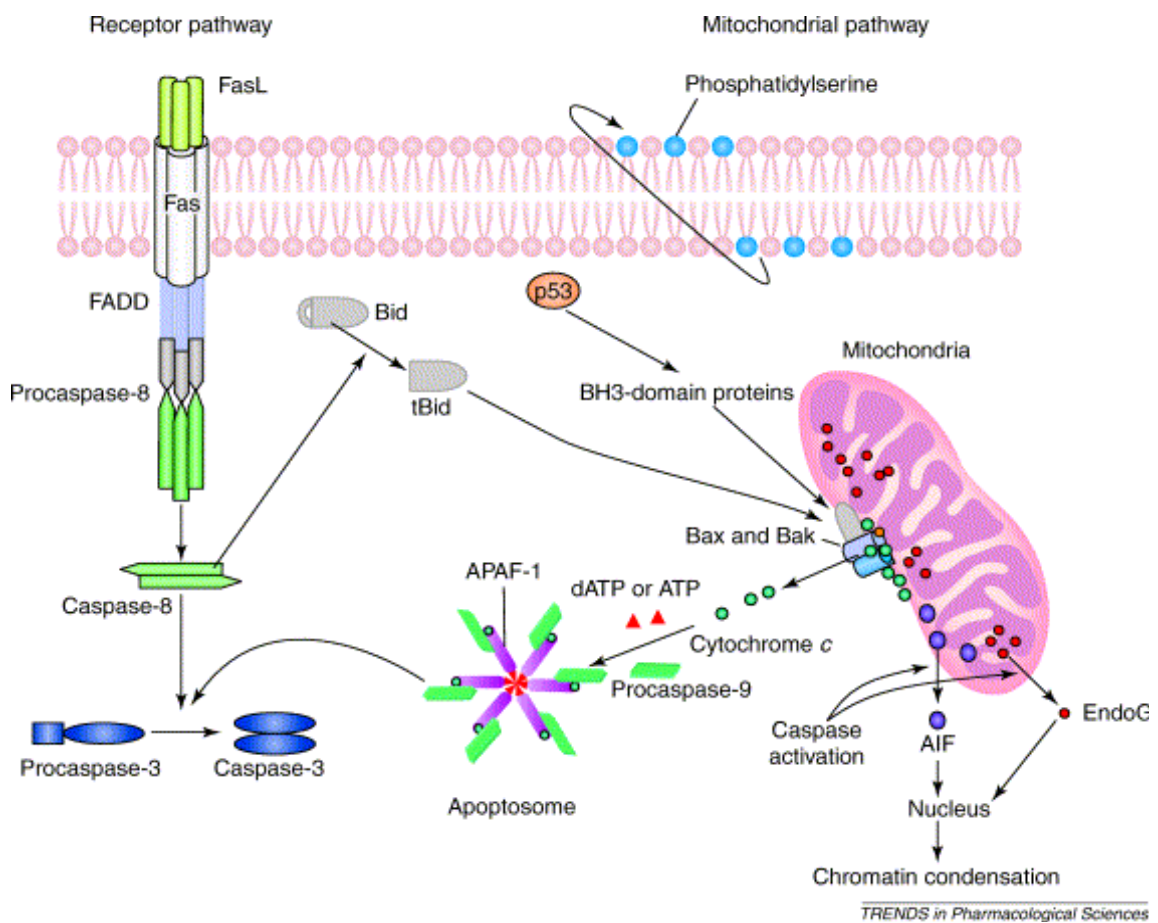
Figure 1.1. General apoptosis pathways (Reproduced from Hong *et al.*, 2004). Apoptotic signals can lead to the activation of BH-3 domain proteins. They translocate to the mitochondrial outer membrane, activate other proapoptotic molecules, and induce protein release, such as cytochrome c, from mitochondria. This release is an irreversible step in apoptosis. It leads to the apoptotic cascade and finally cell death.

Initiation of apoptosis (cytochrome c release)

Understanding the mechanism of apoptosis, especially the initiation of apoptosis is very important in understanding some disease processes, including those occurring in cancer, stroke, heart disease, neurodegenerative diseases, autoimmune disorders, and viral diseases. If we can control the conditions that lead to cell death, we might be able to specifically kill cancer cells, and cells infected with viruses such as AIDS, SARS, etc. We may also be able to prevent the death of neurons in degenerative diseases like Parkinson's disease.

A major objective in the study of apoptosis is to determine how cytochrome c is released from mitochondria. Cytochrome c is a component of the mitochondrial respiratory chain, which carries electrons from complex III to complex IV (Tyler, 1992). Cytochrome c is located in the mitochondrial intermembrane space and some is bound to the outer surface of the inner membrane (Tyler, 1992). Its molecular weight is 13kDa and under normal conditions it cannot permeate through the mitochondrial outer membrane because the VDAC channels in the outer membrane have a molecular weight cut-off of about 5000 (Colombini, 1980b; Zalman *et al.*, 1980). There are many proposed ways of achieving the increase in permeability to cytochrome c: the permeability transition pore (Crompton, 1999), channels formed by Bax oligomers (Antonsson *et al.*, 2000, 2001; Saito *et al.*, 2000), the mitochondrial apoptosis-induced channels (MAC) (Pavlov *et al.*, 2001), BH3/Bax/cardiolipin interactions (Kuwana *et al.*, 2002), Bax induced lipidic pores (Basanez *et al.*, 1999), Bax/ceramide interactions (Belaud-Rotureau *et al.*, 2000; Pastorino *et al.*, 1999), and ceramide channels (Siskind and Colombini, 2000; Siskind *et al.*, 2002).

Ceramide is a sphingosine-based lipid and can be generated via the hydrolysis of sphingomyelin or by *de novo* synthesis from sphingosine and acyl-CoA. It has been shown to induce cytochrome *c* release when added to whole cell cultures (Zamzami *et al.*, 1995; Castedo *et al.*, 1996; Susin *et al.*, 1997; De Maria *et al.*, 1997) and isolated mitochondria (Arora *et al.*, 1997; Di Paola *et al.*, 2000; Ghafourifar *et al.*, 1999). The addition of ceramide to isolated mitochondria results in an increase in the permeability of the mitochondrial outer membrane to proteins (Siskind *et al.*, 2002). This occurs in a dose-dependent and time-dependent manner (Siskind *et al.*, 2002). The molecular weight cut-off for the ceramide channel is about 60 kDa (Siskind *et al.*, 2002), large enough to allow not only the flux of cytochrome c but also that of other pro-apoptotic factors. There was no release of fumarase activity (Siskind *et al.*, 2002) indicating no permeabilization of the inner membrane.

The Bcl-2 family of proteins has been shown to regulate the process of apoptosis. They share sequence homology especially in the BH3 domain, an amphipathic helix required to interact with other Bcl-2 family proteins (Huang and Strasser, 2000). Within this family, Bax, Bim, Bid, Bad are pro-apoptotic; Bcl-2, Bcl-X_L are anti-apoptotic. Following an apoptotic signal, those pro-apoptotic members become active either through translocation to mitochondria and ER such as Bax (Putcha *et al.*, 1999), or through cleavage, such as Bid to t-Bid (Li *et al.*, 1998), or through modification such as dephosphorylation of BAD (Wang *et al.*, 1999), or through oligomerization such as Bax and Bak (Antonsson *et al.*, 2000; Ruffolo and Shore, 2003). Thus they interact with antiapoptotic Bcl-2 family proteins or form their own pathways that favor the release of apoptogenic proteins from mitochondria.

Some of these have been shown to interact with VDAC. Bcl-X_L has been demonstrated to increase the open probability of VDAC channels (Vander Heiden *et al.*, 2001). Bid increase the closure probability of VDAC (Rostovtseva *et al.*, 2004) and Bak is inhibited by VDAC2 (Cheng *et al.*, 2003).

VDAC and its involvement in apoptosis

All the processes above occur in the mitochondrial outer membrane where VDAC resides. VDAC is the major permeability pathway by which metabolites cross the mitochondrial outer membrane. The barrel of the channel is formed by 1α helix and 13β strands (Fig. 1.2; Song *et al.*, 1998a; Blachly-Dyson *et al.*, 1990; Thomas, 1993). A single 30-32 kDa polypeptide forms the channel (Colombini *et al.*, 1996). This secondary structure seems to be well conserved in all species studied even though the primary sequences are quite different (Song and Colombini, 1996). VDAC1, the archetypal VDAC, is highly conserved in fundamental properties including single-channel conductance, selectivity and voltage dependence (Colombini, 1989). The isoforms of VDAC1 share some of the basic properties of VDAC1 but, in addition, have some specialized functions (Colombini, 2004).

Under some conditions, VDAC can close to 40%-50% of its overall conductance. In the open state, VDAC is anion-selective and permeable to multi-valent anionic metabolites including phosphocreatine, phosphate, succinate and ATP (Lee *et al.*, 1998; Xu *et al.*, 1999). In the closed state, the pore size changes from 3nm to 1.8nm, and the positively charged voltage sensor moves out of the channel (Fig. 1.3; Peng *et al.*, 1992; Song *et al.*, 1998b), which makes the channel cation-selective. For small cations, the

permeability becomes even larger (Hodge and Colombini, 1997), while the channel becomes actually impermeable to large anions such as ATP (Colombini, 2004). Thus the gating of VDAC results in a mild reduction of conductance but rather a dramatic change in selectivity (Colombini, 2004).

```
                                K112    F
                                A       N
                                G       L
                                R       H
                                A       F              A S Y Y H K V N S Q V E A G S K A T
                      LT69      N       F          S190                                    W
                       G   V    T       K              F   K T A V E L G V T N G TK S211  N
                       N   T    A       Q              V   Y
                       P   Q    P       S              S   R
   M A V P     N38     K   T    L       N              L   I              E
   -- - -  F A - N - V - D - W - F - F - H- E  - D - P - L - V -  -  -  -  -  -
      D  S7 F    P   A    T       N     S   H   G   G  T183 V  L    T       S
       K  A  I   T   F    F       T     F   G   V   F    A  S  V    L    E282
     S     A     N   K    K       A     I   R   I   L    T  F  N    G     F
       D N A     S   V    G       N     G   A   A   A    I  V  Y    V     T
         L L     K   T    E     A79     E   F   D   G    A  K  A    G     F
      K N   D    V   G    L       L     A   F   I   A    A  G  I    A     S
       F    D    E   K    A       E     K   D   N   S    S  K  A    S     T
        Y        I   S    G       T     L   L   A   A    Y  I  A    F     G
   --    Y   L - H23 - T - T - S - K - G - L -T135- G - T - N - V -D264-  -  -  -  -
        L  A     G   H   T53      V     K   K   P   Y    P  D  G    T     V
         A  A     D   V    E       A           G  D156  A   R240    Q     K
                  K        M       L              V      H         K     H
                       A  D N     I A A K Q             Y               L  T
                           T                           G           D  Q  A
                         G Y S A A V
```

Figure 1.2. The proposed structure of N. crassa VDAC in the open state. From left to right, 1 α helix and 13 β strands span the hydrophobic membrane. (Reproduced from Song et al., 1998a)

- CLOSED ← OPEN → CLOSED +
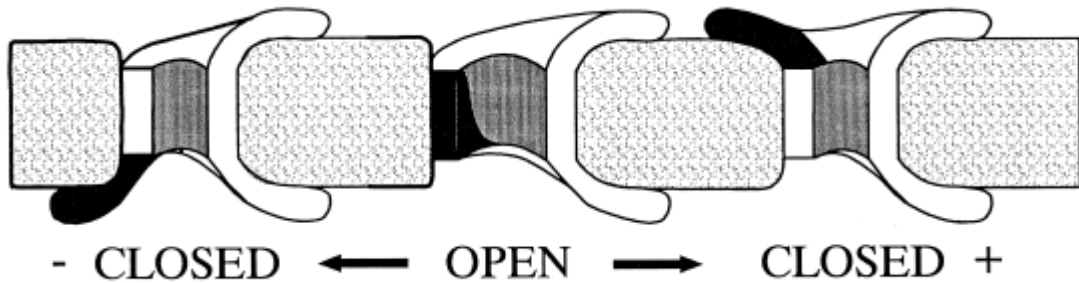
Figure 1.3. The proposed gating model of VDAC. The black region is highly positively charged and forms the selective filter of VDAC. It can move out in both directions in response to transmembrane potential, which reverses the selectivity and decreases the size of the pore.

There are lines of evidences indicating that VDAC's opening and closure is linked to cell apoptosis. For example, when growth factor is removed from the medium of a murine cell line that is dependent on the growth factor, the nucleotide exchange between mitochondria and cytosol becomes poor and somehow leads to cytochrome c release and apoptosis (Vander Heiden *et al.*, 2000). This is an early and reversible event marked by the accumulation of phosphocreatine in the intermembrane space. This accumulation is a signature for VDAC closure rather than some change in the transport across the inner membrane. ATP can get to the intermembrane space from the matrix and creatine (with zero net charge) can cross the outer membrane through the closed state of VDAC, but the product, phosphocreatine has a valence of -2 and thus cannot permeate through VDAC in the closed state. Thus VDAC closure leads to multi-valent anionic metabolite virtual impermeability. It precedes the permeabilization of the outer membrane to proteins and cytochrome c release. The restoration of growth factor prior to cytochrome c release restores the outer membrane permeability and rescues the cells. If Bcl-x_L is overexpressed, the cells can escape apoptosis (Vander Heiden *et al.*, 2000), which is also consistent with the observation that Bcl-x_L is able to favor the VDAC open state (Vander Heiden *et al.*, 2001).

VDAC's gating can be influenced in a variety of ways including voltage, impermeant macromolecules, some small molecules, phosphorylation, and intermembrane space proteins (Colombini, 2004). There is an estimated 40 mV potential negative in the intermembrane space compared to the cytosol (Porcelli *et al.*, 2005), which favors VDAC closure when the channel is reconstituted into phospholipid membranes (V_0=25mV, at which voltage a channel has 50% chance to be closed)

(Colombini, 2004). The non-electrolyte polymers such as polyethelene glycol can favor VDAC closure (Zimmerberg and Parsegian, 1986) and inhibit the mitochondrial outer membrane permeability to ADP (Gellerich *et al.*, 1993). NADH and Mg-NADPH also influence the gating properties of VDAC. The intermembrane space proteins from various species greatly favor VDAC closure (Holden and Colombini, 1993; Liu and Colombini, 1991; Liu *et al.*, 1994). Other proteins including G-actin (Xu *et al.*, 2001), Bcl-X_L (Vander Heiden *et al.*, 2001), dynein light chain (Schwarzer *et al.*, 2002), mtHSP (Schwarzer *et al.*, 2002) all modify the gating properties of VDAC.

VDAC's role in early apoptotic events is still controversial. There is evidence that VDAC is not involved in the apoptosis of S. *cerevisiae* (Gross *et al.*, 2000). There have also been several models for VDAC's participation in early apoptotic events. Many reports claim that VDAC is part of the permeability transition pore (PTP) (Szabo and Zoratti, 1993; Szabo *et al.*, 1993; Crompton *et al.*, 1998; Marzo *et al.*, 1998). PTP is thought to be located at contact sites between the inner and outer membranes, composed of VDAC in the outer membrane, adenine nucleotide translocator (ANT) in the inner membrane, cyclophilin D in the matrix and some kinases (Woodfield *et al.*, 1998; Crompton, 1999; He and Lemasters, 2002). The evidence is that agents targeted to VDAC (particularly Ro 68-3400 and ubiquinone), ANT (particularly bonkretic acid), or cyclophilin D (particularly cyclosporin A) can inhibit PTP opening (Halestrap and Brennerb, 2003; Waldmeier *et al.*, 2003; Cesura *et al.*, 2003). The opening of PTP causes dissipation of the mitochondrial membrane potential and matrix swelling. The trigger for the proposed PTP opening is associated with calcium influx into mitochondria (Hunter *et*

al., 1976). Thus it has been postulated that VDAC opening may promote calcium flow and hence PTP opening and mitochondrial swelling.

In addition, as stated above, it has been shown that VDAC may play a direct role in apoptosis through controlling metabolite permeation through the mitochondrial outer membrane. My results provide evidence that VDAC closure favors apoptosis

G3139 and other phosphorothioate oligonucleotides

G3139 (oblimersen) is an 18mer phosphorothioate oligonucleotide that is anti-sense to the start region of Bcl-2 mRNA (Fig. 1.4). Its efficacy and tolerability is being evaluated in combination with cytotoxic chemotherapy in chronic lymphocytic leukemia (CLL), multiple myeloma (MM), malignant melanoma, and non-small cell lung cancer, non-Hodgkin's lymphoma (NHL), acute myeloid leukemia (AML), and hormone-refractory prostate cancer (Frankel, 2003).
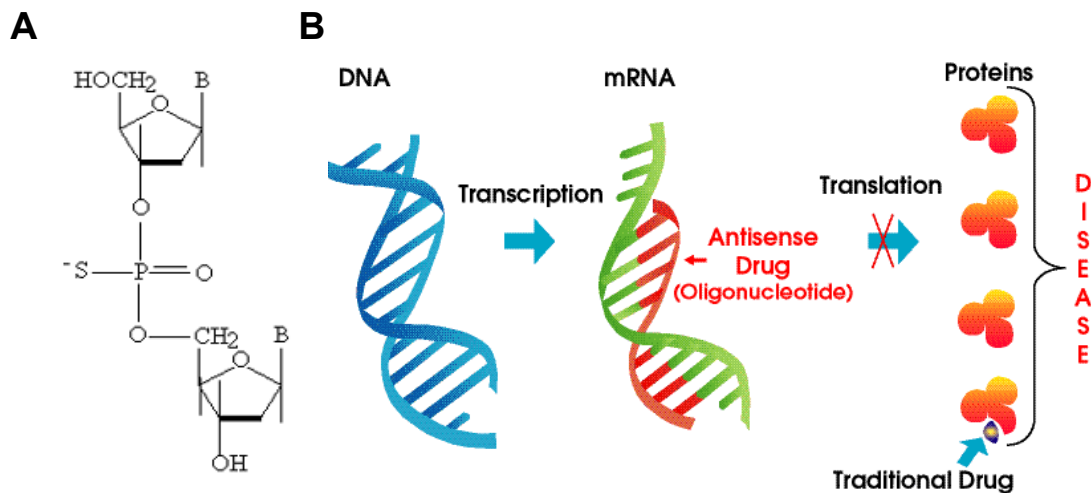
Figure 1.4. (A) Structure of phosphorothioate modification of DNA. One non-bridging oxygen is replaced with sulfur in each phosphodiester linkage. This modification increases its resistance to nucleases. **(B) The mechanism of anti-sense inhibition of protein expression.** The anti-sense oligonucleotide binds to the mRNA and inhibits the translation to proteins. (Reproduced from http://employees.csbsju.edu/hjakubowski/classes/ch331/bind/antisense.GIF)

9

It has been demonstrated that lipid-mediated transfection of G3139 into tumor cells can downregulate Bcl-2 mRNA and protein expression. The basic idea was, by decreasing the Bcl-2 protein level, tumor cells would be more sensitive to proapoptotic agents. However, G3139 induces apoptosis in melanoma cell lines, but does not produce chemosensitization. Furthermore, downregulation of the basal level of Bcl-2 protein does not increase the chemo-sensitization of tumor cells (Raffo *et al.*, 2004). Only forced over-expression of Bcl-2 protein in melanoma cells produces a relatively small amount of chemoresistance.

Further experiments demonstrated that transfection of G3139 with Lipofectamine 2000 resulted in the production of the typical apoptotic pathway intermediates. Nine and one half hours after transfection the simultaneous appearance of the 85kDa cleavage fragment of PARP-1, caspase-3 and tBid were observed. The presence of cytochrome c in the cytosol was observed between 5 and 9 hours. All these rather early changes were in sharp contrast with the fact that mitochondrial levels of Bcl-2 were only reduced after 24 hours of treatment and it took 48 hours to achieve a 40% reduction. These results demonstrate that G3139 induced apoptosis is unrelated to its ability to downregulate the Bcl-2 expression level and it might directly interact with mitochondria.

When isolated mitochondria were treated directly with G3139, changes consistent with the induction of mitochondria-mediated apoptosis were observed. There was an almost immediate reduction in the rate of exchange of nucleotide metabolites between the mitochondria and the medium, consistent with a reduction of outer membrane permeability due to VDAC closure. There was also a hyperpolarization of mitochondria resulting from the same permeability change and this was followed by the dissipation of

the mitochondrial potential and cytochrome c release. This is very similar to published work showing how VDAC closure is a very early step in the apoptotic process. Therefore, G3139 may interact directly with VDAC and thus induce apoptosis.

In contrast, Si3139, which has the same sequence as G3139 but without the sulfur modification, has no direct effect in isolated mitochondrial experiments. Si3139 does reduce the level of Bcl-2 protein in cells but does not induce apoptosis. Thus the sulfur modification seems to be important to the action of G3139. However, the sulfur modification is not sufficient. G4126 is a phosphorothioate oligonucleotide of the same length as G3139 but is not as effective as G3139. G4126 has a 2 codon difference from G3139 and shows weaker and delayed effects in inducing apoptosis. Thus there seems to be some sequence specificity. These results argue strongly that the anti-sense model needs to be abandoned.

My research is aimed at determining whether G3139 does act on VDAC and elucidating just how it acts. This information should help us design phosphorothioate oligonucleotides that are more effective than G3139. Also, my research shows that G3139 could be a specific inhibitor to VDAC, which may help not only in apoptosis studies, but also in the study of mitochondrial function and metabolism. The situation is complicated by the multiplicity of VDAC isoforms found in mammals.

VDAC gating process regulates calcium flux

The gating process of VDAC controls not only the flux of metabolites, it also regulates the flux of small ions. One important ion here is Ca^{2+}, because its flux through VDAC into the mitochondria can lead to mitochondrial swelling and subsequent cell

apoptosis. Because VDAC only shows weak selectivity for monovalent ions ($P_{cl}/P_k \sim 2$), it is speculated to be highly permeable to Ca^{2+} (Gincel *et al.*, 2001). One part of my project deals with the basic ion selectivity of VDAC, which shows that in the presence of $CaCl_2$, this channel shows essentially no permeability to calcium in its normal open state (Pcl/Pca $\sim$ 25) with a reversal potential ($\sim$ 26 mV) very close to the ideal anion selective channel ($\sim$ 30 mV). Those results suggest that the normal weakly anion selective VDAC channel essentially repels divalent cations. This high selectivity could be due to a strong electrostatic barrier to divalent ions.

After VDAC closure, the permeability of calcium could increase as much as 10 times and becomes comparable to that of chloride. Thus in the cell, VDAC closure could favor the flux of calcium into mitochondria and subsequent mitochondrial permeability transition. The bottom line here is that the seemingly weak selectivity change of VDAC in the gating process could show strong selectivity change for divalent ions. Thus this gating process may be important for the cell and mitochondrial calcium homeostasis.

This reexamination of calcium permeability through VDAC argues that calcium normally permeates through the cation selective closed VDAC channels in the mitochondria. Thus the opening of VDAC could hinder this permeation and inhibits mitochondrial swelling. This will be instructive in designing some specific inhibitor and promoter for the mitochondrial calcium uptake and thus could be useful in studying the effect of calcium on mitochondrial function and apoptosis.

PorB and its involvement in apoptosis

There are different types of Porins in the outer membrane of *Neisseria meningitidis*: PorA (class 1) and PorB (class 2/3). Two PorA and one PorB form the functional trimeric β barrels *in vivo*. Interestingly, PorB can insert into mammalian epithelial cells and then translocate into mitochondria, which subsequently inhibits mitochondrial damage induced by an apoptotic signals (Massari *et al.*, 2000). Part of my project is to determine the underlined mechanism by which PorB inhibits apoptosis.

The co-immunoprecipitation of PorB with VDAC (Massari *et al.*, 2000) suggests the localization of this protein in the mitochondrial outer membrane. In addition, based on the knowledge of the involvement of VDAC in apoptosis, it is possible that PorB modulate VDAC function and thus inhibits apoptosis. For example, PorB may open VDAC channels, facilitating metabolite flow, which would be consistent with VDAC opening favoring cell survival.

The purified PorB has also been reconstituted into planar membranes (Song *et al.*, 1998c). It shows a single-trimeric conductance of 1-1.3 nS in 200 mM KCl. Thus each monomeric channel has a conductance of around 0.4 nS under the same conditions. It shows an asymmetric voltage gating with $V_0 = 15$ mV and 25 mV respectively. The steepness of voltage gating is 1.5-1.7. The structure of the channels was proposed to be a 16β barrel. These characteristics are similar to those of VDAC. Considering its localization in the mitochondrial outer membrane, it is also highly possible that PorB may substitute for VDAC functions and increase the metabolite pathways. The

coimmunoprecipitation may be some unspecific binding of PorB with VDAC due to the large amount of the latter protein in the outer membrane.

My research tested for functional interactions between PorB and VDAC, and its possible function in mammalian mitochondria. It is also interesting to observe functional similarities between these two proteins, both important channels in the outer membranes of mitochondria and bacteria.

Significance of the research

Apoptosis is an important biological phenomenon. It happens in our body everyday to balance the increase in cell number arising from cell proliferation. This balance is pivotal to healthy tissues. Less apoptosis would lead to tissue growth and perhaps the generation of tumors. Excessive apoptosis may result in the shrinkage of tissues and dysfunction of organs. Understanding the mechanism of apoptosis is very important in designing drugs, which may promote or inhibit apoptosis so as to treat certain diseases such as cancer and Alzheimer's disease.

My whole study deals with understanding processes that relate to the basic concept of the initiation of mitochondria regulated apoptosis. Using phosphorothioate oligonucleotides as tools, a good correlation was discovered between VDAC closure and cytochrome c release. The calcium study raised the possibility of a physiological significance of VDAC gating in controlling the mitochondrial calcium homeostasis. This also suggests a possible relationship between VDAC closure and calcium uptake by mitochondria, which may leads to permeability transition and cell apoptosis. The

molecular basis by which PorB inhibit apoptosis was investigated in light of our understanding of VDAC's role in apoptosis.

Thus VDAC closure may be an early step in the initiation of cell apoptosis. This step is reversible as the reopening of VDAC can stop the subsequent release of cytochrome c (Vander Heiden *et al.*, 1999; Vander Heiden *et al.*, 2001). This information may lead to the design of efficient inhibitors or promoters of apoptosis by discovering agents that influence the gating of VDAC.

Chapter 2

Methods

Isolation of mitochondria

Mitochondria are isolated from rat liver as described by Parsons et al. (1966). The liver from a young SD rat is removed and washed in chilled buffer (70mM sucrose, 210 mM mannitol, 0.1 mM EDTA, 1.0 mM tris hydroxymethlamino methane, pH 7.2), chopped into small pieces and washed with the same buffer until free from blood. The liver pieces are mixed approximately 10 times the volume of buffer and homogenized with a glass vessel and a Teflon pestle at a speed of 150 rpm. The liver homogenate is spun for 10 minutes at 500 g at 4°C. The supernatant is poured out and spun down for 10 minutes at 9000 g at 4°C. The pellets of mitochondria are coated with a fluffy layer consisting of broken mitochondria and microsomes. The fluffy layer is lightly resuspended in the last few drops of supernatant to be removed and the surface of mitochondria pellet is washed lightly three times with buffer. The mitochondrial pellets are resuspended in buffer with 0.1% BSA. The suspension is spun again at 500 g for 10 minutes, the supernatant removed at the pellet discarded. The supernatant is then spun at 9000 g for 10 minutes, the supernatant removed and the pellet resuspended in buffer without BSA. The pellets are spun again for 10 minutes at 9000g, the supernatant removed as above and the pellets resuspended in a small volume (5 –7 ml) of buffer.

The isolation of mitochondria from yeast follows Daum *et al.* (1982), which follows the basic idea of differential centrifugation. However, the yeast spheroplasts need to be purified first before the lysing and isolation of mitochondria. The details are in Chapter 7.

Mitochondrial protein concentration assay

The protein concentration of the mitochondrial suspension is measured by using 100 mM Tris·SO_4, 0.4% SDS, pH 9.4 solution. (Clarke, 1976) Equal amounts of the solution and the mitochondrial suspension is mixed and the absorbance measured at 280 nm and 310 nm. The concentration of protein is $(A_{280}-A_{310})/1.05$ (mg/ml)

Mitochondrial intactness assay

The intactness of the purified mitochondria is quantified by the rate of cytochrome c-dependent oxygen consumption (Douce *et al.*, 1987). The mitochondrial outer membrane is not permeable to cytochrome c, and the cytochrome c oxidase resides in the inner membrane of mitochondria. Thus, the exogenously added cytochrome c oxidation shows the percentage of mitochondria with damaged outer membrane. The osmotically shocked mitochondria are prepared by incubating the 40 μl of mitochondrial suspension with 1.5 ml of double distilled water. After 3 minutes, 1.5 ml of double concentrated respiration buffer was added to restore the osmotic pressure. The fractional intactness of mitochondria is 1 minus the ratio of KCN-sensitive cytochrome c-dependent oxygen consumption of untreated and osmotically shocked mitochondria.

Measurement of mitochondrial respiration and MOM permeability

A portion of the mitochondrial suspension (about 1 mg mitochondrial protein) was diluted into 3 ml of respiration buffer containing 0.3 M mannitol, 10 mM NaH_2PO_4, 5 mM $MgCl_2$ and 10 mM KCl (pH 7.2). The mitochondrial respiration was measured according to the method of Lee *et al.* (1994). The respiratory control ratio was typically

above 5 (for succinate). Briefly, succinate (5 mM final) was added to the mitochondrial suspension followed by ADP addition (usually 80 μM). The oxygen consumption was measured by using a Clark oxygen electrode and the MOM permeability was obtained by fitting to the theoretical model developed by Lee *et al.* (1994). Since mitochondria respire at a slow rate (state IV respiration rate) even without ADP addition, the state IV respiration was subtracted from state III respiration to obtain the ADP-stimulated oxygen consumption. This result was converted to [ADP] as a function of time by multiplying the [oxygen] by the P/O ratio (2 for succinate as the substrate). The derivative of the [ADP] versus time is the rate of ADP consumption at any time. This curve is fitted using a BASIC program to calculate the MOM permeability.
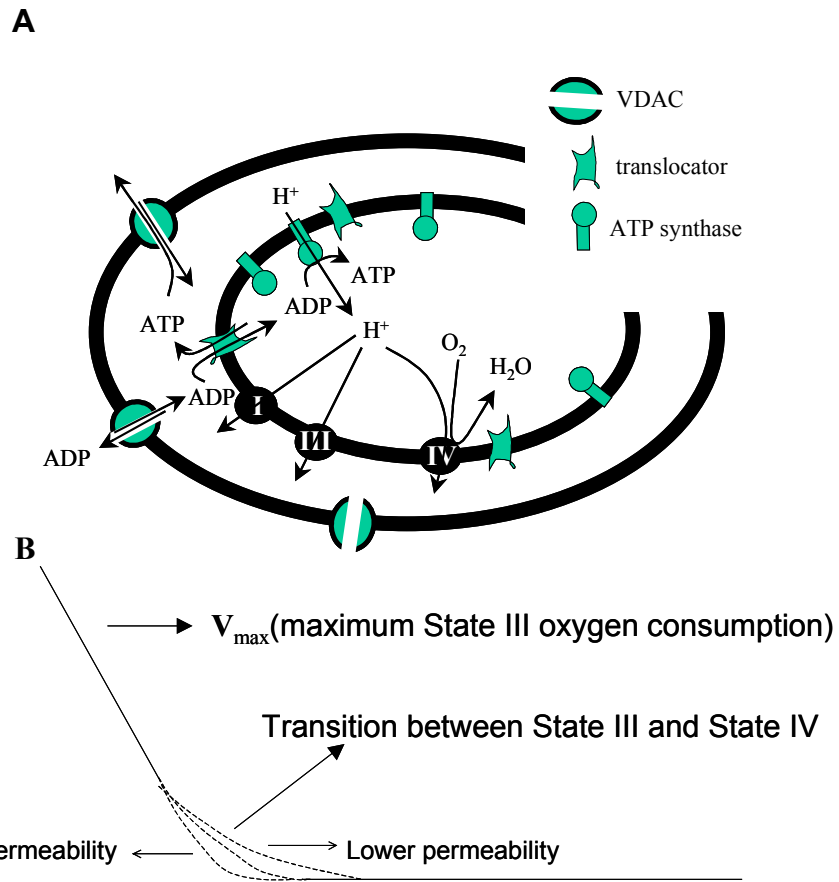
Figure 2.1 MOM permeability assay (A) ADP flux into mitochondria is coupled with mitochondrial respiration or oxygen consumption. **(B)** The illustration of the relationship between ADP stimulated respiration and MOM permeability

Fig. 2.1A shows the basic concept of measuring MOM permeability, When mitochondria undergo State III respiration, ADP needs to permeate through VDAC in the outer membrane, then translocate through the ANT in the inner membrane, and is finally phosphorylated in the matrix, which is quickly coupled to oxygen consumption through the protonmotive force.

At high ADP concentrations, the permeation through the outer membrane is fast and the translocation through inner membrane is saturated, which result in a constant maximum oxygen consumption rate. As ADP is depleting, the flux through the outer membrane becomes more rate-limiting, and intermembrane space ADP concentration will decline faster than the [ADP] in the medium. The transition between State III and State IV then contains the information about the permeability of the outer membrane (Fig. 2.1B).

Isolation of VDAC from mitochondrial membranes

The VDAC is purified according to standard methods (Mannella, 1982; Freitag et al., 1983). The purified mitochondria are hypotonically shocked in 1mM KCl, 1mM HEPES, pH 7.5 and spun at 24,000g for 30min to release the soluble proteins from the membranes. The pellet is resuspended 15% DMSO, 2.5% Triton X-100, 50mM KCl, 10mM Tris·Cl, 1mM EDTA, pH 7.0 and spun in a microcentrifuge at 14,000rpm for 30min. The supernatant is passed through a 1:1 hydroxyapatite/celite column that binds most proteins but allows VDAC to flow through. The VDAC samples are stored at − 80°C. This isolated VDAC would thus possibly contain three isoforms (but mostly VDAC1) if the mitochondria are from a mammalian source (normally rat liver) or two

isoforms if the mitochondria are from yeast (however, only yeast VDAC1 forms functional channels).

Planar phospholipid membrane studies

The planar phospholipid membrane is generated according to standard methods (Montal and Mueller, 1972; Schein et al., 1976, Fig. 2.2). The phospholipid/cholesterol monolayers are formed from a hexane solution containing 0.5% diphytanoylphosphatidylcholine (DPyPC), 0.5% asolectin (soybean phospholipids polar extract) and 0.05% cholesterol. The two monolayers are used to form a bilayer across a 0.1 mm hole in a Saran partition separating the two Teflon chambers. The increase in

Experimental Set-Up for Making Planar Membranes
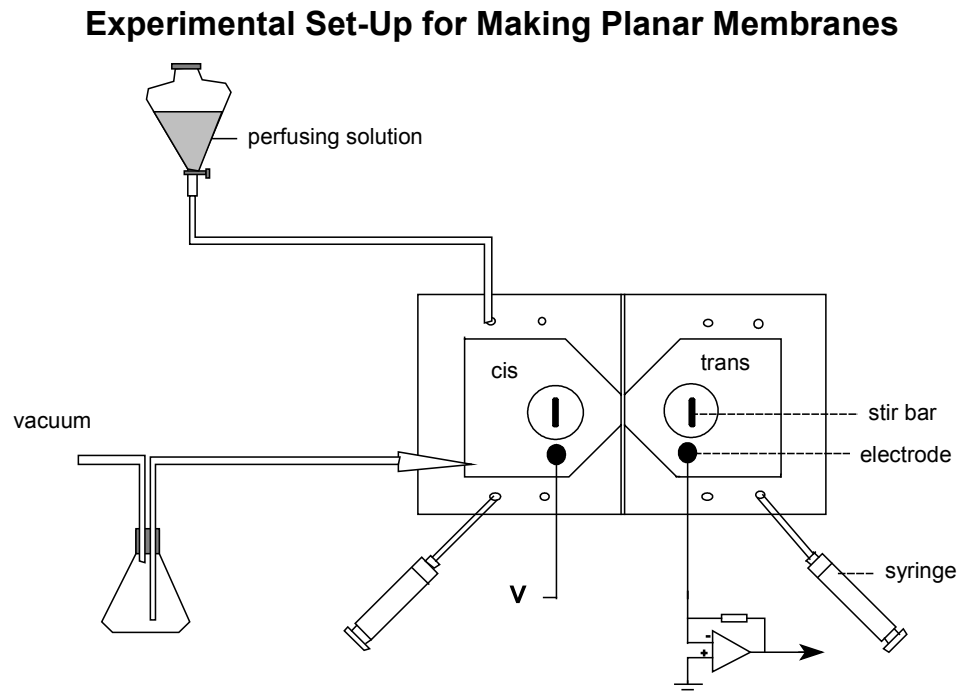
Figure 2.2 The experimental setup for planar membrane. The planar membrane is made in a 0.1mm hole in the saran partition separating two aqueous compartments: *cis* and *trans*, surrounded by Teflon chamber. The purified VDAC was inserted from the *cis* side. The voltage was clamped and the current was recorded. The left part shows the instruments used to change the solution of the *cis* side.

capacitance is used to monitor the formation of the membrane. Generally, membranes with a conductance of less than 0.05 nS were used. The aqueous solution generally contains 1 M KCl, 5 mM $CaCl_2$, 5 mM HEPES (pH = 7.2). All the experiments are performed at room temperature (about 23°C).

The side to which VDAC is added is defined as the cis-side and the other side is the trans-side. The trans-side is kept at ground, while the voltage on the cis-side is controlled as needed. Normally channels are inserted into the membrane by adding (while stirring) 1-5 µl of the VDAC solution to 4-6 ml of aqueous solution on the cis side of the chamber.

Measurement of yeast MOM permeability to NADH

NADH oxidation was measured according to Lee *et al.* (1998). Briefly, a portion of yeast mitochondria (about 250 µg mitochondrial protein) is diluted into the yeast respiration medium containing 0.65 M sucrose, 10 mM HEPES, 10 mM KH_2PO_4, 5 mM KCl and 5 mM $MgCl_2$ with pH at 7.2. NADH oxidation was measured as the absorbance change at 340 nm after the addition of 30 µM NADH. Another portion of mitochondria was mildly shocked by incubation with 2 volumes of distilled water on ice for 10 minutes followed by addition of 5 volumes of yeast respiration medium and 2 volumes of double concentrated yeast respiration medium to restore the osmotic pressure.

The flux of NADH through VDAC restricts the rate of NADH oxidation in the mitochondrial intermembrane space. Thus by assuming 100% permeability of NADH through the MOM in mildly shocked mitochondria, the permeability of the MOM to NADH in unshocked mitochondria can be calculated as previously described (Lee *et al.*, 1998).

Chapter 3

A Pharmacologic Target of G3139 in Melanoma Cells May Be the Mitochondrial VDAC

Running title: G3139 Targets Mitochondrial VDAC

Key words: cytochrome c, phosphorothioate, oligonucleotides

Abstract

G3139, an 18-mer phosphorothioate antisense oligonucleotide targeted to the initiation codon region of the Bcl-2 mRNA, can induce caspase-dependent apoptosis via the intrinsic mitochondrial pathway in 518A2 and other melanoma cells. G3139-mediated apoptosis appears to be independent of its ability to down-regulate the expression of Bcl-2 protein, because the release of mitochondrial cytochrome c precedes in time the down-regulation of Bcl-2 protein expression. In this study, we demonstrate the ability of G3139 and other phosphorothioate oligonucleotides to bind directly to mitochondria isolated from 518A2 cells. Furthermore, we show that this interaction leads to the release of cytochrome c in the absence of a mitochondrial membrane permeability transition. Our data further demonstrate that there is an interaction between G3139 and VDAC, a protein that can facilitate the physiologic exchange of ATP and ADP across the mitochondrial outer membrane. Evidence from the electrophysiologic evaluation of VDAC channels reconstituted into phospholipid membranes demonstrates that G3139 is capable of producing greatly diminished channel conductance, indicating a closed state of the VDAC. This effect is oligomer length-dependent, and the ability of phosphorothioate homopolymers of thymidine of variable lengths to cause the release of cytochrome c from isolated mitochondria of 518A2 melanoma cells can be correlated with their ability to interact with VDAC. Because it has been suggested that the closure of VDAC leads to the opening of another outer mitochondrial membrane channel through which cytochrome c can transit, thus initiating apoptosis, it appears that VDAC may be an important pharmacologic target of G3139.

Introduction

G3139 is an 18-mer phosphorothioate antisense oligonucleotide targeted to the initiation codon region of the Bcl-2 mRNA (Klasa *et al.*, 2002). The ability of G3139 to down-regulate the expression of the proapoptotic Bcl-2 protein has been demonstrated in a series of previous experiments (Leung *et al.*, 2001; Raffo *et al.*, 2004; Lai *et al.*, 2005), and this effect has been correlated with decreased resistance to cytotoxic chemotherapy in animal models (Jansen *et al.*, 1998). On the basis of favorable phase II clinical data (Jansen *et al.*, 2000), G3139 has recently entered phase III clinical trials in combination with dacarbazine for the treatment of advanced melanoma. However, the mechanism of action of G3139 remains somewhat uncertain. siRNA silencing of Bcl-2 protein expression in 518A2 melanoma cells, the preclinical model, did not lead to chemosensitization (Lai *et al.*, 2005). In fact, G3139 induced extensive apoptosis in 518A2 and other melanoma cells, frequently in the absence of any discernable Bcl-2 protein down-regulation (Lai *et al.*, 2005). Caspase-dependent apoptosis in melanoma cells *in vitro* occurred via activation of the intrinsic pathway and was characterized by cleavage of procaspase-3/7 to caspase-3 with subsequent cleavage of many intracellular proteins. In addition, Bid was processed to proapoptotic tBid in a caspase-3/7-dependent manner, without any activation of caspase-8 (Slee *et al.*, 2000). The mitochondrial permeability transition occurred relatively late (Bossy-Wetzel *et al.*, 1998) in the apoptotic process (24 h after the initiation of the transfection with G3139).

The initiation of the apoptotic process via the intrinsic pathway can require the release of cytochrome *c* into the cytoplasm (Liu *et al.*, 1996) from loosely bound sites in the intermembrane space of the mitochondrion (Ott *et al.*, 2002). In the cytoplasm,

cytochrome *c* combines with Apaf-1, dATP, and procaspase-9 to form the apoptosome (Li *et al.*, 1997), in which procaspase-9 is cleaved to caspase-9, which then activates caspase-3/7, resulting in intracellular demolition (Salvesen and Dixit, 1997). We observed (Lai *et al.*, 2005) that the G3139-induced release of cytochrome *c* from the mitochondria in intact melanoma cells occurred very early (9.5 h) after the initiation of the cellular transfection with G3139, much earlier, in fact, than what we typically observed with standard cytotoxic chemotherapy (20–24 h).

G3139 and phosphorothioate oligonucleotides can bind with high affinity to cell-surface heparin-binding proteins (Guvakova *et al.*, 1995; Benimetskaya *et al.*, 1997; Rockwell *et al.*, 1997). Because of this ability, we postulated that the early release of cytochrome *c* from the mitochondria might also be occurring as a result of the interaction of G3139 with a heparin-binding protein present in the outer mitochondrial membrane.

VDAC is a channel-forming protein in the mitochondrial outer membrane responsible for metabolic flux (including nucleotide phosphates) through that membrane (Colombini, 1979; Rostovtseva and Colombini, 1997; Colombini, 2004). VDAC has been widely implicated in the initiation of the mitochondrially mediated intrinsic pathway of apoptosis (Szabo and Zoratti, 1993; Crompton *et al.*, 1998; Vander Heiden *et al.*, 2001). Although the mechanism of action is still quite controversial (Vander Heiden *et al.*, 2000), closure of the VDAC and the subsequent decrease in metabolic flux can precede, and may in fact cause, the permeabilization of the outer membrane to relatively small proteins, leading to apoptosis. The actual protein translocation channel would thus be generated by other, as yet unknown structures as a consequence of decreased metabolic

flux. Because a variety of polyanions favor VDAC closure, we thus deemed it possible

that G3139 could also induce VDAC closure, which would result in cellular apoptosis.

Materials and Methods

Cell Culture and Oligonucleotide Transfections

The mycoplasma-free human melanoma cell line 518A2 was a kind gift from Volker Wacheck (University of Vienna). Cells were grown in DMEM supplemented with 10% heat-inactivated FBS and 100 units/ml penicillin G sodium and 100 µg/ml streptomycin sulfate. Stock cultures of all cells were maintained at 37°C in a humidified 5% CO_2 incubator.

Cells were seeded the day before the experiment in six-well plates at a density of 15×10^4 cells per well, to be 60–70% confluent on the day of the experiment. All transfections were performed in OptiMEM medium (Invitrogen) plus complete media without antibiotics, as previously described (Raffo *et al.*, 2004; Lai *et al.*, 2005). The incubation time for oligonucleotide/Lipofectamine 2000 complexes was 5 h. The total incubation time before cell lysis and protein isolation was from 24 to 72 h at 37°C.

Reagents

The anti-cytochrome *c* monoclonal antibody was purchased from Santa Cruz Biotechnology. The anti-α-tubulin monoclonal antibody was from Sigma-Aldrich. Lipofectamine 2000 was from Invitrogen. MitoTracker Red was from Molecular Probes. Oligonucleotides were kindly supplied by Genta (Berkeley Heights, NJ).

Subcellular Fractionation and Oligonucleotide Treatment of Isolated Mitochondria

Cells were harvested by trypsinization and washed with cold PBS. Cell pellets were resuspended in 300 µl of buffer A (250 mM sucrose/10 mM Tris·HCl, pH 7.4/1 mM

EGTA/50 µg/ml Pefabloc/15 µg/ml leupeptin, aprotinin and pepstatin). Cells were then homogenized on ice in a Dounce homogenizer until 90% of cells were disrupted, as judged by Trypan blue staining. Crude lysates were centrifuged at 1,000 x g for 10 min at 4°C twice to remove nuclei and unbroken cells. The supernatant was collected and subjected to centrifugation at 10,000 x g for 30 min at 4°C. The supernatant was collected as the cytosolic fraction, and the mitochondrial pellets were resuspended in 30 µl of buffer A. In some experiments, mitochondria were highly purified by ultracentrifugation through a Percoll gradient at 100,000 x g.

Western Blot Analysis and Coomassie Blue Staining

Cells treated with oligonucleotide–lipid complexes were extracted in lysis buffer at 4°C for 1 h. Aliquots of cell extracts, containing 25–40 µg of protein, were resolved by SDS/PAGE and then transferred to Hybond ECL filter paper (Amersham Pharmacia). After treatment with the appropriate primary and secondary antibodies, ECL was performed. The typical margin of error for Western blotting is at least 20–25%.

For Coomassie blue staining, gels after electrophoresis were stained with 0.025% Coomassie blue R250 in 40% methanol/7% acetic acid (vol/vol) for 1 h, followed by washing with destaining solution [7% acetic acid/5% methanol (vol/vol)]. The stained gel was then scanned by laser-scanning densitometry, and the bands were quantitated.

Labeling of Mitochondria with Fluorescent G3139 and MitoTracker Red

Cells were transfected with 100 nM FITC-G3139/Lipofectamine 2000 complexes for 5 h as previously described (Raffo *et al.*, 2004; Lai *et al.*, 2005), and incubated for an

additional 19 h before staining with MitoTracker Red, a mitochondrion-selective probe. For live-cell staining, the cell culture medium was replaced with 500 nM MitoTracker Red in prewarmed DMEM, and the cells were incubated for 30 min under standard growth conditions. Then, the stained cells were washed twice with 1x PBS before analysis by flow cytometrically.

Binding of Fluorescinated Oligonucleotides to Mitochondria

Isolated mitochondria were resuspended in 20 µl of energizing buffer B (250 mM sucrose/10 mM Tris-HCl, pH 7.4/1 mM EGTA/50 µg/ml Pefabloc/10 mM KCl/3 mM KH$_2$PO$_4$/5 mM succinate/100 µM ADP/15 µg/ml leupeptin, aprotinin, and pepstatin), which contained increasing concentrations of fluorescent-labeled oligonucleotides (1–40 µM). In some experiments, a competitor of G3139 binding to the mitochondrial surface, a 28-mer phosphorothioate homopolymer of cytidine (SdC28; 20 µM), was added. Incubation was carried out on ice for 10 min before washing twice with cold 1x PBS. After centrifugation at 10,000 x g, the pellet was resuspended in 200 µl of blank buffer B before flow-cytometric analysis.

Planar Phospholipid Membrane Studies

The planar phospholipid membrane was generated according to standard methods (Colombini, 1987a). The membrane was formed of phospholipid monolayers consisting of diphytanoylphosphatidylcholine asolectin (soybean phospholipid polar extract) and cholesterol (1:1:0.1 mass ratio). The aqueous solution generally contained 1.0 M KCl, 5

mM CaCl$_2$, 1 mM EDTA, and 5 mM Hepes (pH 7.2). All experiments were performed at 25°C.

VDAC was purified from mitochondria isolated from rat liver (Freitag *et al.*, 1983; Blachly-Dyson *et al.*, 1990). It was then solubilized in 2.5% Triton X-100, and a 1- to 3-µl aliquot was stirred into 4–6 ml of aqueous solution on the cis side of the chamber. The opposite, trans side was held at virtual ground by the voltage clamp.

Statistical Analysis

Data are expressed as mean ± SD, and significance was determined by Student's *t* test.

Results and Discussion

Phosphorothioate Oligonucleotides Bind to Mitochondria

As mentioned previously, 518A2 melanoma cells treated with G3139 undergo apoptosis characterized by relatively rapid release of mitochondrial cytochrome *c*. We hypothesized that this release might be due to a direct interaction of G3139 with the mitochondrial membrane. Accordingly, we isolated mitochondria from 518A2 cells by differential centrifugation. The purity of the mitochondria was assessed flow cytometrically by nonyl acridine orange (NAO) staining, and subsequently only the NAO-gated population was analyzed. The flow cytometric results of treatment of isolated mitochondria at 4°C with increasing concentrations of either 5'-FITC-G3139 or -4126 (a two-base mismatch) are shown in Fig. 3.1A. The binding is essentially maximal by 30 min and remains undiminished for up to 2 h (data not shown). In contrast to what was observed with these two oligomers, the 5'-FITC-isosequential phosphodiester congener of G3139 (5'-FITC-PO-G3139) did not bind to the mitochondria. This difference in binding affinity between a phosphodiester (low) and an isosequential phosphorothioate (high) oligonucleotide has been long recognized (Guvakova *et al.*, 1995).

In addition, as shown in Fig 3.1B, the binding occurs substantially on the basis of a charge interaction, because it can be 75% competed by SdC28, a longer phosphorothioate oligomer that is a homopolymer of cytidine. Moreover, the ability of the binding to be competed indicates that it occurs predominately at the outer mitochondrial membrane, as opposed to within the organelle itself.

31
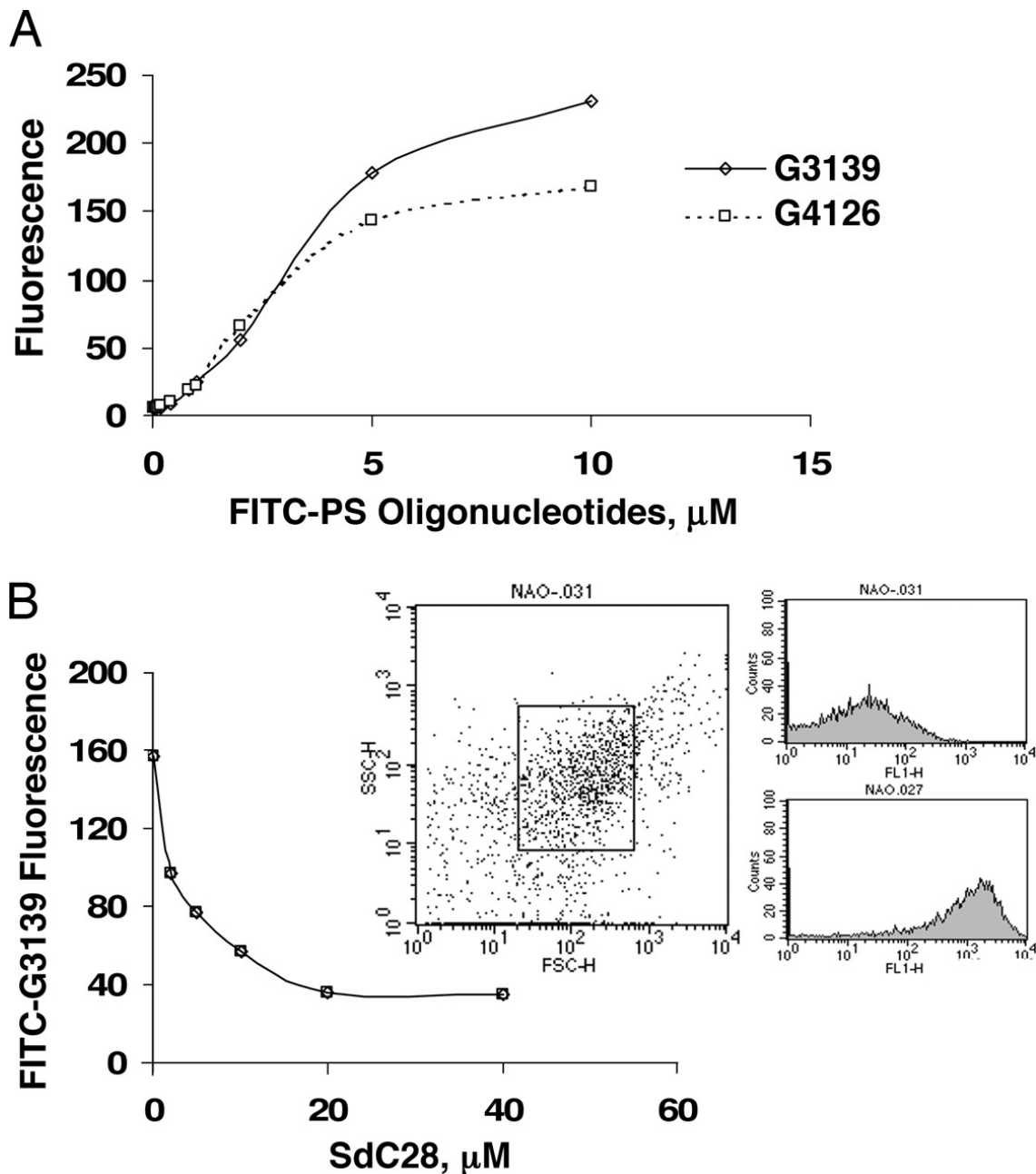
Figure 3.1. Binding of oligonucleotides to isolated mitochondria. (**A**) Isolated mitochondria from 518A2 melanoma cells were incubated with 5'-FITC-G3139 and -G4126 at various concentrations (10 nM to 10 µM), as described in *Materials and Methods*, and the binding was assessed flow cytometrically. (**B**) The binding of 5'-FITC-G3139 can be competed by SdC28 in a concentration-dependent manner (2–20 µM). (*Inset*) Mitochondria were gated flow cytometrically by NAO staining, which specifically stained the mitochondrial cardiolipin.
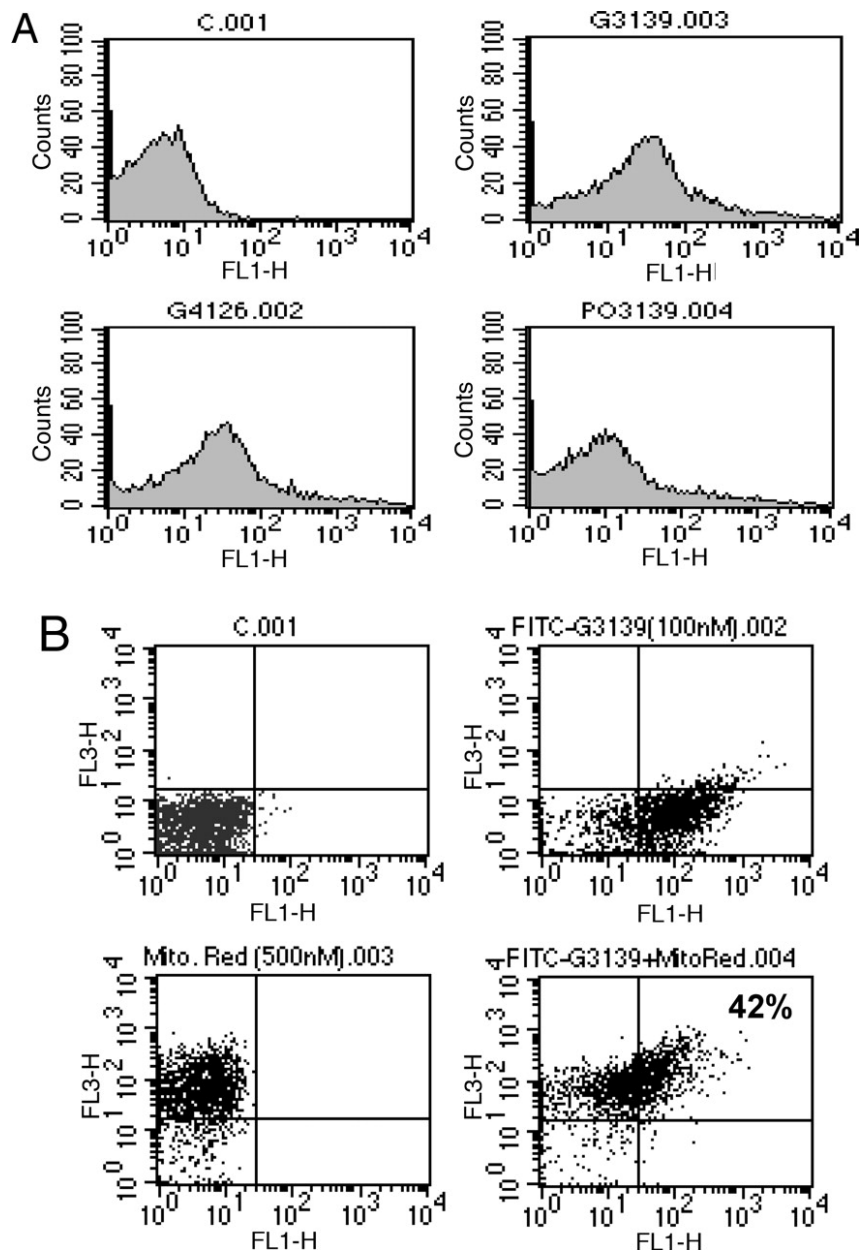
Figure 3.2. Binding of oligonucleotides to mitochondria isolated from intact cells. (*A*) 518A2 melanoma cells treated with 100 nM 5'-FITC-oligonucleotides/Lipofectamine 2000 (1.9 μg/ml) for 5 h were fractionated, and the staining of the mitochondria with FITC-oligonucleotides was assessed by flow cytometry. A minimum of 10,000 mitochondria per sample were analyzed as described in *Materials and Methods*. A >8-fold increase in FL-1 fluorescence was observed in both FITC-G3139 and -G4126-treated samples, whereas FITC-PO-3139 yielded only a very small increase (2-fold) (Table 3.1). (*B*) Intact 518A2 melanoma cells were treated with 100 nM 5'-FITC-G3139/Lipfectamine 2000 (1.9 μg/ml) for 5 h and stained with 500 nM MitoTracker Red. As analyzed flow cytometrically, 42% of the mitochondria were costained with FITC-G3139 and MitoTracker Red, as shown in the dot plot.

Table 3.1. Fluorescence mean channel from Figure. 3.2A

Samples	Fluorescence mean channel
C	6.71
G4126	55.84
G3139	55.55
PO-3139	15.19

We then treated intact 518A2 cells with 100 nM 5'-FITC-G3139/Lipfectamine 2000 (1.9 µg/ml) and other oligonucleotides for 5 h, and then isolated mitochondria. As shown in Fig. 3.2A, substantial mitochondrial staining was observed flow cytometrically in the NAO-gated population after either treatment with 5'-FITC-G3139 or the two-base mismatch 5'-FITC-G4126. In contrast, treatment with the 5'-FITC-phosphodiester analog of G3139 produced only a small increase in mitochondrial staining. We confirmed these observations by treating intact cells with 5'-FITC-G3139 as above and the specific mitochondrial stain MitoTracker Red. Again, flow-cytometric analysis clearly demonstrated that a substantial proportion (42%) of the mitochondrial population stained with both dyes (Fig. 3.2B).

The binding of phosphorothioate oligonucleotides to the mitochondrial membrane does not result in a membrane permeability transition. This permeability transition was assessed flow cytometrically by JC-1 staining in mitochondria isolated from 518A2 cells that were then treated with either 20 or 40 µM G3139.

Treatment of Isolated Mitochondria with Phosphorothioate Oligonucleotides Causes Release of Cytochrome c

When isolated mitochondria were directly treated with 20 µM G3139 (Fig. 3.3A) in energizing buffer B with or without 100 µM Mg^{2+} for 2 h at 10°C, cytochrome c was released into the supernatant, as demonstrated by Western blotting. This release was identical whether mitochondrial were isolated either by low-speed differential centrifugation or ultracentrifugation. The release of cytochrome c is concentration-dependent and Mg^{2+}-independent (Fig. 3.3B) but can easily be observed at a concentration of as low as 5 µM, also by Western blotting. Estimates of the intracellular concentration of 5'-FITC-G3139, based on the data in Fig. 3.1A and Fig. 3.2A, indicate that it may be at least as high as 2–3 µM. This is despite the much lower media concentration of 100 nM, a value that nevertheless has questionable significance because the oligonucleotide, when complexed with Lipofectamine 2000, is particulate and essentially precipitates on the cells in culture at the bottom of the wells. The ability of G4126 to cause concentration-dependent release of cytochrome c from isolated mitochondria was almost identical to that of G3139.

As mentioned above, the release of cytochrome c from mitochondria in response to G3139 or G4126, but not PO-G3139 treatment, is not accompanied by a mitochondria permeability transition. Simultaneous treatment with up to 20 µM MPTP inhibitor cyclosporin A, which binds (Cesura *et al.*, 2003) to cyclophilin D [a PTP regulatory protein (Nicolli *et al.*, 1996)], also does not alter the concentration-dependent increase of cytochrome c release by G3139.
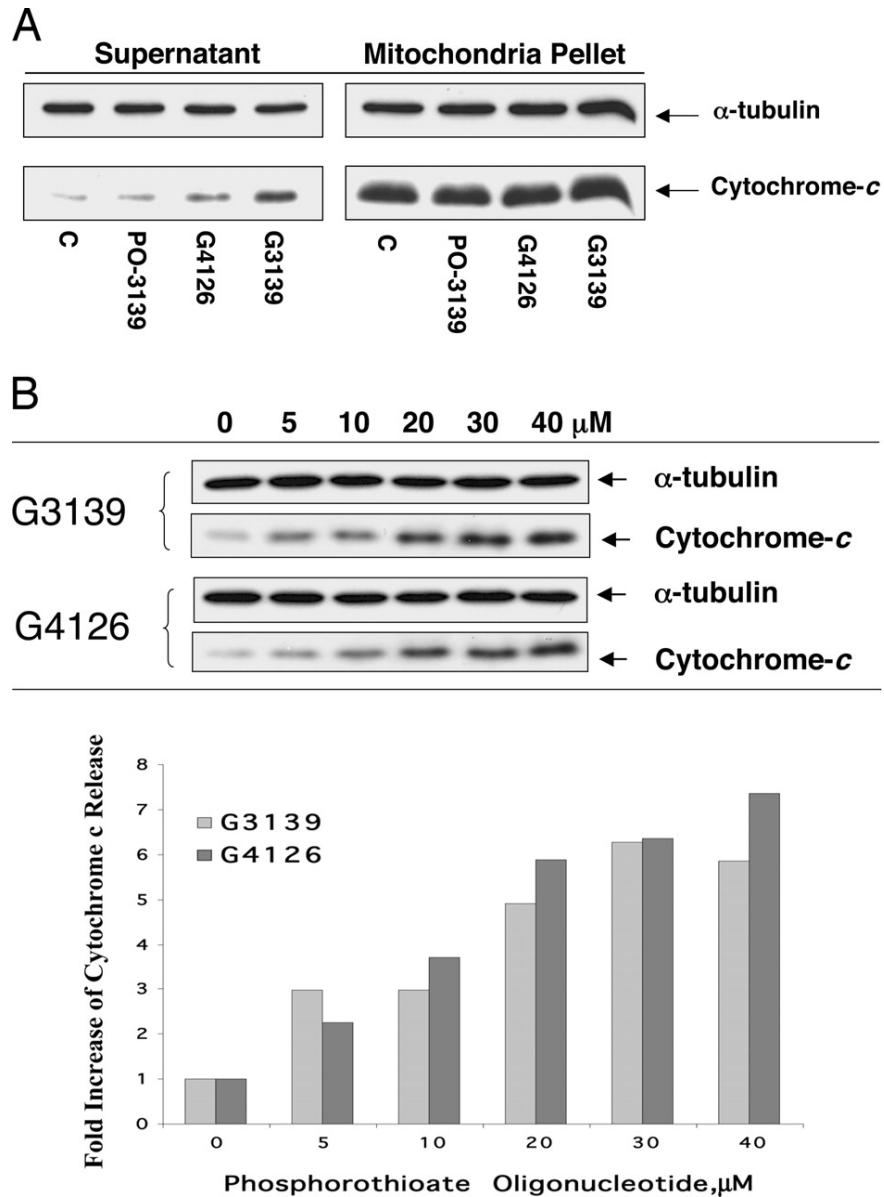
Figure 3.3. Release of cytochrome *c* from isolated mitochondria. (**A**) Isolated mitochondria from 518A2 melanoma cells were treated with 20 μM oligonucleotides (including PO-3139, G4126, and G3139) for 2 h in buffer B, and the supernatants were collected. Cytochrome *c* protein levels in both mitochondrial pellets and supernatant were analyzed by Western blotting as described in *Materials and Methods*. As shown, both phosphorothioate oligonucleotides G3139 and, to a lesser extent, G4126 caused a significant release of cytochrome *c* from the mitochondria. However, PO-3139 did not lead to any detectable release of cytochrome *c* from the mitochondria. (**B**) Western blot of the concentration-dependent profile of cytochrome *c* release by G3139 and G4126 from mitochondria isolated from 518A2 cells.

36

The release of cytochrome *c* from the mitochondria is not accompanied by mitochondrial inner membrane permeabilization. Fifty-kilodalton fumarase is an enzyme present in the mitochondrial matrix (Tuboi *et al.*, 1990), and its release is considered normative evidence of damage/disruption of the mitochondrial inner membrane (Siskind *et al.*, 2002). Treatment of isolated mitochondria with Triton X-100 led to rupture of the mitochondrial membranes and release of fumarase activity, whereas treatment with up to 80 μM G3139 did not lead to the release of any detectable fumarase activity. In addition, treatment of isolated mitochondria also did not lead to release of MnSOD, also a mitochondrial matrix protein. Dextran sulfate (500 kDa; 500–1,000 μg/ml, 2 h, 10°C) and Koenig's polyanion (50–100 μg/ml) are both agents that favor closure of the voltage-dependent anion selective channel (VDAC), a mitochondrial outer membrane protein (Colombini *et al.*, 1987a; Mangan and Colombini, 1987). Treatment of isolated mitochondria did lead, under the same conditions, to the release of cytochrome *c*, but this release occurred only at the highest concentrations. The release of 14-kDa cytochrome *c* from the mitochondria is also customarily associated with the release of other, relatively low molecular weight proteins [e.g., Smac/DIABLO, Htra2/Omi, AIF, and endonuclease G (Debatin *et al.*, 2002)].

These data suggested that the mitochondrial outer membrane target of the phosphorothioate oligonucleotides may be VDAC. These are the proteins that form a large-diameter (3 nm) channel that permits the physiologic exchange of anionic metabolites (e.g., ATP and ADP) across the mitochondrial outer membrane when they are in the open configuration (Vander Heiden *et al.*, 2000; Hodge and Colombini, 1997).

Although controversial, it is believed that antiapoptotic proteins such as Bcl-2 and Bcl-xL maintain this channel in the open configuration (Vander Heiden *et al.*, 2001).

However, as shown in Fig. 3.4, there appears to be a cut-off in the molecular masses of the proteins released from the mitochondria after they are treated by G3139. The relative lack of release of proteins of molecular mass greater than 35 kDa here [and 60 kDa in the work of Siskind *et al.* (2002)] suggests the formation of another channel in the mitochondrial membrane subsequent to VDAC closure. The nature of this channel has been previously postulated to be of oligomerized ceramide (Siskind *et al.*, 2002), but little is actually known about it.
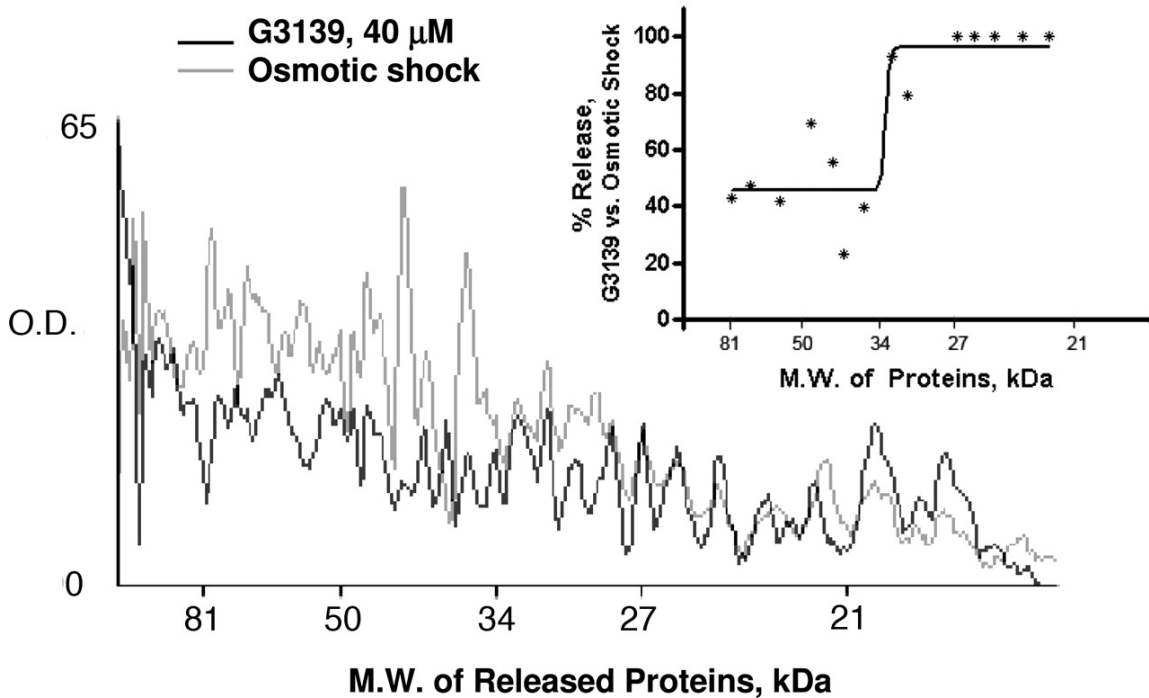
Figure 3.4. Release of proteins from the mitochondrial intermembrane space was characterized by Coomassie blue staining of the supernatants collected either from the osmotic shock of isolated mitochondria in ddH$_2$O or by treatment with 40 μM G3139. G3139-induced protein release was normalized to the total release induced by osmotic shock; peaks representing 14 proteins from the histogram were randomly chosen and quantitated. The profile of protein release by G3139 displayed an approximate 35-kDa molecular-mass cutoff, as shown in the scatter plot (*Inset*).

The interaction between G3139 and the VDAC

To unambiguously determine whether phosphorothioate and other oligonucleotides directly influence the properties of VDAC, evaluations were performed on pure VDAC channels reconstituted into phospholipids membranes. VDAC channels were purified from rat liver mitochondria and inserted into planar phospholipid membranes. Positive and negative 50-mV voltage steps were applied to the membrane, and ion permeability induced by the channels in the membrane was measured as current flow across the membrane. VDAC channels are voltage-dependent and thus the voltage steps induce the opening and closing of the channels. VDAC channels exist primarily in the open state at 0 mV and low voltages, and tend to close at voltages above ± 20 mV. Closing is a slow process and is thus well resolved in a time scale of 1 s (Fig. 3.5). The opening process occurs in a millisecond time scale and thus seems to occur instantly in
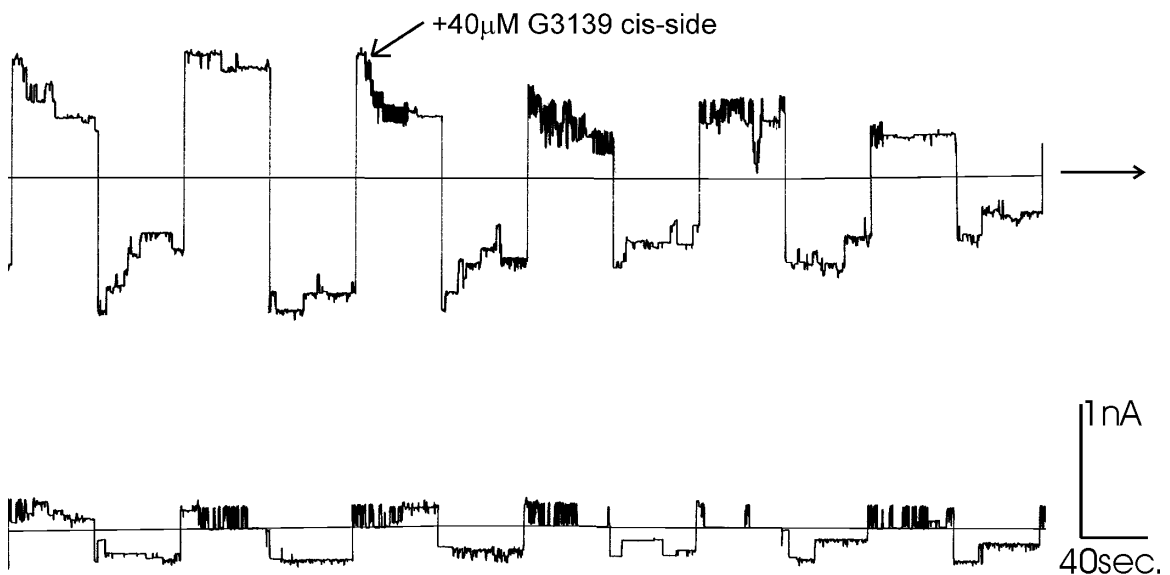
Figure 3.5. A few VDAC channels were reconstituted into a planar phospholipid membrane as described in *Materials and Methods*. The voltage was held at either +50mV or −50mV and alternated every 50 seconds. The long horizontal line indicates zero current. The 40 μM G3139 was added where indicated. The upper and lower traces are a continuous record without any breaks.

the figure. Note that the closed state of VDAC, although impermeable to ATP, allows substantial flux of both K^+ and Cl^- ions; thus, the current drops only to 50–60% of the open-state current.

When 40 μM G3139 was added to the cis side of the chamber (Fig. 3.5), VDAC channels flickered between the open and closed states at high negative voltages (more than −30 mV). Note that the negative potential draws VDAC's voltage sensor to the cis side (Sampson *et al.*, 1998); this voltage sensor may interact with G3139. No flickering was observed under positive potentials where the sensor would be driven toward the opposite, trans side. This flickering effect indicates that there is a direct interaction between G3139 and VDAC. The isosequential phosphodiester G3139, at the identical concentration, does not produce flickering of VDAC (data not shown), demonstrating the importance of the phosphorothioate backbone for the interaction.

The time scale of the flickering is 1 ms, and the amplitude of the conductance fluctuations is close to the conductance of a single VDAC channel. This amplitude is far greater than the conductance difference between the open state and the normal closed states of VDAC (Fig. 3.6). Thus, G3139 is able to induce unusually low levels of VDAC conductance and even a loss of total conductance (note the periods of very low conductance in between the periods of rapid flickering). In Fig 3.5, most channels, except for one single channel, completely lose their conductance. Some channels, in fact, fail to reopen. On the other hand, some channels merely flicker without achieving full closure. This variation may be related to the existence of different forms of VDAC [isoforms (Song *et al.*, 1998b) or splice variants (Liberatori *et al.*, 2004), or other modified versions].
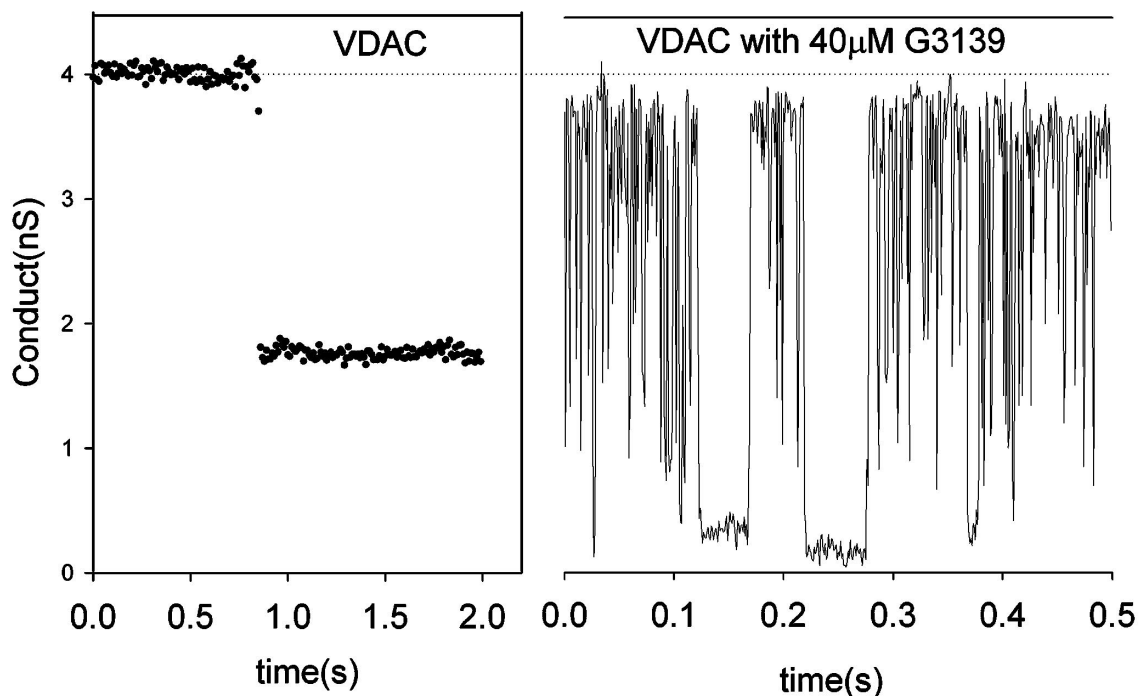
Figure 3.6. A **comparison of VDAC closure** resulting from voltage gating (*Left*) and the rapid conductance fluctuations (flickering) resulting from the addition of G3139. The applied voltage was –48 mV on the cis side, the same side to which G3139 was added.

Correlation between Levels of VDAC1 Expression and Induction of Cytochrome *c* Release by G3139

VDAC1 protein expression was determined in several melanoma and prostate cancer cell lines by Western blotting. In Fig. 3.7, the correlation between these levels, the concentrations of G3139 needed to release cytochrome *c* in mitochondria isolated from these cells, and the amount of cytochrome *c* released are correlated. Note that the PC3 and DU145 prostate cancer cell lines do not undergo apoptosis (Benimetskaya *et al.*, 2004a), except perhaps at very high G3139 concentrations. These two cell lines also have the lowest amount of mitochondrial membrane VDAC1. On the other hand, LNCaP cells,

which do undergo apoptosis in response to G3139 treatment (Leung *et al.*, 2001), have

levels of VDAC1 similar to those found in 518A2 cells.
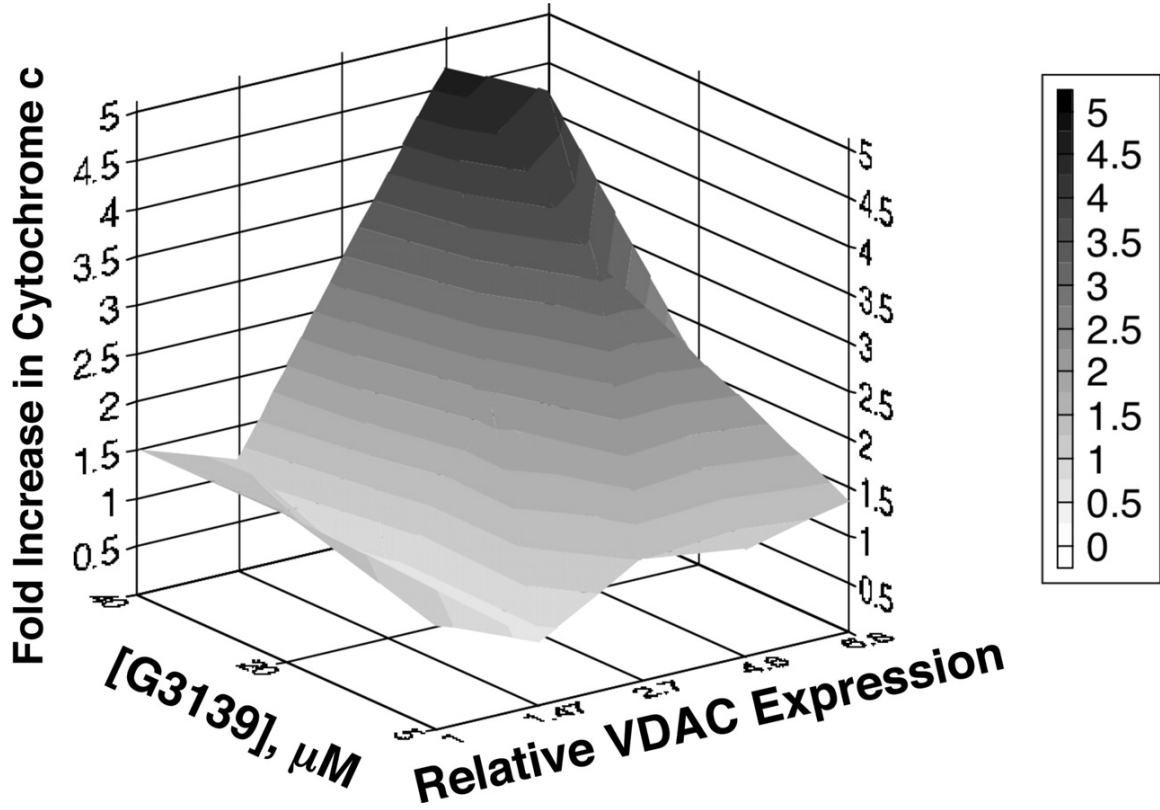
Figure 3.7. Correlation of G3139-induced cytochrome *c* release from isolated mitochondria to the relative VDAC expression from various prostate cancer and melanoma cell lines from which the mitochondria were derived (listed in Table 3.2). G3139 caused significant release of cytochrome *c* from the mitochondria derived from cell lines containing more VDAC protein expression level, in a concentration-dependent manner.

Table 3.2. Relative VDAC1 expression in human tumor cell lines

Cell line	Relative VDAC1 expression
PC3	1
DU145	1.5
LNCap	2.7
518A2	6.8
346.1	5.7
201.2	4.8

Sequence Dependence of the Potency of Phosphorothioate Oligonucleotides

To quantitatively compare the ability of different phosphorothioate oligonucleotides to close VDAC channels, multichannel membranes (>20 channels) were used to average out the channel-to-channel variation. In addition, the dose was reduced to 5 μM. Even at this concentration, G3139 still caused VDAC channels to flicker, but full channel closure was somewhat less pronounced (data not shown).

The identical pulse sequence was used as in Fig. 3.5. The conductance before channel closure was used as the measure of oligonucleotide activity. The addition of phosphorothioate oligonucleotide caused a reduction in this parameter; this corresponds to some of the VDAC channels remaining closed. The fractional drop in this parameter after it reached steady state (Fig. 3.8A) and the half-life of this decay (Fig. 3.8B) are shown for the various oligonucleotides tested. SdT18 demonstrated the strongest ability to close VDAC channels and the most rapid effect (half-life of 10 min). G3139 resulted in a 20–30% reduction in conductance, with a half-life of 15 min. 5'-truncated variants of G3139 as small as 10 mer in length had the same level of potency but also had a more
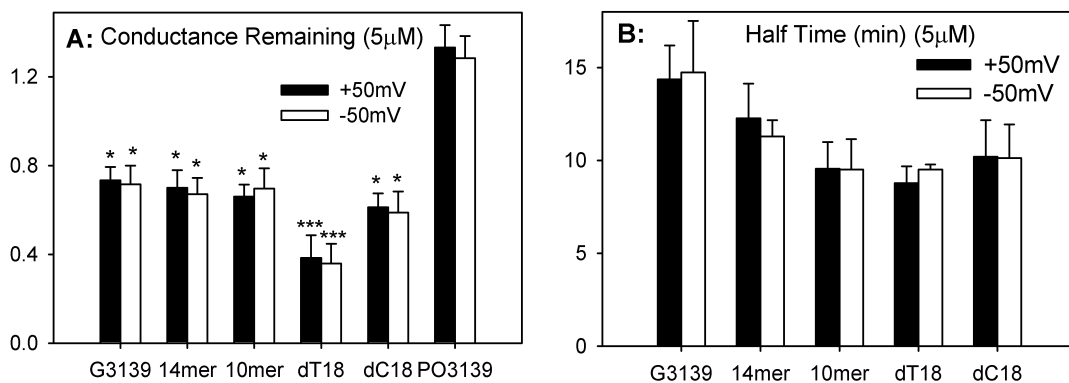
Figure 3.8. Fractional conductance remaining (**A**) and half time of the response (**B**) after treatment with 5 μM oligonucleotides. Each result is the average of 3 experiments, except dT18, which is an average of 6 experiments. The error bars are the standard deviations of independent experiments. Statistical tests indicate significance in the reduction of the conductance. $* < 0.05$; $*** < 0.005$

rapid rate of onset. PO-G3139 at the identical concentration could not close VDAC channels at all. The reproducible increase in conductance was the result of channel insertion.

Length Dependence of Phosphorothioate Oligonucleotides on the VDAC Interaction

The importance of the length of the oligonucleotide on VDAC closure was tested by using a series of phosphorothioate homopolymers of thymidine of different lengths. Once again, multichannel membranes were used. Fig. 3.9 demonstrates the changes in membrane conductance after addition of 5 µM SdT6, -10, -12, -14, -16, or -18. The three longest oligonucleotides (SdT18, -16, and -14) caused significant losses of conductance and also caused flickering of VDAC channels (data not shown). SdT12, on the other hand, had only small and variable effects on VDAC, while shorter oligomers were not active. These data obtained from isolated VDAC channels parallel the length dependence
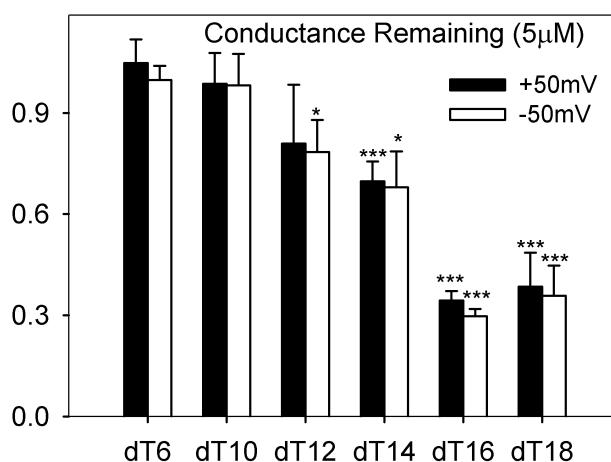
Figure 3.9. Fractional conductance remaining after treatment with 5 µM phosphorothioate homopolymers of thymidine of different lengths. Each result is the average of 6 experiments, except dT6 and dT16, which are averages of 3 experiments. The error bars are the standard deviations of independent experiments. Statistical tests indicate significance in the reduction of the conductance. *< 0.05; ***<0.005

of the release of cytochrome *c* from isolated mitochondria after treatment with G3139, as described previously. The cytochrome *c* release induced by SdT18 and SdT14 is almost equivalent to the release induced by G3139. The release induced by SdT12 is somewhat diminished, but little or no release was observed with either SdT10 or SdT8.

Conclusions

The apoptosis that we have previously observed (Lai *et al.*, 2005) in melanoma cells being treated with G3139 occurs as a result of activation of the intrinsic pathway, which can be initiated by release of cytochrome *c* from the mitochondria. This release is related to the closure of VDAC as a direct result of the binding to G3139, but it should also be recognized that VDAC is most likely not the only mitochondrial outer membrane surface protein to which this oligomer can bind with high affinity.

Among the many ways of initiating apoptosis, blocking the exchange of metabolites across the mitochondrial outer membrane may be sufficient. VDAC closure can occur as a result of growth factor withdrawal or by treatment with polyanions. Normal VDAC closure results in a selective drop in the flux of anions such as phosphocreatine, ATP^{4-}, and HPO_4^{2-}. VDAC permeability to cations can be retained, but as shown here after treatment with G3139, that too is also lost. It is possible that these disturbances in metabolic flux across the outer mitochondrial membrane may lead to the formation of a protein-conductive pathway across the outer membrane allowing cytochrome *c* and other proteins to be released from at least some mitochondria, which hence promotes the initiation of apoptosis. However, a permeability transition does not occur until relatively late in the process of apoptosis (24 h after the initiation of the transfection) compared with the early release of cytochrome *c* (9 h after the initiation of the transfection). In fact, as demonstrated by Bossy-Wetzel *et al.* (1998), the release of mitochondrial cytochrome *c* does not require mitochondrial membrane depolarization. Only a relatively small percentage of the total cytochrome *c* found in the mitochondrial intermembrane space is actually released in the early phases of apoptosis initiation, but

because of the amplifying nature of the process, cellular demolition and diminished $\Delta\psi$m is the inevitable result. The role of at least some of the Bcl-2-family proteins seems to be minimal in preventing G3139-induced apoptosis. Bcl-2 and, more convincingly, Bcl-xL have been shown to favor the open configuration of VDAC. This would thus permit small anion exchange, which would prevent disruption of normal mitochondrial physiological processes that could lead to the release of cytochrome *c*. However, silencing of either Bcl-2 or Bcl-xL by an siRNA strategy (Benimetskaya *et al.*, 2004b) produce neither spontaneous apoptosis nor increased sensitivity to a variety of cytotoxic agents. It also did not produce any alteration in the ability G3139 to induce apoptosis in melanoma cells. Furthermore, Bax has been reported to dock with VDAC1 (Shimizu *et al.*, 2000), and we also observed release of this proapoptotic protein into the supernatants of G3139-treated mitochondria, as might be expected after VDAC1 closure. This observation, however, is not inconsistent with other work (Rostovtseva *et al.*, 2004) that demonstrated that the electrophysiologic properties of VDAC channels reconstituted into planar phospholipid membranes are not affected by addition of either monomeric or oligomeric forms of Bax.

Although polyanions, in general, are known to favor VDAC closure, phosphorothioate oligodeoxynucleotides (and, we anticipate, siRNAs that contain a high percentage of phosphorothioate linkages) seem to be particularly potent, suggesting a relatively selective interaction. However, although there is a clear length dependence to the ability of a phosphorothioate oligonucleotide to induce VDAC closure [which closely parallels results observed with other, heparin-binding proteins such as basic fibroblast growth factor (Guvakova *et al.*, 1995; Rockwell *et al.*, 1997)], the sequence and phosphorothioate content dependency is not as yet fully understood. Nevertheless,

because of the wide variety of sequences, chemistries, and structures that can be investigated, the judicious application of phosphorothioate linkages in synthetic oligonucleotides may be a promising way of generating molecular and potentially therapeutic tools to control the initiation of apoptosis.

Chapter 4

Phosphorothioate Oligonucleotides Reduce Mitochondrial Outer Membrane Permeability to ADP

Running title: G3139 reduces mitochondrial outer membrane permeability to ADP

Keywords: respiration, VDAC, apoptosis, cell death

Foot Notes:

1.   Even at the low ionic strength used, mild hypotonic shocks that damage the outer membrane result in reductions in the rate of state III respiration that can be reversed by addition of cytochrome c.

Abstract

G3139, an antisense Bcl-2 phosphorothioate oligodeoxyribonucleotide, induces apoptosis in melanoma and other cancer cells. This apoptosis happens prior to and in the absence of the downregulation of Bcl-2 and thus seems to be Bcl-2-independent. Binding of G3139 to mitochondria and its ability to close VDAC have led to the hypothesis that G3139 acts, in part, by interacting with VDAC channels in the mitochondrial outer membrane. In this study, we demonstrate the G3139 is able to reduce the mitochondrial outer membrane permeability to ADP by a factor of 6-7 with a K_I between 0.2 and 0.5 µM. Since VDAC is responsible for this permeability, this result strengthens the aforesaid hypothesis. Other mitochondrial respiration components are not affected by [G3139] up to 1 µM. Higher levels begin to inhibit respiration rates, decrease light scattering and increase uncoupled respiration. These results agree with accumulating evidence that VDAC closure favors cytochrome c release. The speed of this effect (within 10 minutes) places it early in the apoptotic cascade with cytochrome c release occurring at later times. Other phosphorothioate oligonucleotides are also able to induce VDAC closure and there is some length dependence. The phosphorothioate linkages are required to induce the reduction of outer membrane permeability. At levels below 1µM, phosphorothioate oligonucleotides are the first specific tools to restrict mitochondrial outer membrane permeability.

Introduction

G3139 (oblimersen) is an antisense 18mer phosphorothioate oligonucleotide that is targeted to the initiation codon region of the Bcl-2 mRNA (Klasa *et al.*, 2002). When transfected into melanoma and other cancer cell lines, G3139 downregulates the anti-apoptotic Bcl-2 mRNA and protein expression (Lai *et al.*, 2005; Leung *et al.*, 2001; Raffo *et al.*, 2004). However, G3139 induces cytochrome c release from mitochondria more than 10 hours before the downregulation of Bcl-2 proteins (Lai *et al.*, 2005) and there is no strict sequence dependence of its pro-apoptotic effect (Lai *et al.*, 2006). The phenotype of G3139 treated prostate and melanoma cell lines is Bcl-2 independent because the siRNA targeted to the Bcl-2 mRNA does not produce apoptosis and has little or no effect on cellular viability (Anderson *et al.*, 2005). Thus G3139 must be exerting its effect in other ways.

Further research has demonstrated direct binding of G3139 to the mitochondrial surface and has correlated its potency to induce cytochrome c release with the level of VDAC (voltage-dependent anion-selective channel) expression in a cell-line dependent manner. G3139 has also been shown to inhibit the conductance of VDAC reconstituted into planar phospholipid membranes (Lai *et al.*, 2006). As VDAC has been widely recognized as a participant in cell apoptosis, these findings suggest a new pro-apoptotic role for G3139.

VDAC is the major permeability pathway by which metabolites cross the mitochondrial outer membrane (Colombini, 2004; Hodge and Colombini, 1997; Rostovtseva and Colombini, 1997). There are claims that pro-apoptotic signals stimulate VDAC (alone or together with pro-apoptotic Bcl-2 family proteins) to form a larger

channel, by which cytochrome c is released into the cytosol (Shimizu *et al.*, 1999; Shimizu *et al.*, 2000; Zalk *et al.*, 2005). These proposals are in conflict with the physico-chemical properties of VDAC and, where tested, have been found to be incorrect (Rostovtseva *et al.*, 2004; Rostovtseva *et al.*, 2005). Indeed, VDAC activity seems to be anti-apoptotic. VDAC2 inhibits the activation of the pro-apoptotic protein Bak, suppressing its ability to induce apoptosis (Cheng *et al.*, 2003). An alternative proposal consistent with this view is that VDAC closure favors mitochondria-initiated apoptosis. VDAC, in its closed states, allows small ion flow but virtually excludes large highly charged metabolic anions such as ADP and ATP (Rostovtseva and Colombini, 1996). VDAC closure results in failure to exchange metabolites between the cytosol and mitochondria. This process, in a still undefined manner, favors the permeabilization of the mitochondrial outer membrane (MOM) and the release of cytochrome c and other proteins into the cytosol. Some of these proteins become components of the apoptosome (Li *et al.*, 1997), activating caspase-9 and initiating the apoptotic cascade.

Addition of G3139 to pure VDAC channels formed in phospholipid membranes results in channel closure (Lai *et al.*, 2006). This demonstrates a direct effect of G3139 on VDAC in the absence of other proteins. Thus**,** G3139 is able to induce VDAC closure, in agreement with the hypothesis that VDAC closure favors apoptosis (Vander Heiden *et al.*, 2001).

In this paper, we report a phosphorothioate-oligonucleotide-specific strong reduction of MOM permeability to ADP by G3139. This is consistent with the inferred *in situ* reduction of VDAC permeability and supports the hypothesis that G3139 induces cytochrome c release by closing VDAC.

Materials and Methods

Measurement of MOM permeability and intactness

Mitochondria were isolated from rat liver (Parsons *et al.*, 1966). A portion of the mitochondrial suspension (about 1 mg mitochondrial protein) was diluted into 3 ml of respiration buffer containing 0.3 M mannitol, 10 mM NaH_2PO_4, 5 mM $MgCl_2$ and 10 mM KCl (pH 7.2). The mitochondrial respiration was measured according to the method of Lee *et al.* (1994). The respiratory control ratio was typically above 5 (for succinate). Briefly, succinate (5 mM final) was added to the mitochondrial suspension followed by ADP addition (usually 80 µM). The oxygen consumption was measured by using a Clark oxygen electrode and the MOM permeability was obtained by fitting to the theoretical model developed by Lee *et al.* (1994). Since mitochondria respire at a slow rate (state IV respiration rate) even without ADP addition, the state IV respiration was subtracted from state III respiration to obtain the ADP stimulated oxygen consumption. This result was converted to [ADP] as a function of time by multiplying the [oxygen] by the P/O ratio (2 for succinate as the substrate). The derivative of the [ADP] versus time is the rate of ADP consumption at any time. Each of the experiments in Figs 4.1, 4.4B, 4.6A, 4.7B has been repeated three times using the same mitochondria. It has also been repeated at least three times using mitochondria isolated on different days.

The intactness of the MOM was calculated (Douce *et al.*, 1987) from the KCN-sensitive rate of oxygen consumption following addition of 2.5 µM cytochrome c and 8 mM sodium ascorbate. This rate was compared to that of hypotonically disrupted mitochondria. Hypotonically disrupted mitochondria were prepared by adding 30 µl

mitochondria into 1.5 ml of double distilled water (on ice) and incubating for 3 minutes, followed by addition of 1.5 ml double concentrated respiration medium.

To measure the respiration of mitoplasts, mildly shocked mitochondria were employed (Lee *et al.*, 1998). These were generated by the addition to the mitochondrial suspension, 2 volumes of cold double distilled water. The shocked mitochondria were incubated for 10 minutes on ice followed by the addition of 5 volumes of respiration buffer. Finally, 2 volumes of double concentrated respiration buffer were added to restore normal osmotic pressure. These steps were used to minimize damage to the inner membrane.

Measurement of MOM Intactness by Adenylate Kinase Release Assay

Mildly shocked mitochondria containing 1 mg protein were pelleted at 14,000 g for 5 minutes at 4°C and the supernatant was kept on ice until assayed. 30 μl of supernatant was added to 700 μl of adenylate kinase reaction mixture (50 mM Tris-HCl, pH 7.5, 5mM $MgSO_4$, 10 mM glucose, 5 mM ADP, 0.2 mM NADP, 10 units of hexokinase, and 10 units of glucose-6-phosphate dehydrogenase) (Sottocasa *et al.*, 1967). The activity of adenylate kinase was detected as an increase in absorbance at 340 nm. Intact mitochondria and mitochondria with lysed outer membranes served as negative and positive controls. The mitochondria with lysed outer membranes were hypotonically shocked by adding 50 volumes of cold double distilled water to the mitochondria.

The assay of protein content

Mitochondrial protein was measured using the BCA method (Pierce, Rockford, IL) following addition of Triton X-100 to the mitochondrial suspension (1% v/v final). Bovine serum albumin was the standard.

Oligonucleotides

G3139 was kindly donated by Dr. R. Brown, Genta Inc (Berkeley Heights, NJ). The N-mers, the oligonucleotides of random sequence, were a generous gift of Trilink Biotechnologies (San Diego, CA).

Planar phospholipid membrane studies

The planar phospholipid membranes were generated according to standard methods (Colombini, 1987a; Montal and Mueller, 1972). The membranes were formed from phospholipid monolayers consisting of diphytanoyl phosphatidylcholine, asolectin (soybean phospholipid polar extract) and cholesterol (1:1:0.1 mass ratios).

VDAC was purified from mitochondria isolated from rat liver (Blachly-Dyson *et al.*, 1990; Freitag *et al.*, 1983). A 1-3 μL aliquot of the VDAC-containing solution (2.5% Triton X100, 50 mM KCl, 10 mM Tris, 1 mM EDTA, 15% DMSO, pH 7.0) was stirred into 4-6 mL of aqueous solution containing 1.0 M KCl, 5 mM $CaCl_2$, 1 mM EDTA, and 5 mM HEPES (pH 7.2) on the cis-side of the chamber. The trans-side, containing the same aqueous solution, was held at virtual ground by the voltage clamp. All experiments were performed at approximately $23^{o}C$.

Cell culture

The mycoplasma-free human melanoma cell line 518A2 was a kind gift of Dr. Volker Wacheck (University of Vienna, Austria). Cells were grown in DMEM supplemented with 10% heat inactivated fetal bovine serum and 100 U/ml penicillin G (sodium salt) and 100 μg/ml streptomycin sulfate. Stock cultures of all cells were maintained at 37°C in a humidified 5% CO_2 incubator.

Subcellular Fractionation and Oligonucleotide Treatment of Mitochondria from melanoma cells

Cells were harvested by trypsinization and were washed with cold PBS. Cell pellets were re-suspended in 300 μL of buffer A (250 mM sucrose, 10 mM Tris-HCl, pH 7.4, 1 mM EGTA, 50 μg/mL Pefabloc and 15 μg/mL leupeptin, aprotinin and pepstatin). Cells were then homogenized on ice in a dounce homogenizer until ~90% of cells were disrupted, as judged by Trypan blue staining. Crude lysates were centrifuged at 1000 g for 10 min at 4°C twice to remove nuclei and unbroken cells. The supernatant was collected and subjected to a 10,000 g centrifugation for 30 min at 4°C. The pelleted mitochondria were resuspended in 20 μL of energizing buffer B (250 mM sucrose, 10 mM Tris-HCl, pH 7.4, 1 mM EGTA, 50 μg/mL Pefabloc, 10 mM KCl, 3 mM KH_2PO_4, 5 mM succinate, 100 μM ADP and 15 μg/mL leupeptin, aprotinin and pepstatin), which contained increasing concentrations of oligonucleotides (10 μM to 40 μM). After 2 hours of incubation at 10°C water bath, samples were centrifuged to pellet the mitochondria and the supernatant was colleted and subjected to Western blotting for Cytochrome c release.

Western Blot Analysis

Aliquots of protein samples, containing 25-40 μg of protein, were resolved by SDS-PAGE, and then transferred to Hybond ECL filter paper (Amersham, Arlington Heights, IL). The filters were incubated at room temperature for 1-2 h in 5% milk in TBS containing 0.5% Tween-20. The filters were then probed with 1:200 dilutions of the anti cytochrome c antibody (Santa Cruz Biotechnology, Santa Cruz, CA) in 5% milk in TBS containing 0.5% Tween-20 at 4°C overnight. After washing in TBS containing 0.5% Tween-20, the filters were incubated for 1 h at room temperature in 5% milk in TBS containing 0.5% Tween with a 1:3,000 dilution of a peroxidase-conjugated secondary antibody (Amersham). After washing (3 x 10 min), ECL was performed according to the manufacturer's instructions.

Results

G3139 reduces the MOM permeability to ADP by interacting with VDAC

Mitochondrial respiration is coupled to ADP phosphorylation through the protonmotive force (PMF). The stimulation of respiration by ADP phosphorylation requires a continuous flow of ADP from the cytosol into the mitochondrial matrix, involving the permeation through the MOM and translocation across the mitochondrial inner membrane (MIM) through the adenine nucleotide translocator (ANT). The phosphorylation of ADP is fast and the two permeation processes are rate limiting. At high extramitochondrial ADP concentrations, the translocation through the MIM is saturated and the mitochondria undergo state III respiration, which is characterized by a constant rate of oxygen consumption. However, as the ADP level declines, the flux through the MOM becomes rate limiting and thus mitochondria consume ADP and oxygen more slowly. When ADP is totally depleted, mitochondria undergo state IV respiration. Thus, the transition between state III and state IV respiration provides information about the MOM permeability to ADP. (Please note that the permeability to ATP should also be reduced but this was not measured.) The broader the transition between the states, the lower is the permeability of the outer membrane (Lee *et al.*, 1994). Following the method of Lee *et al.* (1994), the permeability of the MOM to ADP was calculated from this transition.
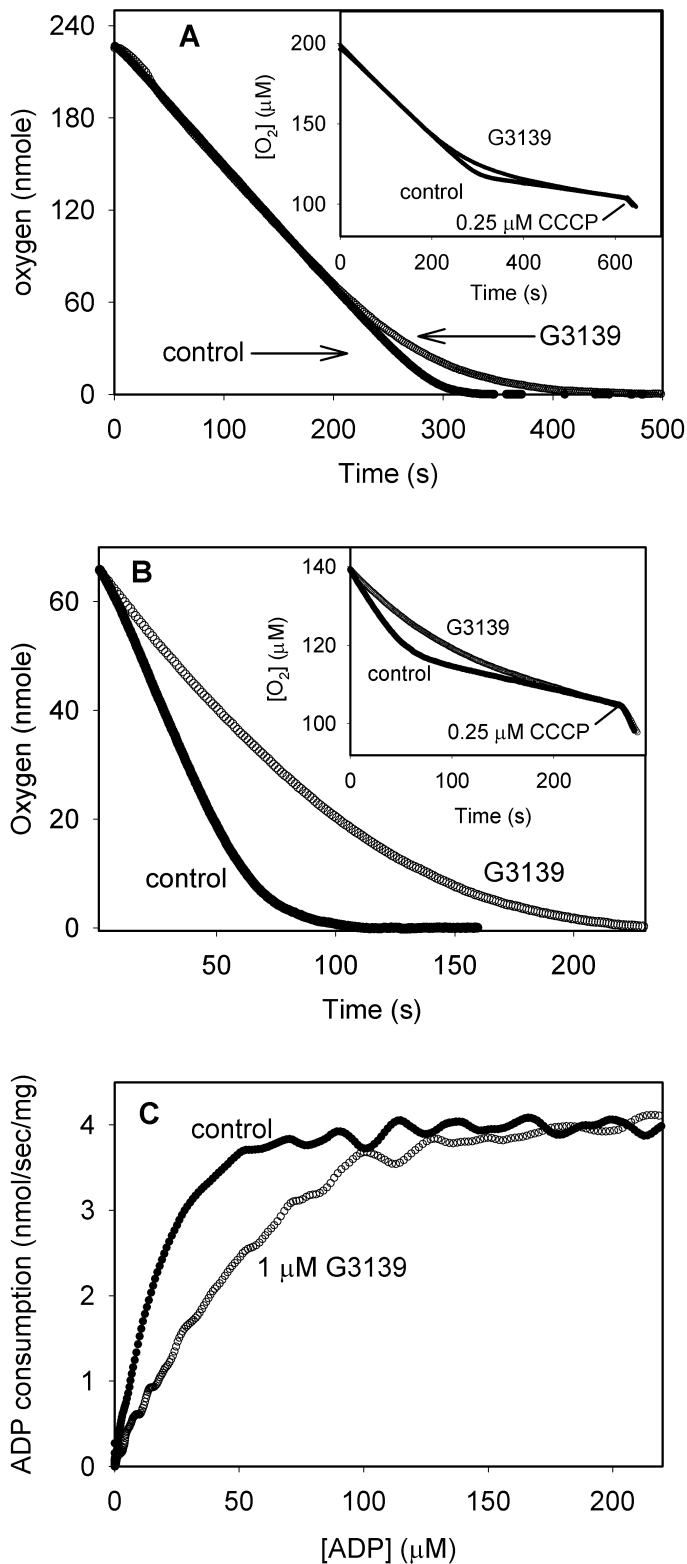
Figure 4.1. An example of G3139-induced reduction of mitochondrial respiration between state III and state IV. (**A**) O_2 consumption following addition of 270 μM ADP to mitochondria in the presence or absence of 1 μM G3139 (inset). The rate of State IV respiration was subtracted from the respiration curve (main figure). (**B**) O_2 consumption following addition of 80 μM ADP to the mitochondria in the presence or absence of 1 μM G3139 (inset). The rate of State IV respiration was subtracted from the respiration curve (main figure). The mitochondrial protein concentration was 320 μg/ml in both panels (a) and (b).

(**C**) ADP consumption rate vs. [ADP]. The ADP consumption rate was calculated from the oxygen consumption rate and the P/O ratio (2 for succinate as the substrate) and divided by the amount of mitochondrial protein present (1mg). The O_2 consumption rate, at each point in figure 1a, was determined by calculating the slope at each point using the linear regression of 13 adjacent points.

As shown in Fig. 4.1A and Fig. 4.1B, when 1 µM G3139 was added to isolated mitochondria, it reduced the rate of respiration in the transition between State III and State IV. The calculated rates of ADP consumption are shown in Fig. 4.1C. In the presence of G3139, the rate of ADP consumption saturates at more than 100 µM external ADP. Without G3139 the rate of ADP consumption essentially saturates at about 50 µM external ADP. At the lower ADP levels, which are more physiological, 1 µM G3139 reduced the rate of State III respiration by as much as 50% (Fig. 4.1C). The presence of adenylate kinase inhibitor, P1,P5-di(adenosine-5')pentaphosphate, does not change G3139 inhibition of mitochondrial respiration, showing that adenylate kinase is not involved (data not shown).

As VDAC is the major pathway for metabolite flux across the MOM (Colombini, 1979; Colombini, 2004; Rostovtseva and Colombini, 1997), the reduced permeability should be due to VDAC closure. This was also observed in planar membrane experiments, which assess the direct interaction between G3139 and VDAC. 40 µM of G3139 was able to fully close a VDAC channel reconstituted into a planar membrane (Fig. 4.2). Channels closed in this way remain closed irrespective of the applied voltage. This effect can be reversed by removing G3139 from the system (Fig. 4.2), demonstrating a reversible interaction. The reversibility was also observed in mitochondrial respiration experiments (Data not shown). The direct effect of G3139 on VDAC indicates that VDAC closure is responsible for the lowered respiration rate observed at low ADP levels. Closure of some of the VDAC channels slows down the permeation of ADP and decreases the intermembrane space and matrix ADP levels.

Figure 4.2. A single VDAC channel was reconstituted into a planar phospholipid membrane as described in the Methods. The voltage was held at either +50 mV or –50 mV and alternated every 50 seconds. The long horizontal line indicates zero current. G3139 (40 μM final) was added where indicated. Before the perfusion, there were 7 minutes of record (deleted to save space) where the channel was fully closed. The side of addition of G3139 was perfused with 30 ml (6 times of chamber volume) of buffer for 5 minutes.
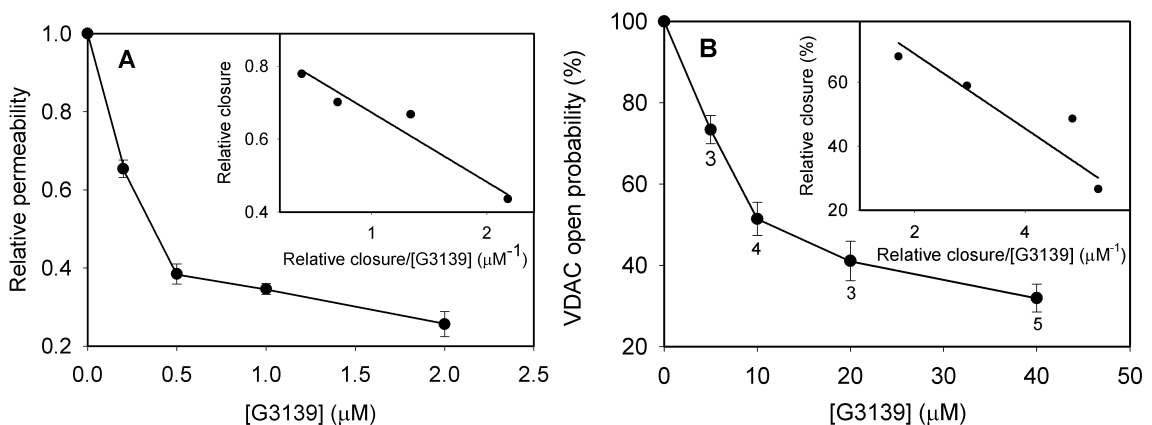
Figure 4.3. (A) The concentration dependence of G3139 induced MOM permeability reduction. This is the average of the results obtained in three independent experiments. Mitochondria were added to 3 ml of respiration buffer with final protein concentration of 370 μg/ml. The results were normalized to the permeability in the absence of G3139. The error bars are the standard deviations of the three independent experiments. **(B) The concentration dependence of G3139 induced VDAC closure.** Each point is the average of at least three separate experiments. The indicated amount of G3139 was added to the cis-side of the chamber. The voltage was held at either +50 mV or –50 mV and alternated every 50 seconds. Relative closure is the fractional decrease in permeability or conductance. The error bars are the standard errors of the indicated number of independent experiments.

Concentration dependence of the potency of G3139

G3139 reduces MOM permeability in a concentration dependent manner (Fig. 4.3A). At a concentration of 1 μM, G3139 is able to reduce the permeability by 70%. This concentration of G3139 is similar to the estimated cellular level required to induce cytochrome c release from mitochondria (Lai *et al.*, 2006). The concentration dependence data can be further analyzed to obtain the concentration at half inhibition K_I, and the maximum permeability reduction P_{max}.

Assuming a 1 to 1 stoichiometry between G3139 (G) and a single permeability unit (V), which forms a closed permeability unit (GV) with the equilibrium constant K, the ratio of active open and closed permeability units is $P_{closed}/(P_{max}-P_{closed})=K[G]$, where P_{closed} is the permeability reduction (i.e. P_{max} minus the remaining permeability). This equation can be rearranged to yield

$P_{closed}=-1/K * (P_{closed}/[G]) + P_{max}$

A linear plot of P_{closed} vs. $P_{closed}/[G]$ was generated to determine K and P_{max} (Figs 4.3A, B). K_I is equal to 1/K. The inset of Fig. 4.3A shows the linearized results that yield a K_I of 0.18μM and maximum permeability reduction of 85%.

G3139 also closes VDAC channels in a concentration dependent manner (Fig. 4.3B). However, a higher concentration is needed for G3139 to induce the same extent of closure as observed in the mitochondrial experiments. The K_I of 9.6μM is about 50 times greater but the maximum conductance drop of 86% is indistinguishable in the two types of experiments (Fig. 4.3B inset). The difference in sensitivity could be due to endogenous mitochondrial factors that influence the closure of VDAC, factors eliminated by VDAC purification and reconstitution into phospholipids membranes. One example

of such a factor is the presence of modulating proteins in the mitochondrial intermembrane space that induce the VDAC closure by favoring the closed states (Colombini, 2004). Despite the quantitative difference, both results are strikingly similar, thus providing evidence that G3139 is actually closing VDAC in the MOM.

G3139 induced mitochondrial respiration reduction is not due to release of cytochrome c

G3139 causes the release of cytochrome c from mitochondria but this release takes time and is evident after 2 hours (Lai *et al.*, 2006). The permeability changes reported here are early and immediate effects. However, we observed that elevated levels of G3139 induced small decreases in light scattering at 600nm, consistent with some mitochondrial swelling (Fig. 4.4A). Large scale mitochondrial swelling is usually due to
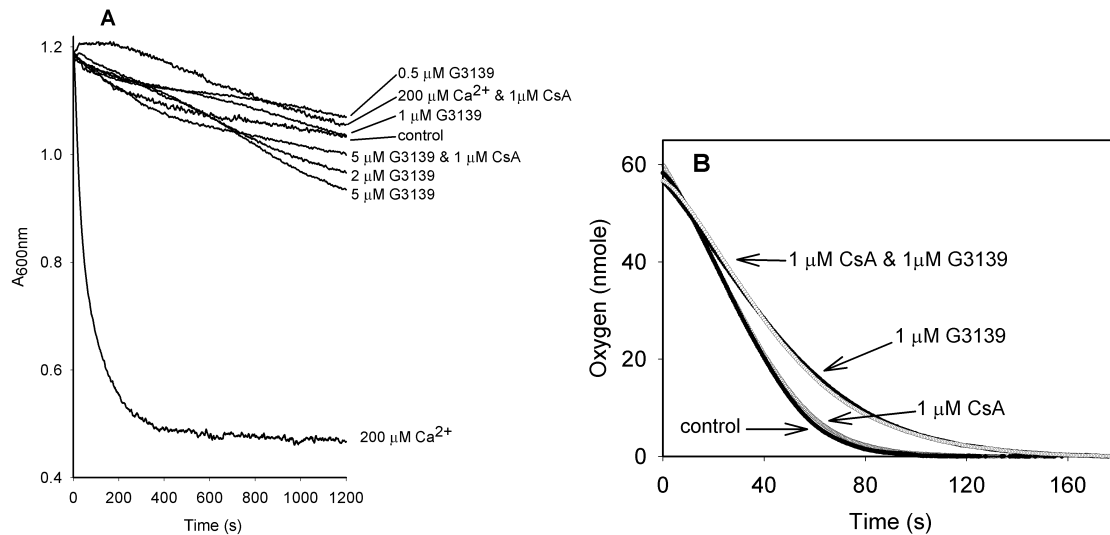
Figure 4.4. (A) Mitochondrial swelling in the absence or presence G3139 and/or cyclosporin A. It was measured as light scattering at 600 nm. Mitochondria were added into the respiration buffer containing 5 mM succinate and 80 μM ADP. The final mitochondrial protein concentration was 320 μg/ml. **(B) Cyclosporin A does not influence the ability of G3139 to reduce MOM permeability to ADP.** Mitochondrial O_2 consumption was recorded following addition of 80 μM ADP. The mitochondrial protein concentration was 350 μg/ml. The rate of State IV respiration was subtracted from the entire respiration curve.

the formation of a permeability transition and this could lead to outer membrane tearing and cytochrome c release[1]. Loss of cytochrome c impairs electron transport and therefore respiration. However, at concentrations between 0.5 and 1 μM, G3139 does not induce significant swelling (n=3, 95% confidence). Even at concentrations of 2 μM or 5 μM, G3139 the apparent swelling is very small compared to swelling induced by calcium ions, associated with the permeability transition. This slight change in light scattering is unlikely to reflect a matrix swelling that would tear the outer membrane and release cytochrome c (Fig. 4.4A).

Cyclosporin A is known to prevent outer membrane damage and cytochrome c release caused by swelling and permeability transition. We find that it partially inhibits G3139-induced mitochondrial swelling (Fig. 4.4A). However, treatment with cyclosporin A doesn't change the G3139-induced reduction of outer membrane permeability to ADP. (Fig. 4.4B, Table 4.1). To confirm that, 2.5 μM cytochrome c was added to the mitochondrial suspension. If the MOM of some of the mitochondria in the

Table 4.1 Cyclosporin A and cytochrome c do not alter the calculated values of the reduction in MOM permeability to ADP induced by G3139. The permeability values given here are the permeability per gram mitochondrial protein (at 400 μg/ml). The values are average ± standard deviation of three to four experiments. All results of the experiments containing 1 μM G3139 are significantly different from control (99.9% confidence)

	Permeability (cm^3/s/g prot.)	% inhibition
No G3139	242 ± 17	
1 μM G3139	116 ± 6	52
1 μM cyclosporin A	210 ± 20[1]	13
1 μM cyclosporin A & 1 μM G3139	120 ± 16[2]	50
2.5 μM cytochrome c & 1 μM G3139	126 ± 5[2]	48
1 μM cyclosporin A & 1 μM G3139 & 2.5 μM cytochrome c	115 ± 2[2]	52

[1] no significant difference from control (95% confidence)
[2] no significant difference from the result obtained with only 1 μM G3139 (95% confidence)

population had become permeable to cytochrome c, respiration of these mitochondria would have been suppressed due to a functional break in the electron transport chain. (We observe this after mild hypotonic shock of the mitochondria.) Restoring the cytochrome c would restore this respiration at least in part. However, addition of cytochrome c did not significantly change the measured respiration rate, the calculated permeability value or the G3139-induced permeability change (Table 4.1). The measured degree of mitochondrial intactness (96% ± 1% (n=3)) shows no significant change (1% ± 1% (n=3)) after treatment with 5 μM of G3139 (95% ± 1% (n=3)) for 30 minutes, which is the time range of each experiment. This is consistent with the published finding that cytochrome c release takes time and is evident after 2 hours of treatment with G3139 (Lai et *al.*, 2006).

The effects of G3139 on the inner membrane cannot explain the permeability change

Despite the fact that G3139 did not damage the MOM nor release cytochrome c during short term incubations, it might still permeate through VDAC and affect the components of the electron transport chain located in the mitochondrial inner membrane. In this way it could reduce the enzymatic activities of the electron transport complexes and thus inhibit respiration. It could also inhibit the ANT on the MIM, thus reducing the rate of ADP/ATP translocation through the inner membrane and lower the matrix ADP concentration, inhibiting respiration.

The effects of G3139 on the vital respiratory functions of the inner membrane were tested by measuring state III, state IV and uncoupled respiration rates as a function of [G3139] (Fig. 4.5). Please note that true state III is only achieved, in the presence of

G3139, at high levels of added ADP. We rationalize that the high levels overcome the reduced outer membrane permeability allowing maximal ADP-dependent stimulation of respiration. Thus at 80 μM ADP there is an apparent reduction in ADP-dependent respiration that probably arises from the reduced permeability of the outer membrane. Even at the high ADP levels used (as in Fig. 4.1A) G3139 reduces state III and increases state IV resulting in a reduced respiration control ratio. However, at 0.5 μM and 1 μM these effects are not significant. The increase in state IV at higher concentrations is consistent with some uncoupling. The decrease of state III respiration rate was mainly caused by inhibition of the electron transport chain, confirmed by the CCCP uncoupled mitochondrial respiration rate (Fig. 4.5B). CCCP eliminates the protomotive force and should result in maximal rates of respiration. At 5 μM G3139 there was a significant drop
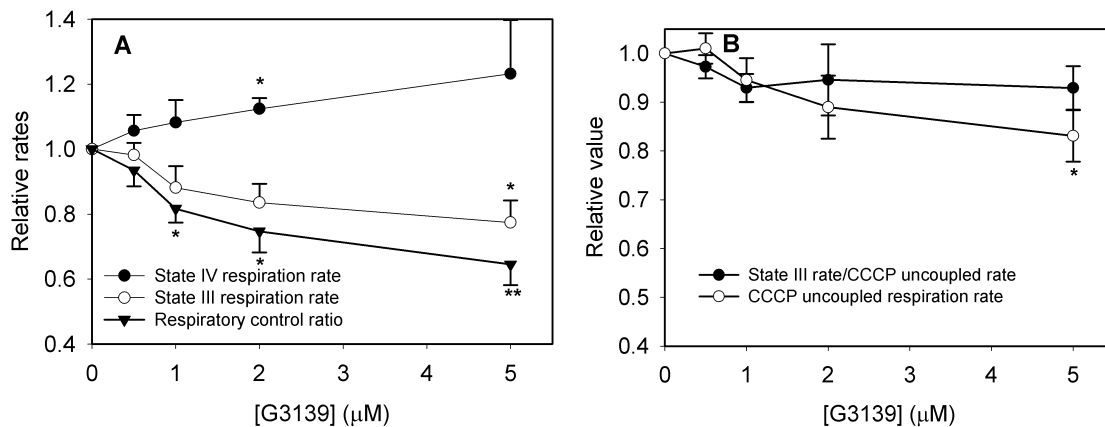
Figure 4.5. The effects of G3139 on mitochondrial state III respiration, state IV respiration, respiratory control ratio, and CCCP uncoupled respiration. The values were normalized to the value in the absence of G3139 (RCR: 6.0 ± 0.7, state III respiration rate: 1.2 ± 0.1 nmole O_2/second/mg mitochondrial protein, state IV respiration rate: 0.21 ± 0.03 nmole O_2/second/mg mitochondrial protein, CCCP uncoupled respiration rate: 1.5 ± 0.2 nmole O_2/second/mg mitochondrial protein). The values were given as the mean ± standard error of four independent experiments with each experiment performed in triplicates. 270 μM ADP was added in those experiments to reach the maximum State III respiration. Statistical tests indicate the significance of the difference compared to control experiments. (* < 0.05, ** < 0.01).

in the rate of respiration in the presence of CCCP. However, even at a concentration of 5 μM, G3139 only influenced state III/state IV respiration by 20% compared to more than 80% reduction in MOM permeability (Fig. 4.5). Thus, effects observed at higher concentrations of G3139 cannot account for the permeability change (Fig. 4.5). Moreover, the ratio of state III to uncoupled rate does not change with increased amounts of G3139, indicating that ANT can fully function at least at high ADP concentrations (Fig. 4.5B).

In isolated mitochondria one can add high levels of ADP to achieve maximal respiration rates but, physiologically, ADP levels are much lower and thus G3139 would reduce ADP-dependent respiration.   For example, when 80 μM ADP was added to mitochondria pretreated with 1 μM G3139, the initial respiration rate was 48% ± 8% of the uncoupled rate, which is significantly less than the ratio of the control (76% ± 4%) experiments (mean ± S.E., 4 independent observations; P<0.05). This reinforces the conclusion that at physiological ADP levels, G3139 can directly inhibit mitochondrial respiration.

Further evidence that G3139 acts by reducing outer membrane permeability, was obtained from mildly shocked mitochondria. The mitochondrial outer membrane was damaged in order to bypass any permeability barrier of this membrane. Both mild hypotonic shock and carefully titrated amounts of digitonin were used for initial trials. Of these the hypotonic shock did the least damage, as assessed by measuring ADP-dependent respiration. There was an unavoidable reduction in respiration following hypotonic shock and a trade-off was achieved between MOM breakage and respiration reduction. The effects of G3139 are clear despite this limitation. The state III/state IV

respiration with and without G3139 is nearly the same, especially as compared with the

huge difference observed with the intact mitochondria (Fig. 4.6A). Even more persuasive,

in the presence of 1 μM G3139, disruption of the outer membrane restored state III

respiration to a level close to the rate observed without G3139, indicating that the major

factor inhibiting respiration is the limitation of the rate of ADP transport through the

outer membrane (Fig. 4.6A). However, it is clear that mildly shocking only partially
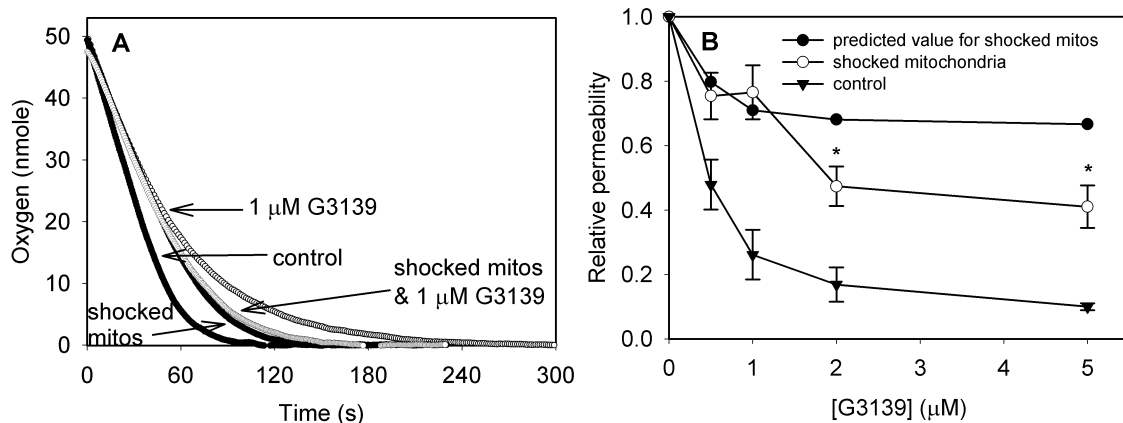
Figure 4.6. Low concentrations of G3139 have a minimal effect on mitochondrial respiration after the outer membrane has been broken. (a) Mitochondrial O$_2$ consumption was recorded as described in Fig. 4b. Mildly shocked mitochondria were obtained by exposing them to a 100 mOsmolar solution for 10 minutes on ice. The normal osmotic pressure was restored as described in Methods**. (b) Comparison of mitochondrial outer membrane permeability changes induced in mildly shocked and normal mitochondria by G3139.** All values were measured after 10 minutes of treatment with G3139. The error bars are the standard errors of four independent experiments. The adenylate kinase activity assay showed that after a mild shock, 37% ± 1% (n=4) mitochondria were still intact. This result was used to generate the predicted change in permeability of mildly shocked mitochondria after G3139 treatment. Statistical tests indicate the significance of the difference between predicted values and measured values (* < 0.05)

restores the permeability value (Fig. 4.6B). Is this a sign that G3139 affects ANT? To

address this quantitatively, one must compensate for the mitochondria that remained

intact following the hypotonic shock. The adenylate kinase activity assay showed that

37% ± 1% (n=4) of mitochondria were still intact after a mild shock. These remaining

intact mitochondria should still respond to G3139 and thus there should still be a small

reduction in MOM permeability upon addition of G3139. Assuming the remaining intact

mitochondria were still inhibited by G3139, we calculated predicted values of changes in

relative permeability upon addition of G3139 (Fig. 4.6B). It is clear that at 0.5 and 1 μM

concentrations, the restoration of permeability following hypotonic shock was complete

(compare experimental values to predicted values). However, at 2 and 5 μM, G3139 had

a greater inhibitory effect than can be accounted for by incomplete MOM damage and

therefore, at these higher levels, G3139 does have effects on inner-membrane processes.

These results demonstrate that G3139 doesn't significantly alter the activity of

ANT or the complexes of the respiratory chain at sub micromolar concentrations. Even at

higher concentrations, the effect of G3139 on the inner membrane cannot explain the

reduction of permeability. Thus, the conclusion we draw is that G3139 can interact with

VDAC channels in the MOM and reduce their ability to translocate ADP.
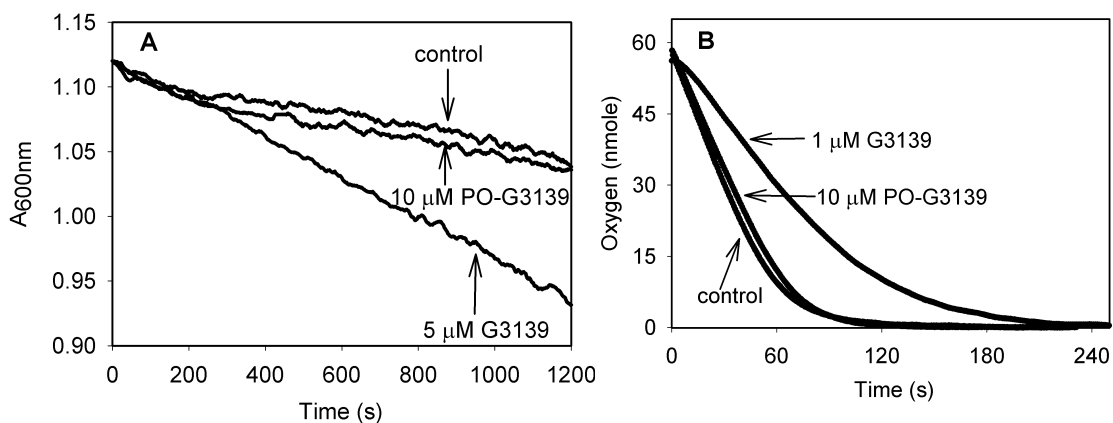
Figure 4.7. The phosphodiester version of G3139 does not induce mitochondrial swelling nor does it reduce the permeability of the MOM. Mitochondrial swelling and O_2 consumption were performed as in Fig. 4.4a and b resp. The mitochondrial protein concentration was 320 μg/ml. This is typical of three independent experiments.

Important features of the oligonucleotide

The isosequential phosphodiester analog of G3139 does not induce mitochondrial swelling and it does not inhibit the respiration of mitochondria (Fig. 4.7). This agrees with our previous findings that this single stranded oligodeoxyribonucleotide does not interact with VDAC and does not induce cytochrome c release from mitochondria (Lai *et al.*, 2006). In fact, there is a small increase of the MOM permeability, which is understandable considering that this highly charged molecule can decrease the voltage difference across the VDAC channels in the MOM (Colombini, 2004) and thus could favor the open state.

To evaluate the importance of the G3139 sequence in its interaction with VDAC, phosphorothioate oligonucleotides with a completely randomized sequence were used. These so-called N-mers (n=12, 14, 16, 18), which contain an equal mixture of each nitrogenous base at each position in the oligonucleotide chain, were added to isolated mitochondria and the MOM permeability was measured. All tested N-mers inhibited this permeability to some extent (Table 4.2). This is consistent with their abilities to induce

Table 4.2 Permeability of mitochondria to ADP in the presence or absence of 0.5 μM **G3139 or N-mers (N=12, 14, 16, 18).** Each result is the average ± standard deviation of 3 experiments. Statistical tests indicate significance in the reduction of permeability (* < 0.01, ** < 0.005). All the results of oligomers except 12mers are not significantly different from that of G3139.

	Permeability (cm^3/s/g prot.)	% Inhibition
Control	244 ± 23	
G3139	$135 \pm 16^{**}$	45
12mers	$168 \pm 13^{*}$	31
14mers	$135 \pm 7^{**}$	45
16mers	$132 \pm 7^{**}$	46
18mers	$116 \pm 20^{**}$	52

cytochrome c release from isolated mitochondria of melanoma cell lines 518A2 (Fig. 4.8). G3139 and N-mers except 10-mers all induce significant release of cytochrome c from isolated mitochondria after 2 hours treatment in a concentration-dependent manner (Fig. 4.8), as demonstrated by Western blotting. Those results indicate that the specific G3139 sequence is not critical for the interaction with VDAC and induction of cytochrome c release from isolated mitochondria. In addition, the interaction is probably not limited to just a small number of sequences because the concentration of any one specific sequence in an N-mer is less than femtomolar. However, as the length increases, the ability of the N-mer to reduce the MOM permeability and induce cytochrome c release also increases (Table 4.2, Fig. 4.8). These data indicate that longer oligonucleotides in the range we tested have a stronger interaction with VDAC channels on the MOM and subsequently a greater ability to induce cytochrome c release from isolated mitochondria. This is also consistent with the length-dependence reported for closure of pure VDAC reconstituted into phospholipid membranes (Lai *et al.*, 2006).
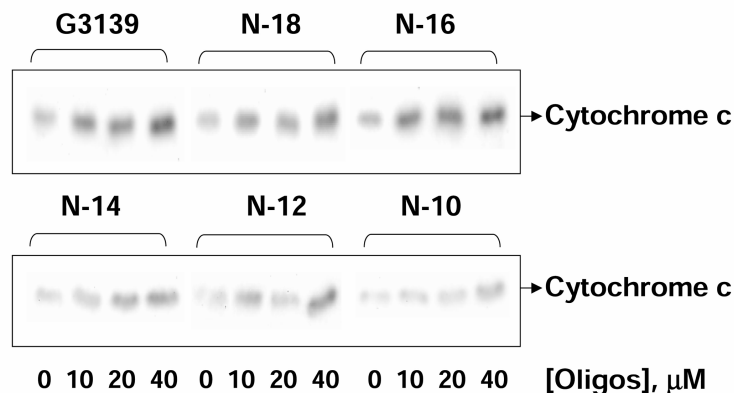
Figure 4.8. G3139 and equivalent random sequences release cytochrome c from mitochondria in a concentration-dependent manner. Isolated mitochondria from 518A2 melanoma cells were treated with 10-40 μM of indicated oligonucleotides for 2 hrs at 10°C in Buffer B and the supernatants were collected. Cytochrome c released into the supernatant from the mitochondria was analyzed by Western blotting.

Discussion

G3139 targets the initiation codon region of the Bcl-2 mRNA. Initially, it was believed that its ability to induce apoptosis in cancer cells relied on the downregulation of Bcl-2 protein, at least in vitro. However, recent work casts doubt on this hypothesis and implicates VDAC as a major target of G3139 (Lai *et al.*, 2006). In this study, we provide direct evidence that G3139 reduces the MOM permeability, building a bridge between G3139 binding to mitochondria and the subsequent release of cytochrome c.

The fact that VDAC is the major pathway for metabolites indicates that G3139 reduces the permeability of the MOM by closing VDAC. This is supported by the fact that phosphorothioate oligodeoxynucleotides induce closure of VDAC reconstituted into planar phospholipid membranes.

The major effect of G3139 is on the MOM

We have demonstrated this in a variety of ways: 1) The G3139 induced reduction of permeability to ADP is not inhibited by cyclosporin A (Fig. 4.4B), indicating that it is not due to a permeability transition. 2) At concentrations less than or equal to 1 μM, the effect of G3139 on the MIM is insignificant (Figs 4.5, 4.6B), and even at higher concentrations, the effect on MIM cannot fully explain the permeability reduction. (Figs 4.5, 4.6B). 3) Damaging the MOM actually restores state III respiration that was inhibited by 0.5 and 1 μM G3139, indicating that the inhibition is on the outer membrane, not on ANT (Fig. 4.6A). 4) The constant ratio of state III to CCCP uncoupled respiration rate confirms that ANT was not inhibited by G3139 (Fig. 4.5B).

Additionally, the mitochondrial permeability reductions induced by G3139 were essentially the same when 5 mM malate and glutamate were used as the substrate (Fig. 4.9), showing that pyridine nucleotides were not depleted from the matrix during G3139 treatment.
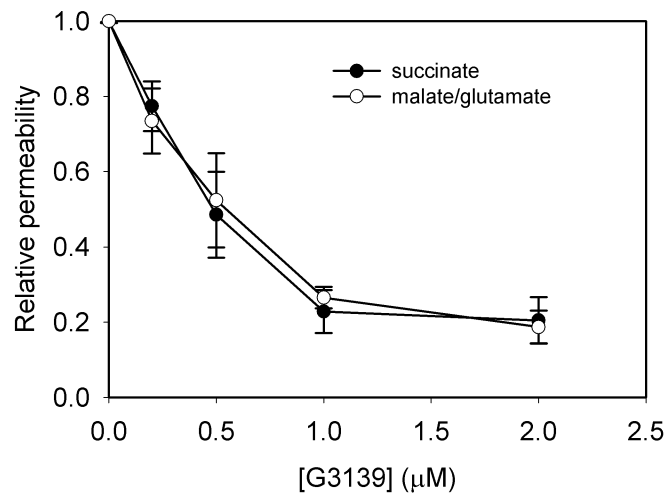
Figure 4.9. Comparison of the concentration dependence of the reduction in MOM permeability induced by G3139 in the presence of 5 mM of either succinate or malate/glutamate as the substrate. The mitochondrial protein concentration was 320 µg/ml. The results shown here were from one experiment performed in triplicates. This is typical of three independent experiments.

Thus, the main effect is that G3139 is able to reduce MOM permeability to ADP by closing VDAC channels in the outer membrane. From the Fig. 4.2, closure of VDAC by G3139 results in a total loss of conductance and thus both ATP and ADP are not permeable through the channels. Thus the remaining permeability of the outer membrane is through VDAC channels that have not been closed by G3139. What we report is an average drop of the mitochondrial outer membrane permeability to ADP. This drop slows down both the steady state ADP influx and ATP efflux, resulting in an inhibition of respiration at physiological ADP level (Fig. 4.1B).

The mechanism and specificity of the oligonucleotide-induced permeability decrease

Our study has shown that the length of the oligonucleotide plays a role in its ability to affect the MOM permeability and cytochrome c release from mitochondria, while the sequence may be less important (Table 4.2). The presence of phosphorothioate linkages in the oligomer is very important for its ability to reduce the MOM permeability (Fig. 4.7) and subsequently induce cytochrome c release and cell apoptosis (Lai *et al.*, 2006).

The importance of the phosphorothioate linkage has also been observed in other oligonucleotide-protein interactions. The binding of a phosphorothioate oligodeoxyribonucleotide to albumin increased with the number of phosphorothioate linkages (Ghosh *et al.*, 1993). The binding of dA_{36} to the g5p protein increases more than 300 fold after substitution of sulfur for oxygen in an oligonucleotide (Mou *et al.*, 2001).

The differences between sulfur and oxygen atoms may provide insight into the requirement for the phosphorothioate linkage. Compared to oxygen, the sulfur atom has less electronegativity and its larger van der Waal's radius decreases its surface charge density, which may allow it to carry a full negative charge in solution. (Florián *et al.*, 1998; Frey and Sammons, 1985). The sulfur also lacks the ability to hydrogen bond with water and so water dissociates more readily from the oligonucleotide. This is critical because the binding energy is the difference between the energy of interaction between the protein and the oligonucleotide and the energies of dehydration of the interacting surfaces. The low charge density of the sulfur also reduces the enthalpy needed to strip small ions prior to binding to VDAC (Cho *et al.*, 1993). This property also increases the

polarizability (Saenger, 1984) of the sulfur atoms strengthening the interaction with lower charge density groups found in proteins.

A simple explanation for the length dependence of the permeability decrease induced by the phosphorothioate oligonucleotides with a randomized sequence is the importance of sheer size. A larger inhibitor would generate a more effective steric block or electrostatic block of the channel. However the reality may be more complex. For example, multiple interactions may be needed to stabilize the complex.

The results are consistent with a one-to-one interaction between G3139 and VDAC. This might indicate a single binding site on VDAC or that electrostatic repulsion precludes the binding of two oligonucleotides. The analysis is complicated by an incomplete reduction in permeability. The latter finding is in harmony with the finding that some VDAC channels are resistant to closure by G3139 (Lai et al., 2006).

The physiological conditions may modify the interaction

The ability of G3139 to influence mitochondrial respiration rates depends on the free [ADP]. At high ADP levels the effects of G3139 are quite small because the lower MOM permeability is compensated by the higher [ADP]. Inside the cell, more than half the ADP is bound to proteins (Brindle *et al.*, 1989; Brown, 1992; Morikofer-Zwes and Walter, 1989). The free [ADP] from various cell types is not directly known but has been estimated to be 6-90 μM (Brindle *et al.*, 1989; Roth and Wiener, 1991; Wan *et al.*, 1993). The failure to detect the ADP by ^{31}P-NMR argues for the real concentration to be in the low end of that range (Brindle *et al.*, 1989; Roth and Wiener, 1991). In any event, this

range is within the concentration range at which G3139-induced MOM permeability reduction limits the rate of ADP phosphorylation.

G3139 induces reductions of MOM permeability at doses that are more than one order of magnitude lower than those needed to achieve comparable reductions in the conductance of a VDAC-containing membrane. These differences in sensitivity between experiments on isolated mitochondria and those performed on pure VDAC in phospholipid membranes indicate that physiological conditions may actually augment the interaction and/or magnify the effect (Figs 4.3A, B). The presence of regulatory proteins and other local factors which favor VDAC closure (Colombini, 2004) may act synergistically with G3139. The voltage difference across MOM may also contribute to the stronger in vivo effect.

Differences in sensitivity also appear among different mitochondria isolated on different days. The K_I values vary between 0.2 to 0.5 μM. These differences could not be attributed to differences in weight/age of the animal. Also all animals were male and were on the same diet. Hence the difference likely arises from differences in the physiological state of the animal: different levels of VDAC regulatory proteins in the intermembrane space, different levels of electrical potential across the outer membrane or different amounts of Bcl-2 family proteins in the MOM. For example, Bcl-xL is anti-apoptotic and has been reported to open VDAC channels and to increase the MOM permeability (Vander Heiden *et al.*, 2001). There may be competition between G3139 and Bcl-2 family proteins.

The apoptotic implication of the interaction

VDAC's role in early apoptotic events is still controversial. There is evidence that VDAC is not involved in the apoptosis of *S. cerevisiae* (Gross *et al.*, 2000) but apoptosis in yeast is very different from apoptosis in multi-cellular organisms. Indeed it is generally believed that VDAC is important in the initiation of apoptosis but different and sometimes conflicting mechanisms have been proposed. Many reports claim that VDAC is a part of the permeability transition pore (PTP) (Crompton, 1999; Marzo *et al.*, 1998; Szabo and Zoratti, 1993; Szabo *et al.*, 1993). The opening of PTP causes dissipation of the mitochondrial membrane potential and matrix swelling, which leads to cytochrome c release and cell apoptosis. Some claim that VDAC can oligomerize (Zalk *et al.*, 2005) or associate with Bax (Shimizu *et al.*, 2000) to form a pathway for the release of proteins from mitochondria. We favor a third mechanism, which is that VDAC closure leads to the initiation of apoptosis (Vander Heiden *et al.*, 2000). A drastic reduction in the rate of exchange of metabolites between the mitochondria and the cytosol leads to unidentified changes that result in the release of proteins from mitochondria. This hypothesis is supported by a variety of observations (Rostovtseva *et al.*, 2004; Vander Heiden *et al.*, 2001) and is consistent with the present findings. G3139 closes VDAC and induces cytochrome c release and apoptosis in cells. The perfect match of the abilities of N-mers to decrease MOM permeability and to induce cytochrome c release from isolated mitochondria (Table 4.2, Fig. 4.8) further implicate VDAC closure as the initial step favoring leading to cytochrome c release from mitochondria.

In conclusion, phosphorothioate oligonucleotides (n>12) are able to reduce MOM permeability through closing VDAC channels. Our findings support the hypothesis that

VDAC closure leads to apoptosis and that G3139 closes VDAC channels in the MOM. In the cell the situation is more complex. G3139 is more potent than a random sequence. Among the possible factors is the presence of CpG motifs (Gekeler *et al.*, 2006). Therefore, the action of G3139 is multi-faceted with VDAC closure being only one of these facets.

VDAC can be viewed as an anti-apoptotic protein, whose open state guarantees the exchange of metabolites through the MOM and inhibits cell apoptosis. It is also a transducer of apoptotic signals, integrating the information and communicating it in the form of a change in MOM permeability (Fig. 4.10).
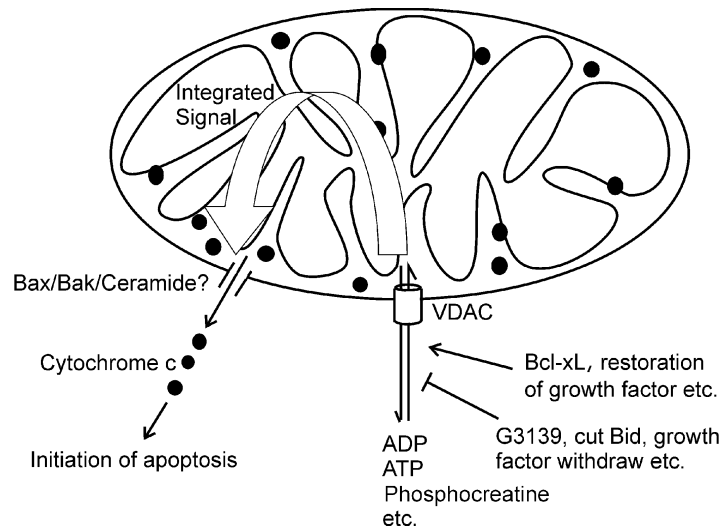
Figure 4.10. Hypothetical model of the role of VDAC in apoptosis. VDAC integrates apoptotic signals changing the propensity for release of intermembrane space proteins. VDAC closure favors cytochrome c release through some not clearly identified mechanism.

Appendix:

D- and L-G3139 cause a similar reduction of the mitochondrial outer membrane permeability

L- and D-G3139 were evaluated in isolated mitochondria from rat liver. The permeability of the outer membrane to ADP was measured at room temperature. D-G3139 has been shown to reduce this permeability with K_I between 0.2 and 0.5 μM. Fig. 4.A1A shows that the L- and D-enantiomers each reduce the outer membrane permeability with a similar concentration dependence. This inhibition happens within 10 minutes. The reduction in mitochondria outer membrane permeability to ADP is attributed to VDAC blockage, because VDAC is the main pathway for metabolite flux through the outer membrane (Hodge and Colombini, 1997; Rostovtseva and Colombini, 1997; Colombini, 2004).
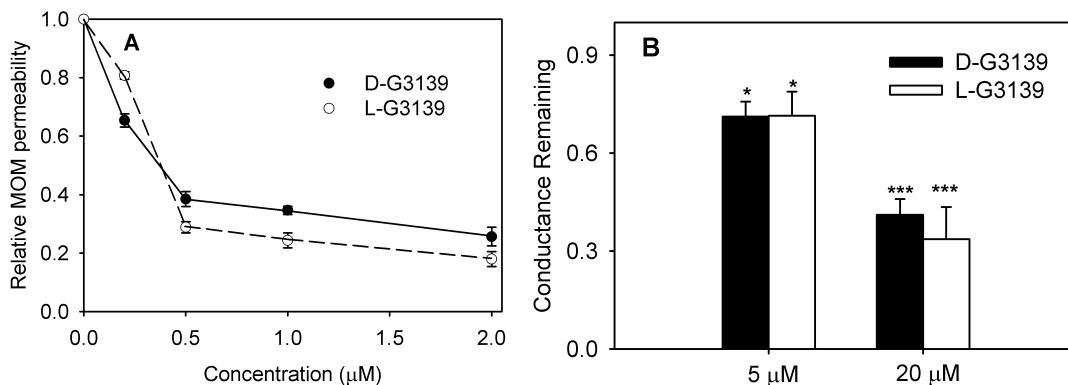
Figure 4.A1. D- and L-G3139 affect MOM and VDAC similarly (**A**) The concentration dependence of D- and L-G3139 induced MOM permeability. Mitochondria were added to 3 ml of respiration buffer with final protein concentration of 400 μg/ml. The results were normalized to the permeability in the absence of G3139s. (**B**) Fractional conductance remaining after treatment with D- or L-G3139. A few VDAC channels were reconstituted into a planar phospholipid membrane as described in the *Methods,* followed by addition of D- or L-G3139. Each result is the average of 3 experiments. The error bars are the standard deviations of three independent experiments. Statistical tests indicate significance in the reduction of the conductance. * < 0.05; ***<0.005

As we have previously described, D-G3139 interacts with VDAC, leading to loss of ionic conductance through this mitochondrial outer membrane channel. Maximal effects were observed at 40 µM, but significant loss of conductance was detected at 5 µM D-G3139. Fig. 4.A1B demonstrates that both D- and L-G3139 have similar inhibitory effects, indicating an indistinguishable potency for the L-G3139 Spiegelmer. Both inhibitors also caused the same flickering of VDAC channels (data not shown), indicating the same underlying inhibitory mechanism.

The similar concentration dependence of D- and L-G3139 affecting MOM and VDAC was also observed in the induction of cytochrome c release from isolated mitochondria. 518A2 melanoma cells were homogenized and mitochondria isolated by differential centrifugation. The mitochondria were suspended in energizing buffer at 10^oC and treated with increasing concentrations of either D- or L-G3139 for 2 h. For each oligonucleotide, the release of cytochrome c into the supernatant (as determined by Western blotting), were similar as a function of concentration, except in some experiments at the highest concentration (40 µM) (Lai JC *et al.*, 2007).

Bcl-2 family proteins modify the interaction

To investigate whether apoptosis related Bcl-2 proteins affect the G3139 inhibition on VDAC, two kinds of BMKs (Baby mouse kidney epithelia cells) were obtained: the wild type cells, and the Bax/Bak double knockout cells. The mitochondria were isolated from these cells and the effects of G3139 on MOM permeability to ADP were measured. Fig 4.A2 clearly shows that at 1 µM G3139, the presence of proapoptotic Bax or Bak strengthens G3139 inhibition on MOM permeability. This result

clearly suggests that the inhibition of MOM permeability to small metabolites is related

with apoptosis. This effect can also be regulated by those apoptosis related proteins such

as Bax or Bak. While at 5 μM G3139, there is no significant difference between

mitochondria obtained from wild type or Bax/Bak double knockout cells. This lack of

difference could be due to the saturation effect of G3139 on VDAC in MOM.
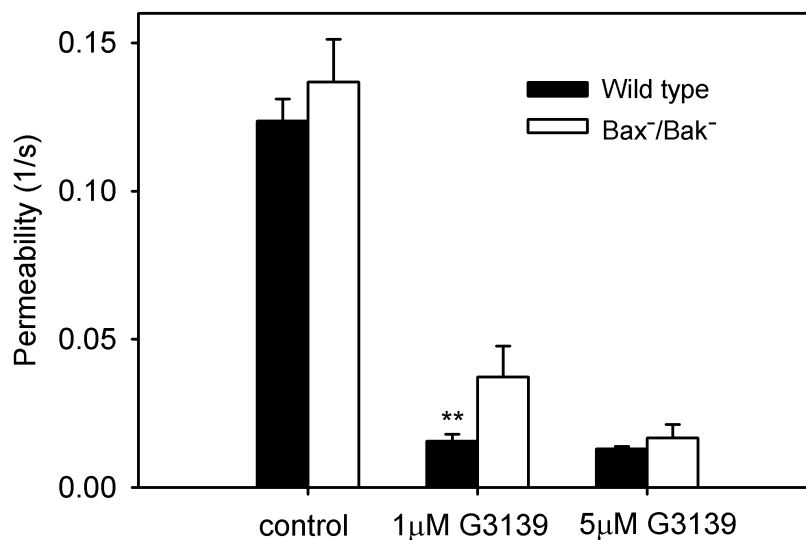
Figure 4.A2. Bak and/or Bak affect G3139 induced MOM permeability reduction.
This is the average of the results obtained in three independent experiments.
Mitochondria were added to 2 ml of respiration buffer with final protein concentration of
320 μg/ml. The error bars are the standard deviations of the three independent
experiments. [**]<0.01.

The results seem to indicate that these proapoptotic proteins favor G3139

blockage of VDAC. This is consistent with our hypothesis that the MOM permeability to

small metabolites regulates the onset of apoptosis. However, the effect could be indirect.

The knockout of proteins often changes the expression level of other proteins. It is also

possible that the knockdown of Bax/Bak may release some anti-apoptotic proteins, which

may compete with G3139 for binding to VDAC. These results need to be followed up

with more direct methods. Purified proteins should be used to determine if Bax or Bak act directly on VDAC or G3139.

Altogether, these findings strengthen the connection between the effect on VDAC and apoptosis. The length dependence, chiral dependence, phosphorothioate dependence of the effects of G3139 on MOM permeability to ADP, on VDAC conductance and on cytochrome c release from mitochondria all agree very well. Some of these also share a similar concentration dependence. These suggest that G3139 induces apoptosis through affecting VDAC channels.

Chapter 5

Phosphorothioate Oligonucleotides Block the VDAC Channel

Abstract

Pro-apoptotic phosphorothioate oligonucleotides, such as G3139 (an 18-mer), induce Bcl-2 independent apoptosis, perhaps partly due to direct interaction with VDAC and reduction of metabolite flow across the mitochondrial outer membrane. Here, we analyzed the interactions at the molecular level. Ten micromolar G3139 induces rapid flickering of the VDAC conductance and, occasionally, a complete conductance drop. These phenomena only occur when VDAC is in the "open" conformation and therefore are consistent with pore blockage rather than VDAC closure. Blockage occurs preferentially from one side of the VDAC channel. It depends linearly on the [G3139] and is voltage-dependent with an effective valence of -3. The kinetics indicate at least a partial entry of G3139 into VDAC, forming an unstable bound state, which is responsible for the rapid flickering (~0.1 ms). Subsequently, a long-lived blocked state is formed. An 8-mer phosphorothioate, poly-deoxythymidine induces partial blockage of VDAC and a change in selectivity from favoring anions to favoring cations. Thus the oligonucleotide is close to the ion stream. The phosphodiester congener of G3139 is ineffective at the concentrations used, excluding a general polyanion effect. This shows the importance of sulfur atoms. The results are consistent with a binding-induced blockage rather than a permeation block.

Introduction

VDAC is the major metabolite pathway across the mitochondrial outer membrane (Hodge and Colombini, 1997; Rostovtseva and Colombini, 1997; Colombini, 2004). It is composed of a single 30-32 kDa polypeptide chain forming a barrel like channel (Blachly-Dyson *et al.*, 1990; Thomas *et al.*, 1993; Song *et al.*, 1998a) with a molecular weight cut off at about 5 kDa for non-electrolytes (Colombini, 1980b). In the open state, VDAC is weakly anion selective and permeable to multi-valent anionic metabolites such as ADP, ATP, and NADH (Colombini, 1979; Lee *et al.*, 1998; Xu *et al.*, 1999). At high positive or negative voltages (> 25 mV), the positively-charged voltage sensor region of VDAC tends to move out of the channel, reducing the diameter of the channel from about 2.5 nm to 1.8 nm, and reversing the ion selectivity (Peng *et al.*, 1992; Song *et al.*, 1998b). This forms the closed states of VDAC. Even though the closure of VDAC only results in a 40% – 60% reduction of conductance and the size of the channel is still larger than a single ATP molecule (Rostovtseva *et al.*, 2002), closed VDAC actually becomes impermeable to ATP (Rostovtseva and Colombini, 1997). Thus, in addition to the channel size, the distribution of the electric charge in the channel wall is very important for controlling the flow of anionic metabolites between the cytosol and mitochondria (Komarov *et al.*, 2005).

This regulation of metabolite permeation through the mitochondrial outer membrane plays a significant role in controlling cell death and apoptosis (Vander Heiden *et al.*, 2000). Recent studies on phosphorothioate oligonucleotides, such as G3139, have strengthened the linkage (Lai *et al.*, 2006). Phosphorothioate oligonucleotides have each phosphodiester linkage modified such that one non-bridging oxygen is replaced by a

sulfur atom. This makes the oligonucleotide resistant to nuclease action. G3139 is an 18-mer phosphorothioate oligonucleotide that is anti-sense to the initiation region of Bcl-2 mRNA (Klasa *et al.*, 2002). It was designed to sensitize cancer cells to chemotherapy agents by downregulating Bcl-2 levels (Leung *et al.*, 2001; Raffo *et al.*, 2004). However, when G3139 was introduced into cells, cytochrome c release preceded the downregulation of Bcl-2. This and the lack of strict sequence dependence (Lai *et al.*, 2005) indicated that another mechanism must be responsible for the pro-apoptotic effect of G3139. Experiments with isolated mitochondria showed that G3139 interferes with metabolite flow through VDAC and this may partly account for the ability of G3139 to induce apoptosis (Lai *et al.*, 2006; Tan *et al.*, 2007).

Interactions between oligonucleotides and protein channels have been intensively studied mainly using the α-hemolysin channel (Kasianowicz *et al.*, 1996; Akeson *et al.*, 1999; Henrikson *et al.*, 2000). α-hemolysin forms a heptameric channel with a diameter of 2.6 nm (Song *et al.*, 1996). Unlike VDAC, the α-hemolysin channel is very asymmetric with a mushroom like domain on one membrane surface (Song *et al.*, 1996). However, its channel size is very similar to the open conformation of VDAC. The permeation of oligonucleotides through α-hemolysin channels (Kasianowicz *et al.*, 1996; Akeson *et al.*, 1999; Henrikson *et al.*, 2000) suggests that they may enter VDAC in a similar manner. This entry may account for blockage of the VDAC channel.

In this work, we investigate the molecular basis for the interaction between phosphorothioate oligonucleotides and VDAC. We propose that partial entry of G3139 into and subsequent binding to VDAC channels account for the apparent result that G3139 induces VDAC closure.

Materials and Methods

Planar phospholipid membrane studies

Planar phospholipid membranes were generated according to standard methods (Montal and Mueller, 1972; Colombini, 1987a). The membrane was formed from phospholipid monolayers consisting of diphytanoyl phosphatidylcholine, polar extract of soybean phospholipids (both from Avanti Polar Lipids, Alabaster, AL) and cholesterol (Sigma, St Louis, MO) in a 1:1:0.1 mass ratio.

VDAC was purified from mitochondria isolated from rat liver (Freitag *et al.*, 1983; Blachly-Dyson *et al.*, 1990). A 0.1 μL aliquot of the VDAC-containing solution (2.5% Triton X100, 50 mM KCl, 10 mM Tris, 1 mM EDTA, 15% DMSO, pH 7.0) was stirred into 4-6 mL of aqueous solution containing 1.0 M KCl, 5 mM $CaCl_2$, 1 mM EDTA, and 5 mM HEPES (pH 7.2) on the *cis* side of the chamber. The *trans* side, containing the same aqueous solution, was held at virtual ground by the voltage clamp.

After a single channel insertion, a triangular voltage wave at a frequency of 3 mHz from −52 mV to +52 mV was applied to the *cis* side. The current was recorded at a rate of 100 μs per point with no filtering unless mentioned otherwise. Its bandwidth is 10 KHz. All experiments were performed at approximately 23°C.

The data were analyzed using the QuB program downloaded from the website (http://www.qub.buffalo.edu/wiki/index.php/Main_Page) of the State University of New York – Buffalo.

Ion selectivity measurement

These were performed in a similar way as above except that KCl concentration gradients (0.50 M KCl vs. 0.10 M KCl; other components are: 0.5 mM CaCl$_2$, 1 mM HEPES, pH 7.2) were used and recordings were made at 1 ms per point with 2 kHz filtering. The salt activity coefficients of 0.5 M KCl and 0.1M KCl are 0.651 and 0.770 respectively. The reversal potential was measured by a linear fit to the current-voltage curve. The ion selectivity was estimated using the Goldman-Hodgkin-Katz theory.

Oligonucleotides

G3139 was kindly donated by Dr. R. Brown, Genta Inc (Berkeley Heights, NJ). Phosphorothioate homopolythymidine 8- or 14-nucleotides in length was synthesized using standard automated phosphoramidite chemistry on an ABI Model 3400 DRNA/RNA synthesizer. 3H-1,2-benzodithiol-3-one 1,1-dioxide was used as the sulfurizing agent. The 5'-dimethoxytrityl-derivatized oligonucleotides were released form the support by treatment with 400 µL of a solution containing concentrated ammonium hydroxide and 95% ethanol (3:1 v/v) for 3.5 h at 55˚C. The dimethoxytrityl derivatized oligonucleotide was dissolved in 50 mM sodium phosphate (pH 5.8) and the solution then loaded onto a C-18 reversed phase SEP PAK cartridge (Watters Inc). The cartridge was washed sequentially with 10% acetonitrile in 50 mM sodium phosphate buffer, water, 2% trifluoroacetic acid and water. The detritylated oligonucleotide was then eluted with from the cartridge with 50% aqueous acetonitrile. The purity of the oligonucleotide was confirmed by reversed phase HPLC.

The phosphodiester congener of G3139 was synthesized by standard automated phosphoramidite chemistry. The oligonucleotide was deprotected as described above and purified by strong anion exchange HPLC.

Results

G3139 induces complete conductance loss of VDAC

VDAC is a voltage-dependent channel. When reconstituted into planar membranes, it is open at low voltages and tends to enter low-conducting, closed states, at high voltages (> 25 mV) (Colombini, 2004). There are 2 independent sets of closed states, one at positive and the other at negative potentials. The normal VDAC closure only results in a partial conductance loss (Fig. 5.1A) with the remaining conductance generally between 40% - 60% of that of the open state (Fig. 5.2). When 10 μM G3139 was added to the *cis* side of the planar membrane (same side as the addition of VDAC), rapid flickering of VDAC conductance occurred in the millisecond time scale. However, flickering was only observed when negative voltages were applied (Fig. 5.1, B and C).
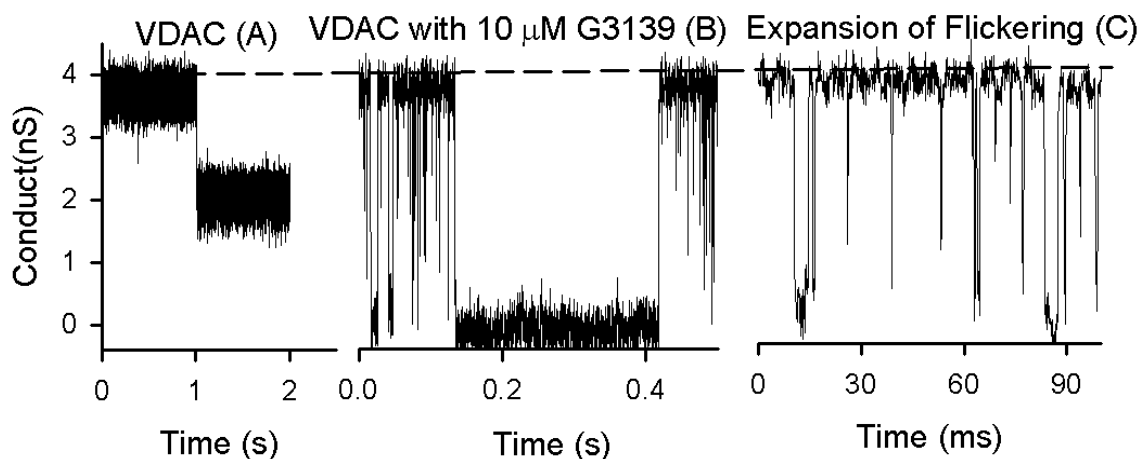
Figure 5.l. Comparison of normal VDAC closure and G3139 induced VDAC closure. These figures are from a typical experiment performed with the same single VDAC channel in response to -50mV potential. (**A**) An example of voltage-dependent VDAC closure. (**B**) An example of G3139 induced rapid flickering and complete conductance loss of VDAC after addition of 10 μM G3139 to the same side as the VDAC addition. (**C**) An expanded scale to show G3139 induced rapid flickering of VDAC channels. These results were obtained at 0.1 msec per point and are presented without any filtering.

This is consistent with the field driving the negatively charged G3139 toward the lumen of the channel. Each time-resolved conductance drop during the flickering process reaches a conductance level that is close to zero. This is clearly evident in the very long-lived events (Fig. 5.1C).

The G3139-induced closure of VDAC is clearly different from voltage-induced closure. While both processes are voltage-dependent, the kinetic properties are quite different. G3139 induces rapid gating accompanied by long-lived closing events. Without G3139, channels close with slow kinetics. The extent of closure is much greater (Fig. 5.2) in the presence of G3139. This closure often represents a complete loss of conductance. This complete closure requires the direct interactions between G3139 and VDAC and suggests that G3139 induced VDAC closure is distinct from the normal VDAC closing process.
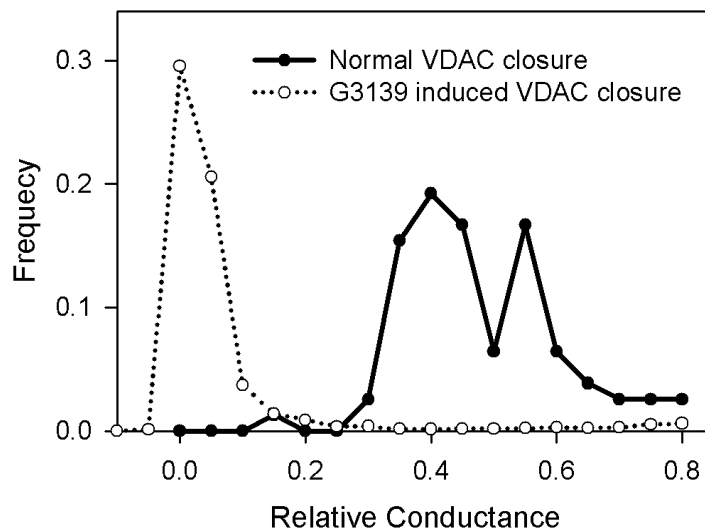
Figure 5.2. A comparison of the distribution of relative conductance of normal VDAC closure and G3139 induced VDAC closure. Ten micro-molar G3139 was added to the same side as the VDAC addition.

The closed states of VDAC have been shown to be favored by a variety of polyanions (Colombini *et al.*, 1987b). In these cases, the closure is not distinguishable from normal VDAC closure. Indeed, the evidence strongly indicates that polyanions act on the normal gating process by interacting electrostatically with the positively-charged voltage sensor forming part of the wall of the aqueous pore and favoring its translocation to the membrane surface (Mangan and Colombini, 1987). However, what appears to be G3139-induced VDAC closure may actually be blockage of VDAC by G3139. This mechanistic distinction is reinforced by the fact that the equally charged phosphodiester congener of G3139 does not induce VDAC flickering or conductance loss (Lai *et al.*, 2006). It also has little effect on VDAC at the concentrations used to observe the effects of G3139.

G3139 directly bind to a specific conformation of VDAC

There are several possible molecular mechanisms that could account for the observed conductance fluctuations following the addition of G3139 to VDAC channels. G3139 could induce a conformational change in VDAC resulting in the occlusion of the pore. This seems unlikely because VDAC does not normally close completely. Alternatively, G3139 could permeate through VDAC channels. Its large size and multiple negative charges might block the channel completely. Thus, the flickering would reflect the transit time of G3139. However, one could also propose that G3139 simply binds to the mouth and inner wall of the channel but does not translocate through the membrane to the other side. Long-lived occlusions would result from conformers of G3139 that bind tightly to the walls of the channel. A particularly pertinent observation

that addresses this issue was made by varying the location of G3139 addition. Addition of G3139 to the same side of the membrane as VDAC addition (*cis* side) resulted in rapid flickering in ~90% of all experiments. Addition of G3139 to the opposite (*trans*) side, resulted in very little flickering (~ 10 events per sec in 2 kHz filtering). When G3139 was added to both sides, flickering was almost exclusively observed when the *cis* side was held at a negative voltage (Fig. 5.3A). Recall that the G3139 side must be made negative to induce flickering. The difference in the rate of flickering was quantitated by measuring the time constant for channel closure (τ_{on}, or mean duration of the open state) obtained using the QuB program (see Methods). When the *cis* side was at −50 mV compared to the *trans* side , τ_{on} = 9.8 ± 0.8 ms, when the *trans* side was at −50 mV compared to the *cis* side, τ_{on} ≈ 100 ms. This asymmetric effect could arise from a permeation blockage but is more consistent with an asymmetric binding site.
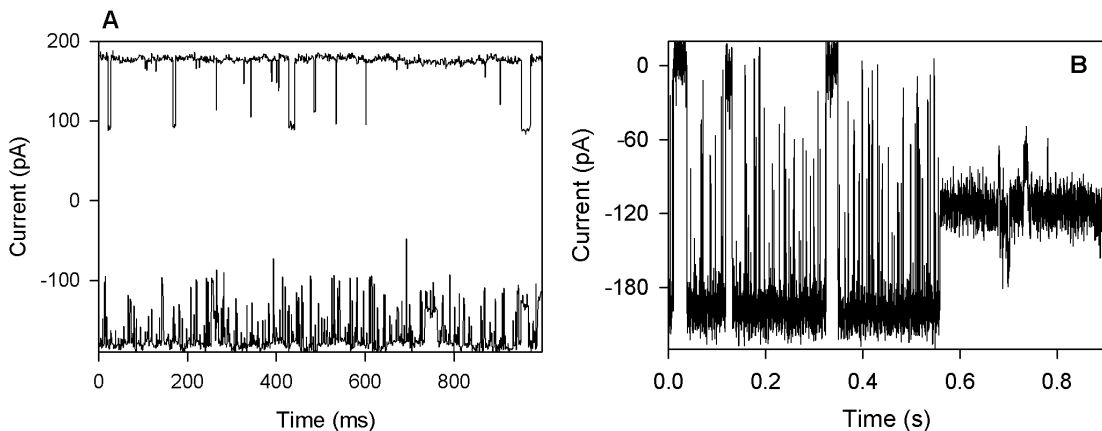
Figure 5.3. (A) Asymmetrical flickering of VDAC induced by 40 μM G3139 present on both sides of the membrane.** Minus 50 mV was applied to the *cis* side (lower trace) and to the *trans*-side (upper trace). Two VDAC channels were present in the membrane. Recordings were made at 1 ms per point with 2 kHz filtering. **(B) No flickering occurs when VDAC enters a normal closed state.** This is a typical experiment of a single VDAC with flickering induced by 10 μM G3139 in *cis* side. The applied voltage was −50 mV.

The asymmetric nature of the G3139-induced flickering reveals the asymmetric insertion of VDAC (from rat liver) into planar membranes. This observation agrees with recent findings about the asymmetric insertion pattern of VDAC from mammalian sources (Rostovtseva *et al.*, 2006), which is different from observations made with yeast VDAC (Zizi *et al.*, 1995).

These observations also strengthen the hypothesis that G3139 specifically interacts with one area of the channel's surface. The asymmetry reveals specificity for a region of the protein. There is also specificity for the ligand because the phosphodiester congener does not induce channel blockage. The focus is clearly on the phosphorothioate backbone of G3139 as the specific sequence of bases is unimportant (a phosphorothioate composed of just thymidine also induces flickering and full blockage, see Fig. 5.6). Thus there must be some specific affinity between the phosphorothioate and some region or domain of the VDAC molecule.

The existence of a specific interacting domain on VDAC is further supported by the observation that G3139 induces flickering almost exclusively when VDAC is open. When VDAC is closed (i.e. in a low-conducting state), there is nearly no flickering (Fig. 5.3B). This suggests some specific interactions between G3139 and the mobile region of VDAC, the voltage-sensor region (Song *et al.*, 1998b). This is a positively charged region and thus ideal for interacting with G3139. When that positively charged region moves out of the channel (the gating process of VDAC, Song *et al.*, 1998b), G3139 is likely to still bind to this region that is mostly outside the pore. This binding would not induce VDAC flickering or complete closure.
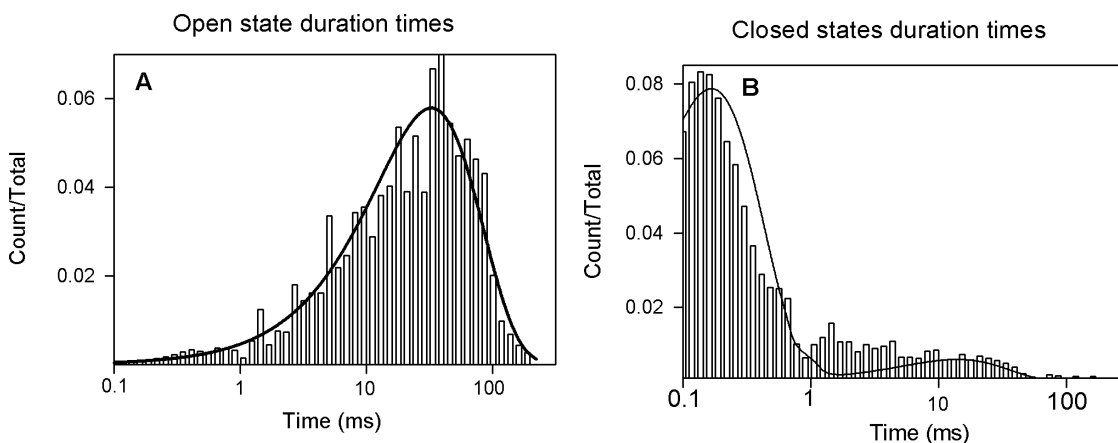
Figure 5.4. **An example of the distributions of the duration of the open state (A) and blocked states (B) of G3139-induced rapid flickering** of a single VDAC channel with 5 µM G3139 added to the cis side and –40 mV applied voltage.

The kinetics of the interaction

Because G3139 is a charged molecule, the mechanism just presented would predict the existence of a voltage-dependence to the blocking action of G3139. The QuB program was used to analyze the kinetics of the flickering events. For these experiments, G3139 was only added to the *cis* side.

Fig. 5.4 shows the distribution of the duration of the open and blocked states of VDAC channels under the influence of 5 µM G3139 and –40 mV. There is a single distribution of open times indicating a single open state. However, the distribution of blocked times indicates multiple blocked states. Some blocked states open quickly as evidenced by events below 1 ms (Fig. 5.1, B and C). However, some states are stable for very long times resulting in events longer than 0.1s. Clearly, these are not the same states. To simplify the analysis, one open state and two blocked states were used to model G3139 induced VDAC closure:

$$\text{open state} \xrightarrow{\;\;k\;\;} \text{blocked state 1} \xrightleftharpoons{\;\;\;} \text{blocked state 2} \qquad\qquad (5.1)$$
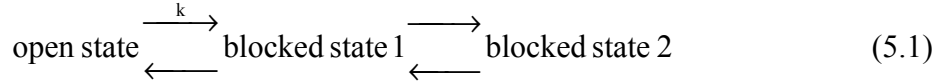
(k is the forward rate constant of the first reaction.)

Clearly, one could fit the data with more blocked states. There may be a variety of ways for G3139 to bind to VDAC: different conformers of G3139 and different ways of binding to the site on VDAC. It is possible that, with time, G3139 may adapt to the VDAC surface, increasing the strength of the interaction and thus decreasing the rate constant of dissociation. This latter process is what is modeled in Eq. 5.1.
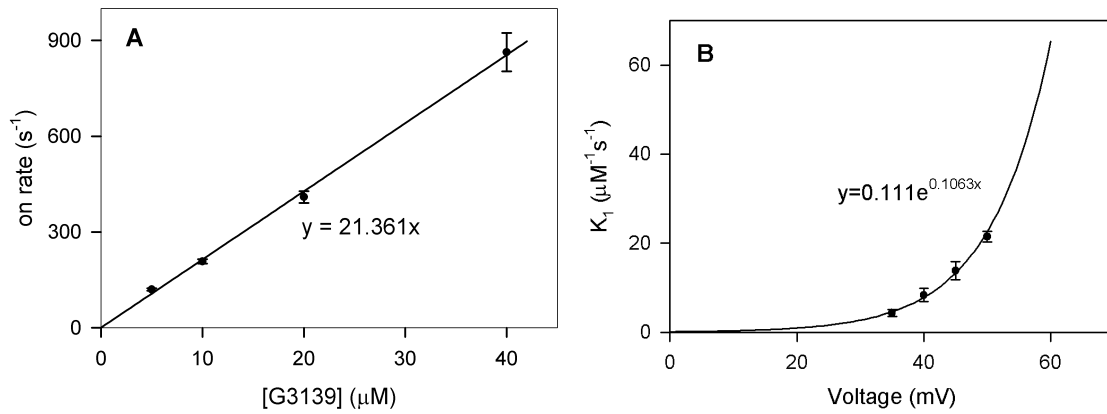
Figure 5.5. (**A**) Concentration dependence of the "on" rate of G3139-induced rapid flickering of a single VDAC channel at −50 mV. The error bars shown are the standard errors of a single experiment generated by QuB. The equation in the graph is the result of a linear fit. (**B**) Voltage dependence of k_1. The error bars shown are the standard errors of the slope calculated from the linear regression in the concentration dependence curve. The equation in the graph is the result of an exponential fit. These results are typical of three independent experiments.

Fig. 5.5A shows a linear dependence of the on rate on the concentration of G3139. This suggests a one-to-one binding of G3139 to VDAC. The reverse rate constant is about 2000 − 3000 s^{-1} and does not depend on the concentration of G3139.

The rate constants between the two blocked states are known with less confidence because these events are very heterogeneous. Thus:

$$G3139 + VDAC \text{ (open)} \underset{k_{-1}}{\overset{k_1}{\rightleftharpoons}} G3139 - VDAC \text{ (blocked1)} \underset{k_{-2}}{\overset{k_2}{\rightleftharpoons}} G3139 - VDAC \text{ (blocked2)}$$

(5.2)
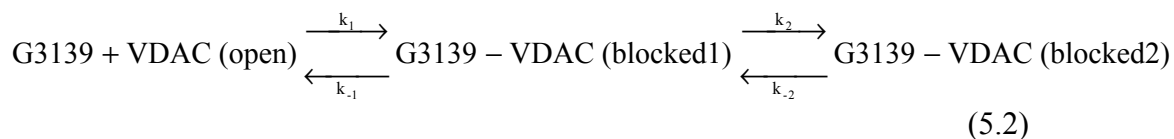
(k_1 and k_{-1} are the forward and reverse rate constants of the first reaction respectively; k_2 and k_{-2} are the forward and reverse rate constants of the second reaction respectively.)

Fig. 5.5B shows that k_1 is voltage dependent. This is not surprising since the applied voltage changes the activation energy between the open and the first blocked state. The energy change is equal to nFV (n is the effective valence of the block, F is the Faraday constant and V is the applied voltages). Thus $k_1 = k_0 \exp(nFV/RT)$ (k_0 is the rate constant of the same reaction with no applied voltage, R is the gas constant and T is the temperature). Fitting the results to this equation (Fig. 5.5B) yields an effective valence of -2.9 ± 0.1 (n=3, mean ± SE) (T = 295K). Even though, formally, G3139 bears a net charge of 18, experiments indicate that an oligonucleotide composed of 18 bases has a net charge of 9 due to the screening by counterions (Li *et al.*, 2001). In the narrow confines within the channel, the screening effect may be quite different. In any event, the voltage dependence suggests that at least part of G3139 moved through the electric field by entering the pore of the channel.

Oligonucleotide binding induces changes in selectivity

If the oligonucleotide enters the pore of the channel, its negative charge should alter the ion selectivity. However, G3139 results in a virtually complete block to ions. Thus we tested shorter phosphorothioate oligonucleotides in order to achieve incomplete
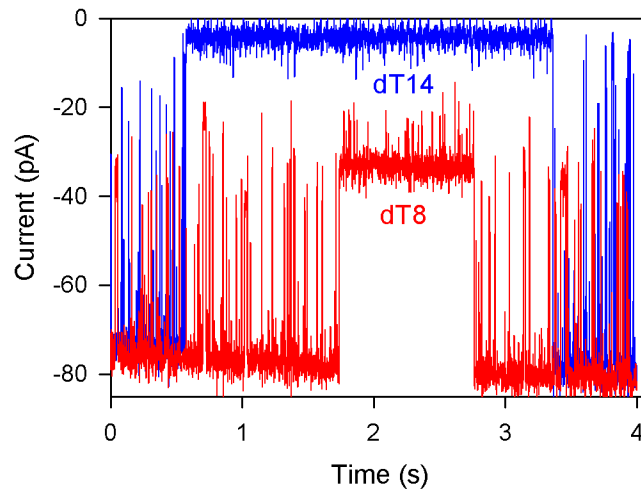
Figure 5.6. Comparison of VDAC flickering induced by phosphorothioate oligonucleotides of different length: dT_8 (red trace) and dT_{14} (blue trace). These were added only to the *cis* side. The voltages applied are from –49 mV to –53 mV. These are typical examples from experiments with KCl gradient (0.50 M KCl vs. 0.10 M KCl; other components are: 0.5 mM $CaCl_2$, 1 mM HEPES, pH 7.2).

block and thus detect any change in ion selectivity. Phosphorothioate oligonucleotides composed entirely of the base, thymidine, are readily made and those of comparable length are as effective on VDAC as G3139. Even the 14mer, dT14 has similar abilities to induce rapid flickering and complete conductance loss of VDAC channels (Fig. 5.6). However, the shorter version, dT8, only reduces the conductance to about 40% - 60% of that of an open VDAC channel.

The residual conductance remaining after the binding of dT8 is cation selective ($P_K/P_{Cl} = 2$) with a reversal potential of –14 mV ± 2 mV (mean ± S.E., n = 9). This is substantially different from the selectivity of the open VDAC channel ($P_K/P_{Cl} = 0.5$). This change in ion selectivity supports the proposed model that the flickering may be a result of the interaction of the phosphorothioate oligonucleotides and the inner wall of VDAC. dT8 may not be long enough to fully occlude the pore. dT10 causes about 70-80% of full blockage and dT12 causes of about 80%-90% of full blockage.

Discussion

Attempts to make cancer cells sensitive to chemotherapy agents by knocking down the anti-apoptotic protein, Bcl-2, have resulted in the generation of a phosphorothioate oligonucleotide that blocks VDAC channels. This blockage does not depend on the sequence but on the phosphorothioate backbone. These molecules are the most specific VDAC blockers available to date. They will likely be useful tool to study the role of VDAC in cellular function.

The blockage of VDAC by G3139 is linearly dependent on the [G3139] indicating a 1:1 complex. It is also voltage-dependent indicating that G3139 is entering the lumen of the channel at least to some extent. dT8 that is 8 nucleotides long only produces a partial block. Full blockage requires a length of about 14 nucleotides. From a molecular dynamics simulation of a single-stranded DNA oligonucleotide inside a 2.4nm hole (which is similar in size to the VDAC pore), the oligonucleotide has a similar conformation as a B-form helix, which has a distance of 0.34 nm between each base and pitch of 10 bases per turn (Cui, 2004). However, in the simulation the oligonucleotide had no affinity for the wall of the pore resulting in a helix with an outside diameter on 2.0 nm. Affinity for the wall and the larger size of the VDAC pore (2.5 to 3 nm) should result in a helix with a greater pitch, perhaps 12. A minimum of a full turn of the helix would be needed to achieve complete block so this explains why dT8 only achieves an incomplete block. This also explains the almost linear increase in blockage with oligonucleotide length.

Our analysis indicates that blockage results in the effective translocation of 3 charges through the entire potential difference across the membrane. If the

oligonucleotide were located entirely within the pore, the 18 charges would be moving an average of half way through the transmembrane potential difference. This should result in an effective valency of -9 if there is no charge screening or about -5 with charge screening (as in Li *et al.*, 2001). Thus it appears that only part of the oligonucleotide is located inside the channel.

The ability of phosphorothioate oligonucleotides, like G3139, to block VDAC channels seems to arise from their ability to bind to VDAC preferentially from one side of the channel. The substantial asymmetry of the rapid flickering of conductance (Fig. 5.3A) argues against the possibility of a permeation block, blocking in transit. VDAC is functionally and structurally rather symmetrical (Colombini, 2004; Mannella *et al.*, 1992), forming a simple cylindrical pore. Thus VDAC would be expected to allow oligonucleotides to permeate equally well in both directions. Single-stranded phosphodiester oligonucleotides of 30 – 200 bases have been shown to block the current flow through α-hemolysin (Akeson *et al.*, 1999; Kasianowicz *et al.*, 1996; Henrickson *et al.*, 2000) as they flow through the channel. The flickering arising from this transient blockage is asymmetrical (Henrickson *et al.*, 2000; Cescatti *et al.*, 1991). However this asymmetry is understandable considering the highly asymmetrical structure of α-hemolysin (Song *et al.*, 1996). Indeed α-hemolysin is also functionally asymmetric, rectifying even in KCl solutions (Cescatti *et al.*, 1991). VDAC normally shows essentially no rectification in its open state (Xu *et al.*, 2001). Despite all this structural and functional asymmetry, α-hemolysin shows a lower level of asymmetric nucleotide block (only 6 fold) as compared to over 10 fold for VDAC exposed to G3139.

An additional difference between the G3139 block of VDAC and the observations with α-hemolysin is the much longer oligonucleotides (200 bases) that must be added to α-hemolysin to obtain blockage lifetimes of similar magnitude as those reported here (Kasianowicz *et al.*, 1996). This indicates that transit times of short oligonucleotides are too short to account for the blockage lifetimes we observe without substantial slowing of the transit by interactions with the walls of the pore.

A variety of experimental observations provide further evidence for a "binding block" as opposed to a permeation block. 1) Phosphodiester oligonucleotides of similar size and charge should have a similar ability to permeate VDAC channels as the phosphorothioate congener, yet these fail to cause flickering (Lai *et al.*, 2006). This is easily explained by the binding but not the permeation model. 2) The voltage-independence of the unbinding rate for the rapid flickering suggests that dissociation of the oligonucleotide is the rate-limiting step. Diffusion away from the site against the field is not rate limiting. In the permeation blockage model, unblockage should be voltage-dependent. Indeed, for α-hemolysin there is an inverse voltage-dependence of the poly[U] induced blockage time (Kasianowicz *et al.*, 1996) demonstrating that unblockage is voltage dependent. 3) The long-lived complete closure of VDAC induced by G3139 cannot be cleared by reversing the polarity of the transmembrane potential. When permeation of poly[U] through α-hemolysin results in long-lived blockage, the channels can be unblocked by reversing the sign of the potential, consistent with permeation block (Kasianowicz *et al.*, 1996). 4) The shorter phosphorothioate oligonucleotides, such as dT8, cause only a partial blockage. Note that the permeation blockage model would predict that the length of the oligonucleotides should only

determine the blockage time (Kasianowicz *et al.*, 1996), not the extent of blockage. Therefore, the binding of G3139 to the inner wall of VDAC and subsequent conformational changes appear to be the mechanisms for the observed flickering and complete conductance loss.

One observation that remains mysterious is the long delay between addition of G3139 and onset of flickering. The rapid flickering of conductance only occurs after about 3-5 minutes after the addition of the phosphorothioate oligonucleotide. For G3139, which has a diffusion coefficient of 2 x 10^{-6} cm^2/s (Li *et al..*, 2001), it takes about 6 seconds to diffuse through 50 μm unstirred layer next to the planar membrane. Thus it seems that G3139 needs to adapt to VDAC before flickering occurs. Indeed, when the concentration of G3139 is increased, it takes about another 3-5 minutes for the flickering effect to increase. These results suggest that there might be some conformational change of G3139 after addition to the buffer solution bathing the membrane. We have tried to incubate G3139 with the buffer solution and heat it before adding it to the system but there was still a delay. Another explanation for the delay might be a slow process of interaction between G3139 and the phospholipid membrane, which may sensitize VDAC to G3139 by changing, for example, the surface potential. Regardless of the fact that, at this stage, we don't have a good explanation for this phenomenon, this delay doesn't affect the proposed mechanism by which G3139 acts on VDAC.

For a VDAC channel, the transient blocked state (first step in Eq. 5.2) is clearly unfavorable because the k_{-1} is 2000-3000 sec^{-1}. The on-rate, k_1, is concentration and

voltage-dependent: $0.11[G3139]\exp(0.11\text{Voltage})\ \mu M^{-1}sec^{-1}$. At 1 μM G3139 and no applied voltage, the on rate is $0.11\ sec^{-1}$. Thus, the equilibrium constant is 4×10^{-5} with an unfavorable free energy change of 25 kJ per mole or 10 kT. The high off-rate can be compensated for by a higher on-rate. A higher concentration and the application of a negative voltage obviously favor binding and make the process feasible. Rapid unbinding of G3139 from VDAC suggests the instability of the transient G3139-VDAC complex. However, the occurrence of longer complete closures clearly shows that the intermediate transient state can be stabilized. The analysis shows a slow on-rate k_2 and off-rate k_{-2} of the second interaction step in Eq. 5.2, suggesting that both those interactions may involve some slow conformational change of VDAC and/or G3139. These structural changes make the bound state more energetically favorable and lead to complete, long-lasting VDAC closure.

Thus, the G3139-blocked VDAC channel is composed of an "open" VDAC channel and G3139 binding from one aqueous surface. Good candidates for surfaces forming the binding site are the positively charged voltage sensor and some adjacent region outside the pore. This explains why the lower-conducting, closed states, whose pore size was estimated to be 1.8 nm (Mannella et al., 1992; Colombini, 1987b; Mannella, 1989), show virtually no flickering despite being large enough to accommodate the oligonucleotides. However, the unfavorable net charge in the pore of the closed state of VDAC may also explain the lack of flickering. Another possible binding site is the nucleotide binding site in the inner wall of VDAC (Rostovtseva *et al.*, 2002; Florke *et al.*, 1994). This site may not be distinct from the voltage sensor region. The importance of phosphorothioate may be a greater affinity for the binding site on

VDAC, allowing the formation of a long-lived block to metabolites. In any case, the binding of G3139 to the inner wall forms the completely blocked state and the shorter oligonucleotides do not have the capacity to fully block the channel (Fig. 5.6). Obviously, the sulfur group is very important for the binding, as the phosphodiester congener does not cause VDAC flickering and complete closure (Lai *et al.*, 2006).

Phosphorothioate oligonucleotides are, presently, the most specific inhibitors of VDAC channels. Their potency of blockage/closure of VDAC channels in isolated mitochondria, is 50-fold higher than observed for the experiments on pure VDAC reconstituted in planar membranes (as presented here). Perhaps a VDAC-associated protein or lipid increases the affinity of VDAC for the phosphorothioate. In any case, the present work provides a mechanistic foundation for understanding effects in cells and organelles.

Chapter 6

VDAC closure increases calcium ion flux

Key words: permeability, PTP, mitochondria, apoptosis, voltage gating, swelling

Abstract

VDAC is the major permeability pathway in the mitochondrial outer membrane and can control the flow of metabolites and ions. Therefore Ca^{2+} flux across the outer membrane occurs mainly through VDAC. Since both Ca^{2+} fluxes and VDAC are involved in apoptosis, we examined the relationship between Ca^{2+} and VDAC isolated from rat liver. The voltage gating of VDAC does not require Ca^{2+} and it functions normally with or without Ca^{2+}. Additionally, VDAC generally shows a higher permeability to Ca^{2+} in the closed states (states with lower permeability to metabolites) than that in the open state. Thus VDAC closure, which induces cell death, also favors Ca^{2+} flux into mitochondria, which can also lead to permeability transition and cell death. These results are consistent with the view that VDAC closure is a pro-apoptotic signal.

Introduction

Mitochondria are the governors of both cell life (e.g. energy generation) and cell death. Some regulation of both of these functions occurs at the level of the outer membrane in that it controls the flow of metabolites and the release of intermembrane space proteins into the cytosol. These two functions are connected in that a drastic reduction in metabolite flow through the outer membrane, associated with VDAC closure, can lead to protein release and apoptosis (Vander Heiden *et al.*, 2000; Tan *et al.*, 2007). However, Ca^{2+} induced mitochondrial swelling and subsequent cell death may require an increase in Ca^{2+} flux and thus an increase in outer membrane permeability. Perhaps these apparently conflicting changes in outer membrane permeability may be understood if VDAC closure is irrelevant to a small ion such as Ca^{2+} and the Ca^{2+}-induced mitochondrial swelling is strictly an inner-membrane phenomenon.

It is generally believed that mitochondrial swelling is caused by the opening of PTP (permeability transition pores). The pore has a molecular mass cut-off of 1500 Da. Many have proposed that PTP involves both the inner and outer membrane through the participation of VDAC. However, knockout of VDAC1 does not seem to affect the formation of PTP (Krauskopf *et al.*, 2006), making the participation of VDAC in PTP questionable. Nevertheless, it is generally believed that Ca^{2+} should flow easily through VDAC channels because VDAC shows only a weak selectivity for small mono-valent ions (Colombini, 1980a; Hodge & Colombini, 1997). Indeed, in a recent study (Gincel *et al.*, 2001), the authors concluded that VDAC opening promotes calcium flux into mitochondria followed by PTP and mitochondrial swelling, i.e., VDAC opening induces cell death.

This conclusion is in sharp contrast to the findings that VDAC closure is a pro-apoptotic signal. For example, the anti-apoptotic protein, Bcl-x_L, favors the opening of VDAC channels (Vander Heiden *et al.*, 1999; Vander Heiden *et al.*, 2001), while the pro-apoptotic oligonucleotide, G3139 closes VDAC (Lai et al, 2006; Tan et al., 2007). In addition, removal of required growth factors from cell lines leads to decreased MOM permeability to metabolites, such as phosphocreatine, and subsequent apoptosis. This is also consistent with VDAC closure. It is possible that apoptosis induced by VDAC closure is through a different pathway from calcium induced PTP. To clarify the role of VDAC gating in Ca^{2+} flux through the outer membrane, we examined the permeability of VDAC to Ca^{2+} in the open and closed states. The states with higher Ca^{2+} permeability are different from the state traditionally considered to be the open state.

Materials and Methods

Planar phospholipid membrane studies

Planar phospholipid membranes were generated according to standard methods (Montal & Mueller, 1972; Colombini, 1987a). The membrane was formed from phospholipid monolayers consisting of diphytanoyl phosphatidylcholine, polar extract of soybean phospholipids (both from Avanti Polar Lipids, Alabaster, AL) and cholesterol (Sigma, St Louis, MO) in a 1:1:0.1 mass ratio.

VDAC was purified from mitochondria isolated from rat liver [12-13]. In the ion selectivity measurements, a 0.1 µL aliquot of the VDAC-containing solution (2.5% Triton X100, 50 mM KCl, 10 mM Tris, 1 mM EDTA, 15% DMSO, pH 7.0) was stirred into 4-6 mL of aqueous solution containing 80 mM $CaCl_2$ aqueous (unless stated otherwise) solution on the *cis* side of the chamber. The *trans* side, containing 20 mM $CaCl_2$ aqueous solution (unless stated otherwise), was held at virtual ground by the voltage clamp. The solutions were unbuffered and no other ions were deliberately added. After a single channel insertion, a triangular voltage wave at a frequency of 3 mHz from −52 mV to +52 mV was applied to the *cis* side. The current was recorded at a rate of 1 ms per point with 2 kHz filtering. All experiments were performed at approximately $23^{o}C$.

Results and Discussion

The voltage gating of VDAC channels is not affected by Ca^{2+}

Detergent solubilized VDAC was added to a solution containing no calcium ions (0.4mM EGTA was added to chelate any possible calcium contaminations) bathing a planar phospholipid membrane (Fig. 6.1). VDAC channels inserted into the membrane and these events were recorded as increases in current. In the absence of calcium ions, VDAC can remain in the open state and closes in response to a 50 mV applied potential. The kinetics of the closure are indistinguishable whether in the absence or presence of 1.6 mM Ca^{2+} (Fig. 6.1). Moreover, the presence or absence of Ca^{2+} does not change the conductance of VDAC. In 1.0 M NaCl the conductance is 3.3 ± 0.3 nS (mean ± S.D.) in the presence of 0.1 mM EGTA and 3.4 ± 0.1 nS (mean ± S.D.) in the presence of 1 mM $CaCl_2$.
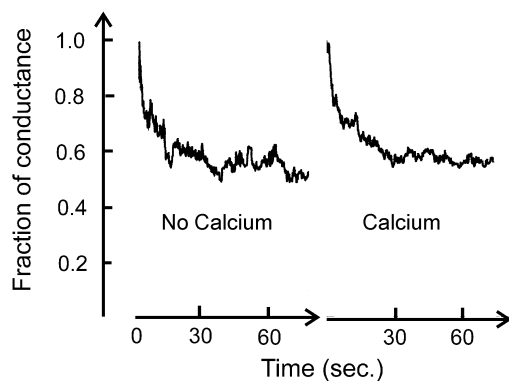
Figure 6.1 VDAC was reconstituted into a planar phospholipid membrane composed of 0.5% PC, 0.5% asolectin and 0.05% cholesterol in the presence of 1.0 M KCl, 20mM HEPES, pH=7.2. 0.4mM EGTA was then added to each side of the chamber to chelate any possible trace amount of Ca^{2+}. 2mM Ca^{2+} was added later to compare VDAC's gating in the presence and absence of Ca^{2+}. (Note: there is enough buffer to control the pH even after acid is released following chelation of some Ca^{2+}.) VDAC's gating was recorded by applying 50 mV (cis side is ground). The total conductance in the absence and presence of Ca^{2+} is 115 nS and 179 nS, respectively. There is an 18-minute gap between these records and the conductance increased because of VDAC insertion. The percent conductance drop and the rate of decay are essentially the same with and without free Ca^{2+}.

Measurement of the permeability of VDAC to Ca^{2+} and Cl$^-$

The permeability of VDAC to small ions includes Ca^{2+}, which was reported to permeate both the open (Gincel *et al.*, 2001) and closed states (Schein *et al.*, 1976; Rostovtseva, T.K., unpublished data) of VDAC. VDAC is the most abundant channel in the MOM (mitochondrial outer membrane). Thus its permeability to Ca^{2+} is very important as this may affect calcium homeostasis and cell death signaling. However, the value of the ion flux of Ca^{2+} through VDAC has never been directly and accurately determined. Here, CaCl$_2$ was used to measure the ion flow through VDAC.

The current carried by cations and anions are given by GHK current equation (constant field equation):

$$I_s = P_s z_s^2 \frac{VF^2}{RT} \frac{\alpha_{si} - a_{so} \exp(-z_s FV / RT)}{1 - \exp(-z_s FV / RT)} \tag{6.1}$$

Where I_S is current carried by ion S, z_S is the charge of s, P_S is the permeability of VDAC to S, α_S is the activity of S (i denotes *cis* side, o denotes *trans* side), V is the potential difference across the membrane, F is the Faraday constant, R is the gas constant and T is the temperature. The single-ion activities were obtained from the salt activity coefficients. For CaCl$_2$, the activity coefficient is 0.5355 for 80 mM solution (*cis* side) and 0.6644 for 20 mM solution (*trans* side) (Staples & Nuttall, 1977).

At any given voltage, all the parameters except I_S and P_S are known in equation 6.1. Thus we can define:

$$X_s = z_s^2 \frac{VF^2}{RT} \frac{\alpha_{si} - a_{so} \exp(-z_s FV / RT)}{1 - \exp(-z_s FV / RT)} \tag{6.2}$$

which is a known parameter, thus

$$\sum PsXs = I \qquad\qquad (6.3)$$

where I is the recorded current. If each X_S is different, equations 6.2 and 6.3 can be combined to fit the current voltage curve to generate the permeabilities to each ion. A four-fold gradient of $CaCl_2$ (with ionic strength in the physiological range) was used as mentioned in the *Materials and Methods.*

A single VDAC channel was used for the current-voltage measurements. The parameters were calculated by fitting to the current voltage curve. The slope at zero voltage is defined as the conductance of the VDAC channel, the zero-current intercept is V_{rev} (reversal potential) and the zero-potential intercept is I_0 (zero potential current).
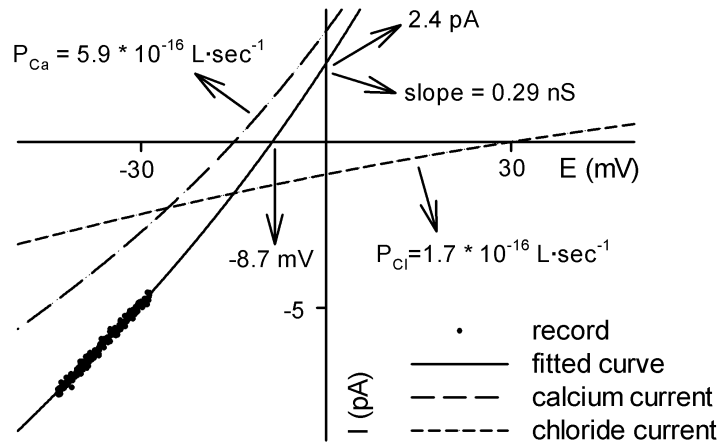
Figure 6.2 An example of fitting equations 6.2 and 6.3 to a segment of a single-channel current-voltage record representing one state of a VDAC channel (a closed state here). A four-fold gradient of $CaCl_2$ was present (see *Materials and Methods*). The arrows and associated numbers indicate the parameters obtained from the fitting.

Fig. 6.2 shows an example of the fitting of equation 6.2 and 6.3 to a segment of a current-voltage record. The recorded current was divided into two currents: calcium current and chloride current. The permeabilities were directly obtained from the fitting.

V_{rev} (reversal potential) and I_0 (zero potential current) for each state were determined by extrapolating the current-voltage curve to intercept the appropriate axis.

This method is more accurate than the calculation of ion permeabilities from a linear extrapolation of the current-voltage curve to the axes. The linear extrapolation is not justified because the current shows rectification.

In the open state, the conductance, $G = 0.520 \pm 0.005$ nS, $V_{rev} = 25.5$ mV ± 0.2 mV, $I_0 = -12.4 \pm 0.1$ pA (mean $\pm$ S.E., n = 15). In the positively closed states, $G = 0.20 \pm 0.02$ nS, $V_{rev} = 15 \pm 2$ mV, $I_0 = -2.8 \pm 0.5$ pA (mean $\pm$ S.E., n = 19). In the negatively closed states, $G = 0.29 \pm 0.05$ nS, $V_{rev} = 2 \pm 3$ mV, $I_0 = 0 \pm 1$ pA (mean $\pm$ S.E., n = 15).

The distributions of conductance, V_{rev}, I_0 are very narrow for the open state and very broad for the closed states. This is consistent with previous observations (Hodge & Colombini, 1997; Colombini, 1986), indicating the presence of multiple closed states. More interestingly, there is a clear difference ($P < 0.001$) between the states observed at negative and positive voltages. The anion preference drops in both cases as compared to that of the open state but states achieved at negative potentials are more favorable to Ca^{2+} flux.

Fig. 6.3 shows the fitted values of the permeability of VDAC to Ca^{2+} and Cl^- in the open state (the units are always 10^{-16} L·s^{-1}), $P_{Ca} = 0.94 \pm 0.05$, $P_{Cl} = 22.6 \pm 0.2$ (mean $\pm$ S.E., n = 15); in the positively closed states, $P_{Ca} = 1.4 \pm 0.2$, $P_{Cl} = 6.3 \pm 0.9$ (mean $\pm$ S.E., n = 19); And in the negatively closed states, $P_{Ca} = 4 \pm 1$, $P_{Cl} = 5 \pm 1$ (mean $\pm$ S.E., n = 15). Clearly, the VDAC channel is highly selective for chloride ions over calcium ions in the open state. When it is closed by high potentials, the permeability to chloride ions

and calcium ions becomes comparable, especially in those states observed in the negative potential region.

There is a significant increase in Ca^{2+} permeability in both sets of closed states but in the negatively closed states the permeability is more that 4 times that of the open state (Fig. 6.4). In some states, the increase can be more than 10 times (Fig. 6.3).
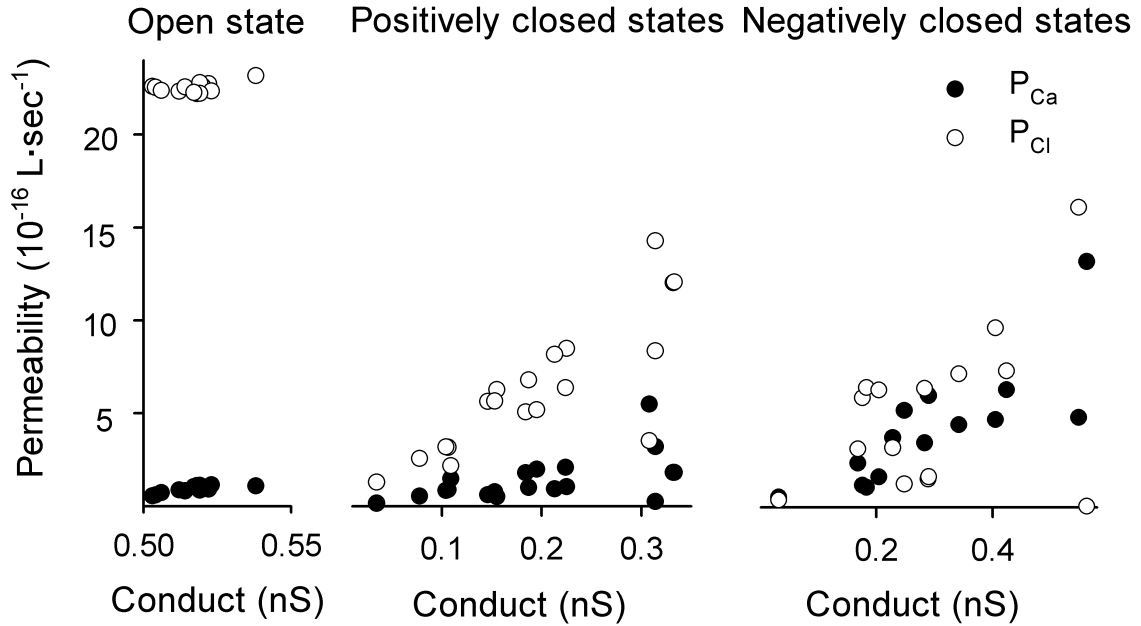
Figure 6.3 Permeability of VDAC to calcium and chloride ions as a function of the total conductance of the channel. Each value is obtained directly as in Fig. 6.2.
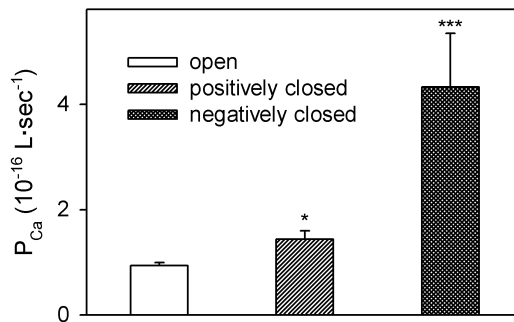

Figure 6.4 Comparison of the permeability of Ca^{2+} through VDAC in different states. The values are mean ± S.E. of 15 measurements in the open state and the negatively closed states and 19 measurements in the positively closed states. (*P < 0.05, *** P < 0.001, compared to the open state)

Discussions

The gating of VDAC channels is not influenced by the presence of Ca^{2+} in the medium, but the flow of Ca^{2+} through VDAC is affected by VDAC gating. In its open state, VDAC is poorly permeable to Ca^{2+}. Extrapolating our results down to a more physiological Ca^{2+} concentration of 1 μM, the flux would be 20 ions per sec. This increases 4 fold when VDAC closes but in some states to as much as 10 fold (Fig. 6.3,6.4). It is possible that some signals may lock VDAC in the more Ca^{2+} conducting states and expedite the Ca^{2+} flux.

In order to obtain accurate estimates for permeability and flux, one needs to have accurate values for activity coefficients. Unfortunately, only salt activity coefficients are available and thus we used these to convert concentrations into activities. However, one can estimate single-ion activity ratios by measuring the reversal potential for salt gradients using ion exchange membranes. Using the salt activity ratios, the calculated permeability ratio of chloride over calcium for the open state of VDAC is more than 25 fold, which is very close to ideal anion selectivity. The permeability ratio doubled if one uses the single ion activity ratios. Thus the calcium flux through VDAC in the open state is even lower, and therefore VDAC closure could enhance calcium flux even more than the value we report.

High-conducting states can be permeable to Ca^{2+}

We observed VDAC functional states that have a similar conductance as that of the open state, but with higher permeability to Ca^{2+} (Fig. 6.3). This is consistent with previous publications (e.g. Zhang and Colombini, 1990) and the "cationic state" of

VDAC previously reported (Pavlov *et al.*, 2005). In our experiments, those states only occur rarely at high negative voltages. They are considered closed states because they are expected to have reduced permeability to metabolites, most of which are anionic. In the Ca^{2+} experiments, these states occurred exclusively at negative potentials.

Ca^{2+} and VDAC gating

We observed no significant Ca^{2+} influence on the voltage gating property of VDAC. A possible reason for the difference between the results presented here and those of Báthori *et al.* (2006) is the different methods used to make planar membranes. We use the monolayer method of Montal and Mueller (1972) to generate solvent-free membranes. The hole in the partition that supports the planar membrane is coated with petrolatum (a hydrocarbon mixture ranging from C_{20} to C_{90}), then phospholipids in hexane are layered on the top of the buffer solution. Once the hexane has evaporated, the planar membranes are made by apposing monolayers from the two sides of the membrane. In contrast, Báthori *et al.* (2006) made the planar membrane by directly painting a decane solution of phospholipids across the hole on the partition separating two sides of the chamber.

The major difference here is the solvent and its propensity to partition into the planar membrane. At room temperature, hexane, which has a vapor pressure of 0.172 atm (Jordan, 1954), evaporates very quickly from the monolayers and thus does not contaminate the membrane. On the other hand, decane, with the vapor pressure of 0.00136 atm, two orders of magnitudes lower than that of hexane (Jordan, 1954), evaporates much more slowly than hexane. In addition, the painting method for making

planar membranes directly applies the decane solution to the hole, which has already been submerged into the buffer solution. Considering the virtual insolubility of decane in water, all the decane will remain with the lipids. Indeed, the decane annulus is necessary to allow the bilayer to interface with the much thicker plastic partition. Unlike the petrolatum coating used in the monolayer method, decane molecules are 5 times smaller and diffuse easily into phospholipid membranes. This solvent increases the membrane thickness by 1 nm and may change such properties as the surface tension and fluidity of the membrane and affect the stability, conductance and voltage gating of VDAC. In addition, Ca^{2+} can interact with charged lipids and spontaneously thin the membrane, favoring channel formation.

Ionic strength and VDAC permeability to Ca^{2+}

The permeability to calcium measured here is very different from that reported by Gincel *et al*., 2001. They measured a P_{Ca}/P_{Cl} of 0.38 and claim a high flux of calcium through the open VDAC channel. This conclusion supports their hypothesis that the open state of VDAC favors Ca^{2+} flux, mitochondrial swelling and cell death. The main observed difference between their experiments and results shown here is the measured reversal potential in $CaCl_2$ gradients. Their observed reversal potential of 10 mV is less than half of what is measured here. This is most likely due to the difference in salt concentration (Table 6.1).

Table 6.1 Comparison of the conditions and results

	This paper	Gincel *et al*., 2001
$CaCl_2$ gradient	80 mM: 20 mM	250 mM: 150 mM
Ionic strength	150 mM	600 mM
Debye length	0.78 nm	0.39 nm
P_{Ca}/P_{Cl}	0.04	0.35

Assuming a linear concentration gradient inside the channel, the difference in CaCl$_2$ concentration between the two sets of experiments is 50 mM vs. 200 mM. The ionic strength is 150mM vs. 600mM. Thus our ionic strength is at a physiological level. The difference in ionic strength translates into a difference in screening of charges within the channel. The calculated Debye Length at room temperature is:

$$\frac{1}{\kappa} = 0.3044I^{-0.5}nm \tag{6.4}$$

Thus the Debye length is 0.78 nm for our experiments vs. 0.39 nm. Hence, in the higher ionic strength there are fewer electrostatic interactions between the positive charges in the inner wall of VDAC and Ca^{2+} ions permeating through the VDAC.

In addition to the difference in ionic solutions, Gincel *et al.* (2001) did not compare the Ca^{2+} flow through VDAC in open and closed states. Perhaps, even under their conditions, the closed states of VDAC could be more permeable to Ca^{2+}.

The physiological impact of VDAC gating

In our observations, the permeability of Ca^{2+} through VDAC is different in the states observed at positive versus negative voltages (Figs 6.3,6.4). This clearly shows an oriented insertion of mammalian VDAC into planar membranes and an asymmetrical VDAC function. The impact of VDAC gating on the regulation of Ca^{2+} flux will depend on the orientation of VDAC in mitochondria and the sign of the potential across the outer membrane.

At present, there is no way of relating the orientation of VDAC in planar membranes and that in the mitochondrial outer membrane. However, it is still interesting to consider the impact of VDAC closure and selectivity change on the calcium flux. Fig.

6.5A shows the open probability of VDAC in response to voltages. By combining this information with the permeability of VDAC to Ca^{2+} in the different states, one can calculate the time-averaged permeability of VDAC to calcium in response to voltages. If we assume that VDAC in mitochondria is in the orientation, whose closure greatly favors calcium flux from the cytosol into mitochondria, the calcium flux in response to 1 μM cytosolic Ca^{2+} can be calculated (Fig. 6.5B).

Porcelli and coworkers (2005) measured the pH difference between the mitochondrial intermembrane space and the cytosol. Considering the highly-buffered nature of these compartments, it is reasonable to conclude that protons will be at equilibrium between these two compartments and thus calculate the potential difference across the outer membrane. This turns out to be 40 mV negative potential in the intermembrane space compared to the cytosol (Porcelli *et al.*, 2005). Thus, from Fig. 6.5 there is a 3 fold increase of calcium flux if VDAC closes with a 40 mV potential. Considering that there are the VDAC modulator (Liu & Colombini, 1992; Holden & Colombini, 1993) and other proteins which may favor VDAC closure and may favor particular closed states, the actual effect could be even larger. Thus the closure of VDAC actually favors Ca^{2+} flux, even though the closed states has a smaller pore diameter (1.8 nm in the closed states compared to 2.5 nm in the open state, Peng *et al.*, 1992; Song *et al.*, 1998b).
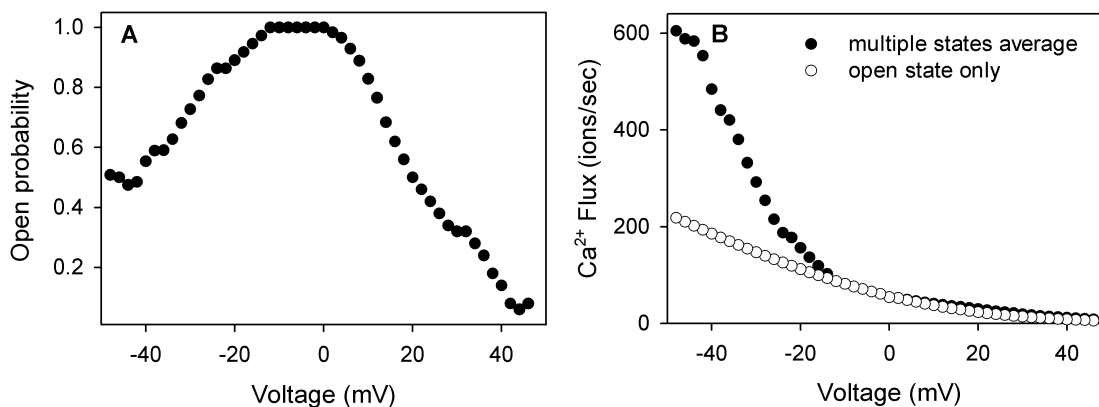
Figure 6.5 (A) The open probability of VDAC in response to voltage. **(B)** A comparison of the average calcium flux through a single VDAC channel in response to voltage in the presence of 1 μM cytosolic Ca^{2+}. The filled circles are the weighted average flux of Ca^{2+} through the open and closed states, assuming the same voltage gating property as in panel A. The open circles are assuming that VDAC is always in the open state.

Accumulating evidence links VDAC gating with apoptosis (Vander Heiden et al., 2001; Tan et al., 2007). It is clear that the open state of VDAC facilitates metabolite flow and thus maintains mitochondria in a healthy state, preventing cytochrome c release. In addition, in the open state, Ca^{2+} permeability is low. In the closed state, VDAC reduces metabolite flux, increases Ca^{2+} permeation, and thus sensitizes mitochondria to apoptotic signals. The gating process of VDAC is not only an interesting biophysical phenomenon, it also changes the properties of VDAC to initiate or be in harmony with changes in the physiological state of the cell.

Chapter 7

On the search: PorB channel

and its mechanism of inhibiting apoptosis

Running tile: PorB channels and metabolite flow

Keywords: metabolites, transfection, VDAC, mitochondria

Abstract

During a *Neisseria meningitidis* infection of human epithelia cells, its outer membrane protein, PorB, can first insert into the plasma membrane of these cells and then localize in mitochondria. This localization is associated with an inhibition of apoptosis. The co-immunoprecipitation of PorB with VDAC raises the possibility that its involvement in apoptosis is through interaction with VDAC. This notion is consistent with the hypothesis that the mitochondrial outer membrane permeability influences cytochrome c release from mitochondria. The possibility that one channel-former might influence the gating properties of the other was investigated and the results were negative. However, experiments on liposome containing PorB showed that PorB is able to facilitate the efflux of ATP indicating that PorB might inhibit apoptosis by allowing metabolites to cross the mitochondrial outer membrane when VDAC channels are closed. Attempts to test this hypothesis by expressing PorB in yeast cells lacking VDAC was unsuccessful. PorB reached the mitochondria in yeast cells but was unable to substitute for VDAC in the knockout cells. There was also no PorB-induced increase of mitochondrial outer membrane permeability to metabolites. Perhaps PorB does not form functional channels in yeast.

Introduction

Porins are channel-forming proteins in the outer membrane of Gram-negative bacteria (Schulz, 1996). Each functional unit is a trimer, composed of three channels. In *Neisseria meningitidis*, two PorA and one PorB form the functional unit in the native state. Surprisingly, after N. meningitidis infection of human epithelial cells, PorB localizes intracellularly to the mitochondrial compartments (Massari *et al.* 2000). This localization is associated with protection of mitochondria from damaging stimuli and prevention of cell apoptosis (Massari *et al.* 2000; Massari *et al.* 2003). Co-immunoprecipitation experiments show a possible interaction between PorB and VDAC, which is the major metabolite pathway through MOM and involved in mitochondria induced cell apoptosis (Massari *et al.* 2000). This interaction could possibly explain the inhibition of apoptosis by PorB proteins.

In the planar membranes, the purified PorB shows a conductance comparable with that of VDAC (Song *et al.*, 1998c). The structure of both channels was proposed to be a β barrel. The anion-selectivity and voltage-gating of PorB is also similar to that of VDAC (Song *et al.*, 1998c). These similarities in characteristics suggest similar functions. Thus PorB may substitute for VDAC functions in mitochondria and inhibit apoptosis. In this chapter, the PorB gene was introduced into yeast lacking VDAC1, so that its function in the mitochondrial outer membrane could be studied without the interference from VDAC. Note that yeast does not undergo apoptosis and does not have the built-in apoptosis machinery. Thus the yeast mitochondria are ideal for modeling the metabolite or protein channel forming capacity of a molecule. However, we have not found any VDAC-like functions of PorB in the yeast system.

Materials and Methods

Planar phospholipid membrane studies

Planar phospholipid membranes were generated according to standard methods (Montal and Muller, 1972; Colombini, 1987a). The membrane was formed from phospholipid monolayers consisting of diphytanoyl phosphatidylcholine, polar extract of soybean phospholipids (both from Avanti Polar Lipids, Alabaster, AL) and cholesterol (Sigma, St Louis, MO) in a 1:1:0.1 mass ratio.

PorB was a kindly gift from Dr. Lee Wetzler (Boston University). The protein was refolded in 1 mM Tris Cl, 10 mM EDTA, 0.1% Zwittergent (pH 7.5). 1% Triton X-100 was added before $2 - 5$ μl aliquots were added into the 4-6 ml of aqueous solution bathing the planar membrane (solution A: 0.1 M KCl, 1 mM $MgCl_2$, 5 mM HEPES, pH 6).

VDAC was purified from mitochondria isolated from rat liver (Freitag *et al.*, 1983; Song *et al.*, 1998a). A $2 - 5$ μL aliquot of the VDAC-containing solution (2.5% Triton X100, 50 mM KCl, 10 mM Tris, 1 mM EDTA, 15% DMSO, pH 7.0) was stirred into the solution A.

After channel insertions, a triangular voltage wave at a frequency of 3 mHz from −52 mV to +52 mV was applied to the *cis* side. All experiments were performed at approximately $23^{o}C$.

Liposome studies

The liposomes with or without PorB were generated according to Colombini (1980b). Essentially 2 mg DPyPC, 0.5 mg egg PS, 0.1 mg cholesterol, dissolved in

chloroform was mixed together and dried down with nitrogen gas and kept in vacuum overnight. 200 μl of buffer (0.1% dextran, 100mM KCl and 5mM HEPES, pH=7.2) with C^{14}-dextran (10^5 cpm), H^3-glucose (10^6 cpm), ATP (10^{-4}M) and with or without 20 μg PorB was added to the dried lipids. The mixture was sonicated (0-5°C) and freeze-thawed and then extruded through a polycarbonate membrane filter to produce uniform single walled liposomes, 100 nm in diameter. The liposomes were separated from the buffer solutions through gel-filtration (Sephacryl S-200). The ATP level retained in the liposome was measured by the luciferin-luciferase assay. The dextran and glucose levels were measured according to its radioactivity. The volume of liposomes was determined by dividing the ^{14}C radioactivity in the liposomes by radioactivity per unit volume of the medium. A similar calculation yields an apparent ATP and glucose volume. These volumes reflect the amount of ATP and glucose that have not leaked out of the liposomes and was used to determine the degree of channel formation and the ability of ATP to permeate through the wall of the liposome.

Transfection of PorB into VDAC knockout yeast

The PorB3 gene in Topo 2.1 plasmid (Invitrogen) was a gift from Dr. Sanjay Ram (University of Massachusetts Medical School). The pRS316 (with ADH promoter) yeast plasmid was a gift from Dr. Mike Forte (Vollum Institute). The PorB3 gene and the yeast plasmid were cut by the restriction enzymes SpeI and HindIII (both from Promega) and subsequently subjected to 1% agarose-gel electrophoresis and separated. The desired fragments (the PorB3 and pRS316 cut with SpeI and Hind III) were recovered from the agarose gel using QIAEX II gel extraction kit (Qiagen) and ligated using T4 ligase (Promega). The ligation mixture was subsequently transfected into Top 10 cells

(Invitrogen) and the yeast plasmid pRS316 with PorB3 was purified following Qiagen midi prep kit (Qiagen). A portion of the DNA was subjected restriction enzyme treatment and electrophoresis to check for successful ligation of the yeast plasmid and PorB3 gene (Fig. 7.1). Another portion of the DNA and the empty plasmid pRS316 ADH were transfected into VDAC knockout yeast following the method of Gietz and Woods (2002). The PorB3 gene, the 1kb band in lane 3 (Fig. 7.1), was sequenced (DNA sequence facility, University of Maryland Biotechnology Institute) to confirm the presence of PorB3 gene.
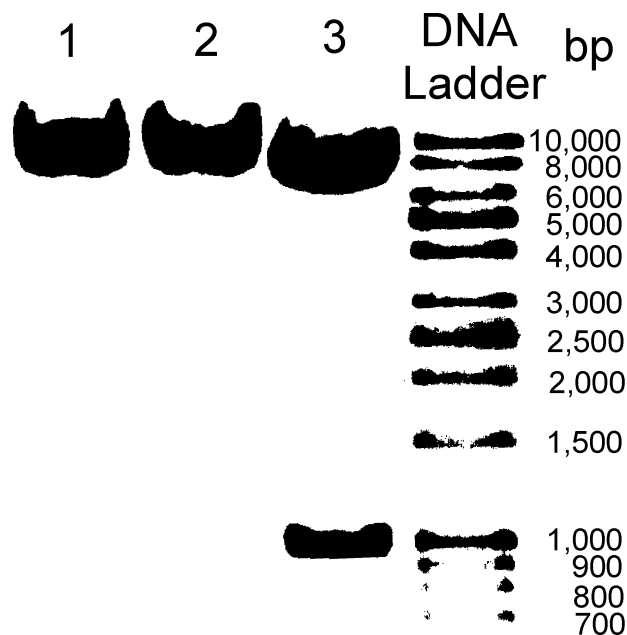

Fig. 7.1 Electrophoresis of restriction enzyme treated pRS-ADH-PorB3 plasmid.
Restriction enzyme treatment: lane1 - SpeI, lane 2 – HinIII, lane 3 – SpeI/HindIII.
The total amount of DNA in each lane is 4 μg.

Preparation of Yeast Cells

To facilitate cell growth and harvesting, stock cultures were prepared. A colony of yeast cells (PorB3 and control), was inoculated into 100 ml of medium consisting of 670 mg of yeast nitrogen base (DIFCO LABORATORIES, Detroit, MI), 77 mg of CSM-URA (Q-BIOgene, Carlsbad, CA), and either 2.4 ml of 85% lactic acid (NADH experiment) or 2 g dextrose (adenylate kinase activity experiment). The pH was adjusted to 5.0. When the cells reached an O.D. (600nm) of between 1.0 and 1.2, they were stored at 4°C for later use. For mitochondrial isolation, 20 ml of yeast stock solution was inoculated into each flask containing one liter of the same medium and grown with shaking at 30°C. An O.D. (600nm) between 1.0 and 1.2 was reached at 40 hours (lactic acid media) or overnight (dextrose media) after inoculation. Typically, 1 - 2 grams of cells were obtained and used for the isolation of mitochondria.

Isolation of Intact mitochondria

Mitochondria were isolated from both yeast phenotypes (PorB3 and control) essentially as published by Daum *et al.* (1982) but modified as previously described (Lee et al., 1998). The mitochondrial pellet was suspended in approximately 200 µl of medium containing 0.65 M mannitol, 10 mM HEPES, 10 mM KH_2PO_4, 5 mM KCl and 5 mM $MgCl_2$, pH 7.2 in order to measure NADH oxidation. The protein concentration of the mitochondrial suspension is measured by using 100mM Tris·SO_4, 0.4% SDS, pH 9.4 solution (Clarke, 1976). Equal amounts of the solution and the mitochondrial suspension is mixed and the absorbance measured at 280nm and 310 nm. The concentration of protein is $(A_{280}-A_{310})/1.05$ (mg/ml). Typically, the final protein concentration was about 20 mg/ml.

NADH oxidation measurement

NADH oxidation was measured according to Lee *et al.* (1998). Briefly, a portion of yeast mitochondria (about 250 μg mitochondrial protein) was diluted into the yeast respiration medium containing 0.65 M sucrose, 10 mM HEPES, 10 mM KH_2PO_4, 5 mM KCl and 5 mM $MgCl_2$ with pH at 7.2. NADH oxidation was measured as the absorbance change at 340 nm after the addition of 30 μM NADH. Another portion of mitochondria was mildly shocked by incubation with 2 volumes of distilled water on ice for 10 minutes followed by addition of 5 volumes of yeast respiration medium and 2 volumes of double concentrated yeast respiration medium to restore the osmotic pressure.

Adenylate kinase activity (ADP/ATP permeability) assay

In order to estimate the MOM permeability to ADP/ATP, a method similar to that described for NADH was used. The flux of ADP/ATP across the MOM was determined by comparing the activity of adenylate kinase of intact and mildly shocked mitochondria. The intermembrane space enzyme adenylate kinase was assayed by a standard method (Sottocasa, 1967), using a coupled enzyme system (hexokinase and glucose-6-phosphate dehydrogenase) and detecting the rate of $NADP^+$ reduction to NADPH, measured as the absorbance increase at 340 nm. The permeability was calculated according to a published method (Colombini, 2007).

Samples of intact mitochondria were prepared from a 200-fold dilution of the mitochondrial suspension ($\sim$ 20 mg/ml of total protein) with A-medium (0.6 M sucrose, 50 mM Tris-Cl, 5mM $MgSO_4$, 10 mM Glucose, 0.2 mM $NADP^+$, 20 μg/ml atractylosides, 0.2 mM KCN, pH 7.5). Mildly shocked mitochondria were obtained by

mixing the mitochondria with 2 volumes of distilled water and incubated in ice for 10 min, followed by addition of 5 volumes of A-medium and 2 volumes of double concentrated A-medium to restore the osmotic pressure. An aliquot containing ADP (250 μM final concentration), hexokinase and glucose-6-phosphate dehydrogenase (10 units each) was added to start the reaction.

SDS-PAGE electrophoresis and western blot

To determine whether PorB proteins are expressed in the transfected yeast and determine their localization, the spheroplasts and mitochondria from both phenotypes were mixed with sample buffer and subject to SDS-PAGE electrophoresis using a 12% pre-made gel from Pierce with Trip-HEPES buffer, according to the manual. The proteins were subsequently transferred to nitrocellulose using a Genie blotter (Idea Scientific, Minneapolis, MN). The PorB protein was detected with rabbit anti-PorB serum (a gift from Dr. Lee Wetzler) and goat anti-rabbit AP 10 western blotting kit (Oxford Biomedical Research) (see Fig. 7.6A).

Results and Discussion

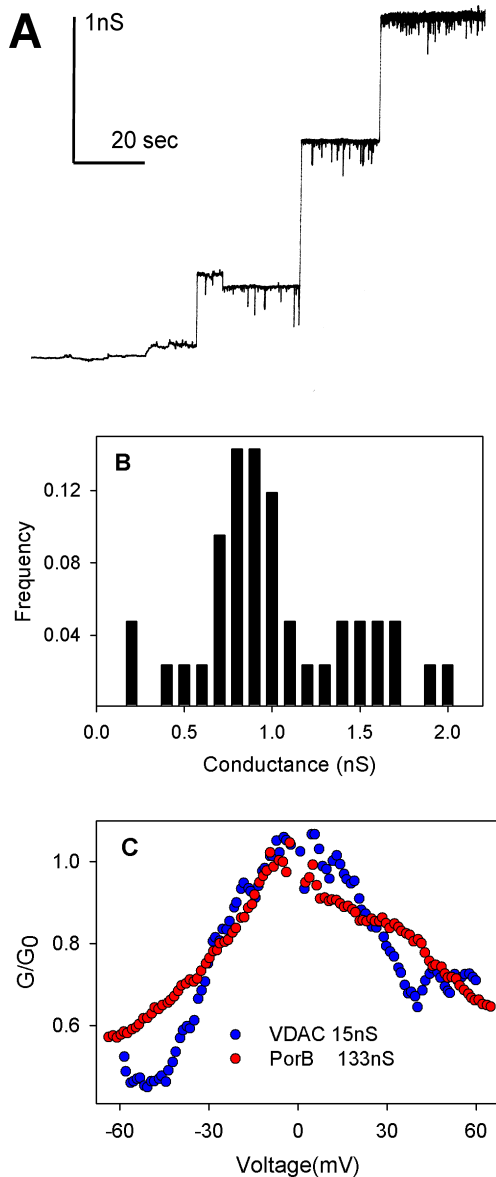## PorB forms VDAC-like channels in planar membranes

Figure 7.2 The electrophysiological characteristics of PorB (A) An example of the insertion of PorB into planar membranes. **(B)** The histogram of the sizes of single insertion events. **(C)** Comparison of the voltage dependence the reconstituted VDAC and PorB channels.

In an effort to test for functional interactions, purified PorB and VDAC were both reconstituted into planar membranes and the channel properties compared.

Detergent refolded PorB proteins were added to the aqueous solution on one side of a phospholipid membrane, and the conductance increases were recorded. Fig. 7.2A shows the insertion pattern of PorB channels into the planar membranes. In the reconstituted systems, the observed single channel conductance is about 0.9 nS (Fig 7.2B). Because PorB is a trimer, each monomer would thus have a conductance of 0.3 nS. The reconstituted channel is also voltage-gated, similar to VDAC (Fig. 7.2C). These results are consistent with those of a previous study on PorB channels (Song *et al.*, 1998c), which also shows a similar ion selectivity of both channels.

Possible interactions between VDAC and PorB

We generated an experimental plan to understand the possible interactions between VDAC and PorB. VDAC was added to the planar membranes first. After several channel insertions, the voltage gating properties were recorded. Then the chamber was perfused to remove any VDAC that had not formed channels. PorB was then added to the planar membranes and after several insertions of PorB channels, the voltage gating was recorded again. When the PorB conductance was at least 10 times more than the original VDAC conductance, the voltage gating pattern was assumed to be the property of PorB (Fig 7.3A). In order to generate the PorB conductance/voltage plot in the presence of VDAC, the conductance/voltage curve of VDAC alone was subtracted from the total (i.e. PorB and VDAC together).

To our surprise, the mixed VDAC and PorB channels show a higher tendency to enter the closed states than that of the calculation (Fig. 7.3B). It seems that either VDAC tends to close PorB or PorB tends to close VDAC. Because PorB is able to inhibit
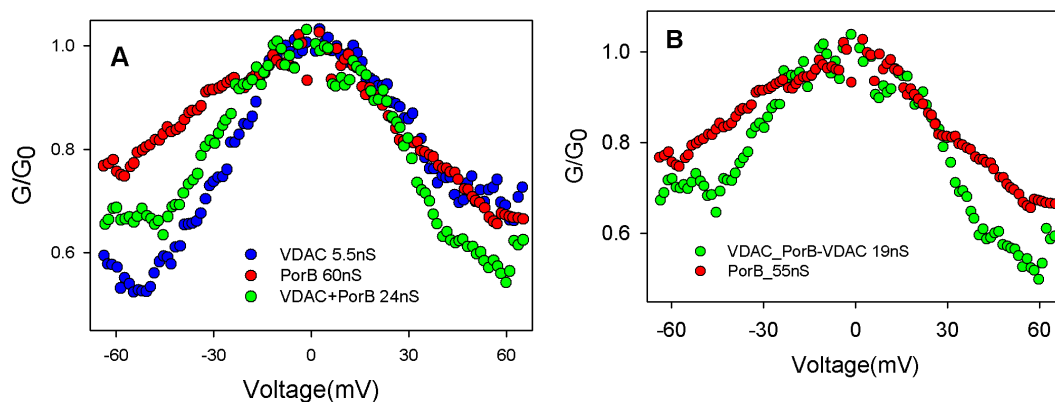

Figure 7.3 (A) The voltage gating of VDAC, PorB individually and together. The channels were reconstituted into the planar membrane in the sequence described in the text. **(B) The comparison of the voltage dependence of the conductance of PorB in the presence (calculated values from A) or absence (experimental values) of VDAC.**

apoptosis, this result seems to be in conflict to our hypothesis that closure of VDAC favors apoptosis.

However, there is a correlation between the voltage dependence and conductance of PorB proteins (Fig. 7.4A). Multiple channel membranes generally show less voltage dependence. This is not due to leakage as La^{3+} ions are still able to inhibit those conductances (Fig. 7.4B). The possible reason for the loss of voltage dependence with
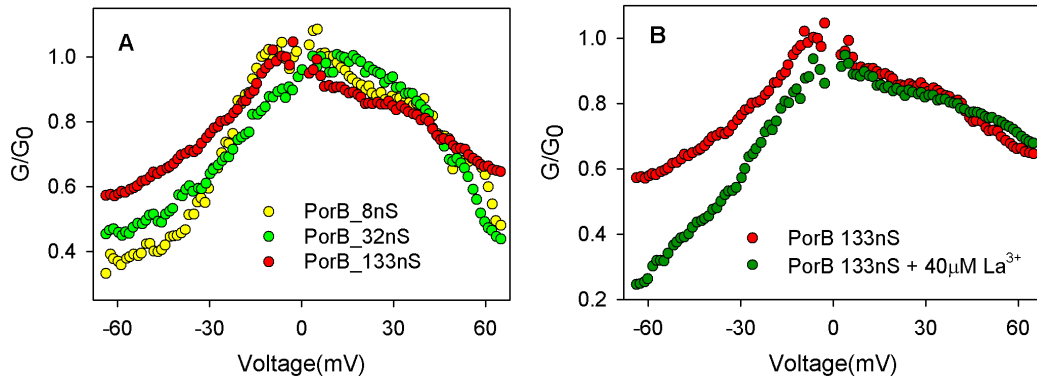
Figure 7.4 (A) The loss of voltage dependence of PorB channels with increasing conductance. **(B)** The steep voltage dependence in the presence of 40 μM La^{3+}.

increased conductance could be due to the increase of access resistance and hence the decrease of actual applied voltage through the pore, which can be calculated from the conductance change theoretically following the equations below (Jeans, 1925; Hall, 1975):

$$R_{channel} = R_{pore} + R_{access} = (l + \frac{\pi a}{2})\frac{\rho}{\pi a^2}$$ (7.1)

$$R_{pore} = \frac{\rho l}{\pi a^2}$$ (7.2)

$$R_{acess} = \frac{\rho}{2a}$$ (7.3)

where R is the resistance, l is the length of the pore, a is the radius of the pore and ρ is the resistivity of the solution.

The above equations only calculate the channel conductance when there is no selectivity or interactions between ions and the channel, which is not true for channels such as VDAC or PorB. For example, the single channel resistance (R_0) of VDAC in 0.1 M KCl solution is 2.5 GΩ, while equation 7.1 gives a value of 1 GΩ. Therefore, practically

$$R_{pore} = R_0 - R_{acess} = R_0 - \frac{\rho}{2a} \tag{7.4}$$

VDAC channels normally insert into the membrane cooperatively, which is also observed for PorB channels (Data not shown). It is possible that they form a large circular aggregate or patch in the planar membrane. Thus for n channels,

$$R_{pores} = \frac{R_0 - \frac{\rho}{2a}}{n} \tag{7.5}$$

$$R_{acess} = \frac{\rho}{2a\sqrt{n+(\frac{n-1}{3})}} \approx \frac{\rho}{2a\sqrt{n+\frac{n}{3}}} = \frac{\sqrt{3}\rho}{4a\sqrt{n}} \tag{7.6}$$

for hexagonal close packing. This approximation ignores the thickness of the channel.

Therefore, assuming $K = 4aR_0 - 2\rho$,

$$\frac{R_{pores}}{R_{channels}} = \frac{R_{pores}}{R_{pores} + R_{acess}} = \frac{K}{K+\sqrt{3}\rho\sqrt{n}} \tag{7.7}$$

$$V_{applied} = \frac{K}{K+\sqrt{3}\rho\sqrt{n}}V_{total} \tag{7.8}$$

Thus the actual voltage applied to the pores is less than the actual value and decreases with increased channel insertions, hence the channels have less tendency to close. Therefore, the observed closure of PorB-VDAC mixed channels is actually due to the fact that the voltage gating of PorB is underestimated. Thus, in the planar membranes, we don't observe any significant interactions between VDAC and PorB channels.

PorB is permeable to small metabolites such as ATP

PorB is able form a VDAC-like channels in the planar membranes. It is possible that PorB can function like VDAC in the MOM, allowing ATP flux through the channel. To determine if PorB is permeable to small metabolites such as ATP, liposome containing ^{14}C-dextran (average MW 70KDa), ^{3}H-D-glucose and ATP was generated. Presumably, the high molecular weight dextran will be completely retained, i.e. be 100% trapped in the liposome. Therefore the retention of other molecules can be compared with that of dextran by calculating the fraction of the dextran volume that contains the
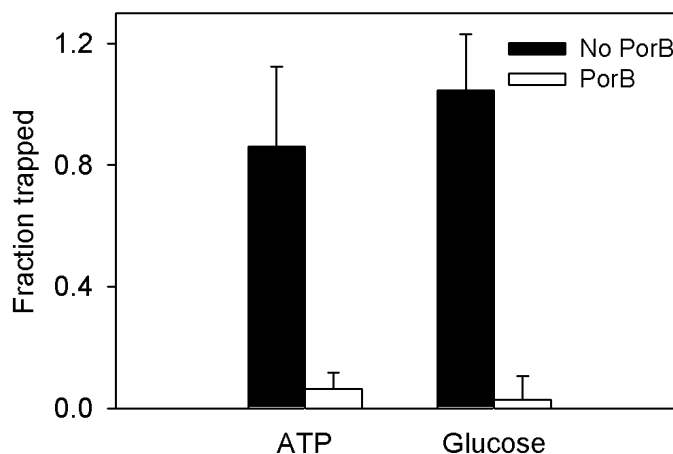

Figure 7.5 PorB containing liposome is permeable to ATP and glucose. The results are mean ± S.E of three independent experiments.

other molecules. From Fig.7.5, it is clear that PorB containing liposomes are permeable to ATP. The release of glucose confirms channel formation and its release in indistinguishable from that of ATP. Further, there is no channel activity in the control experiments indicating that the liposome membranes are effective at retaining all the constituents.

PorB failed to restore VDAC-like function in VDAC⁻ yeast

Since PorB is able to insert into the mitochondrial outer membranes and the channel itself allows ATP to permeate, it is possible that it may function as a metabolite permeation channel *in vivo*. To test this hypothesis, the PorB gene was transfected into VDAC1 knockout yeast as indicated in the *Materials and Methods* (Fig. 7.6A). The PorB transfected VDAC1⁻ yeast grows at a similar rate as the empty plasmid transfected VDAC⁻ yeast (Fig. 7.6B). This is similar to the rate of VDAC1⁻ yeast and much slower than the rate for VDAC containing wild type yeast (Lee *et al.* 1998). In the exponential
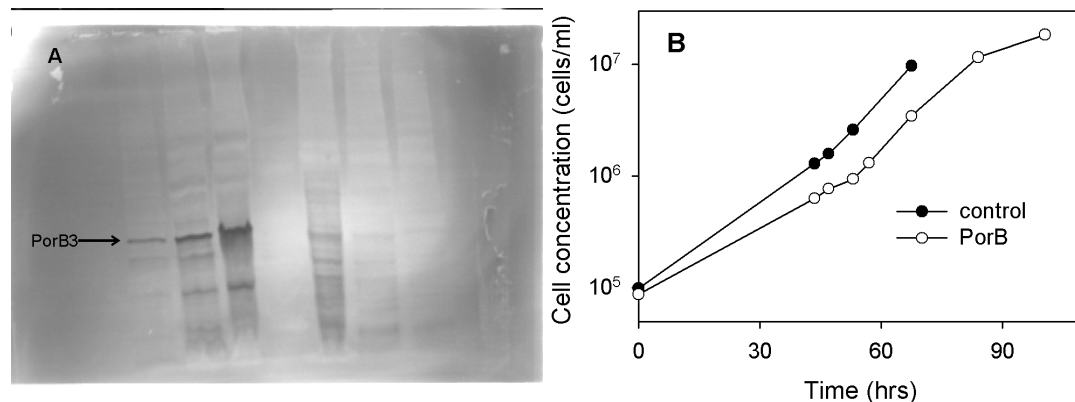
Figure 7.6 (A) The transfection of PorB3 gene into VDAC1⁻ yeast and its localization in the mitochondria. This is the western blot as described in the methods. The lanes are from left to right are: mitochondria (protein amount) 1.5 μg, 4.5 μg, 15 μg, molecular marker, spheroplasts 20 μl, 6μl, 2μl. (B) The growth curve of PorB transfected VDAC1⁻ yeast (PorB) and empty plasmid transfected VDAC1⁻ yeast (control) in the lactic acid medium.

growth region, the doubling time is about 9 hours for both strains. In addition, PorB

expressing VDAC1⁻ yeast failed to grow in the glycerol medium at 37˚C. This

temperature-sensitive phenotype is diagnostic of VDAC1 knock-outs. These results

suggest that PorB cannot restore the functions lost by the loss of VDAC1.
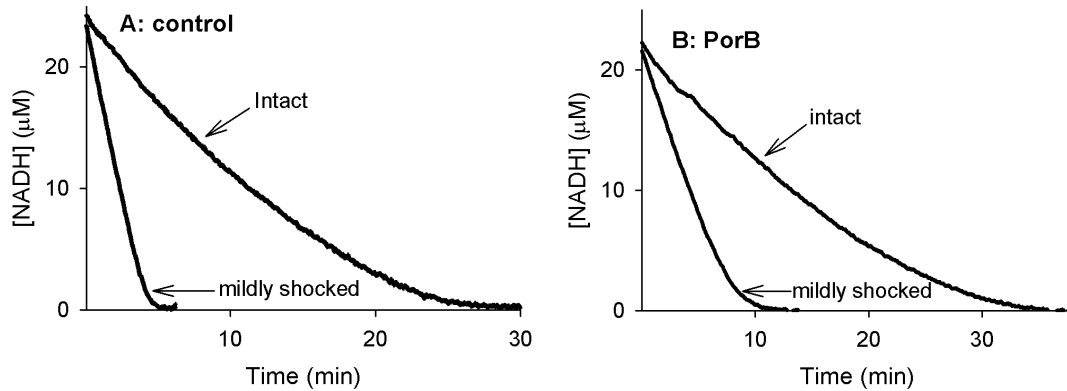
Figure 7.7 NADH oxidation by mitochondria isolated from empty plasmid (A) or
PorB (B) transfected VDAC1- yeast. The amount of mitochondria applied is 125
μg/ml and 94 μg/ml protein concentration in control experiment and PorB experiment
respectively.

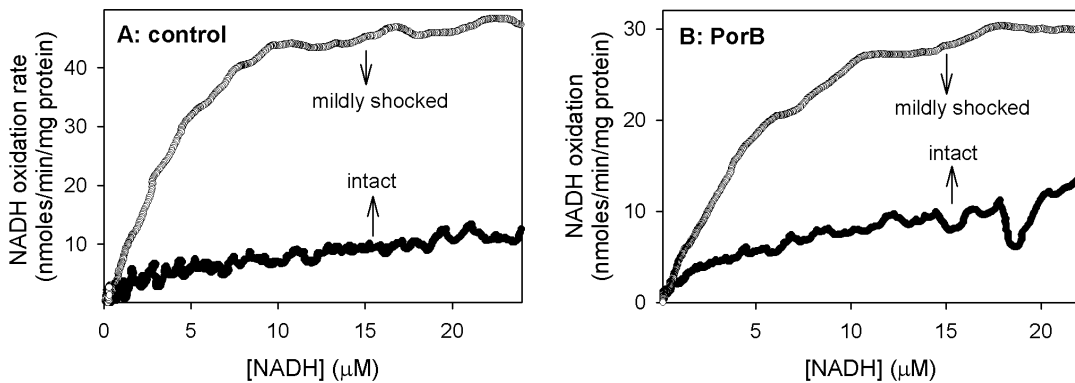**Figure 7.8 NADH oxidation rate** by mitochondria isolated from empty plasmid (A)
or PorB (B) transfected VDAC1⁻ yeast. The rates are calculated from the figure 7.7

The mitochondria of the transfected yeast were isolated and NADH oxidation

measured (Fig. 7.7). It is clear that, in the cells expressing PorB, the outer membrane is

still a major barrier to NADH permeation. This barrier slows down the rate of oxidation

of NADH as compared to that of the mildly shocked mitochondria, which have disrupted outer membranes. By contrast, in VDAC1-expressing yeast, damaging the outer membrane increases the rate of NADH oxidation by only a small amount (Lee *et al.* 1998). These results demonstrate the inability of PorB to significantly increase NADH through the mitochondrial outer membrane in VDAC1⁻ yeast.

The experimental traces of NADH oxidation can be converted into plots of the rate of NADH oxidation as a function of the medium [NADH] (Fig. 7.8). For intact mitochondria, the permeability to NADH can be thus quantified following the methods of Lee *et al.* (1998):

$$\frac{d[NADH]}{dt} = \varphi_{NADH} = P_{NADH}([NADH]_o - [NADH]_i) \qquad (7.9)$$

where φ is the flux of NADH across the mitochondrial outer membrane, P is the permeability of the outer membrane to NADH, "o" and "i" denote the [NADH] in the medium and in the mitochondrial intermembrane space. The [NADH]$_i$ is determined from the [NADH] that yields the same rate of NADH oxidation in the mildly shocked mitochondria. Thus the permeability can be calculated (Fig. 7.9).
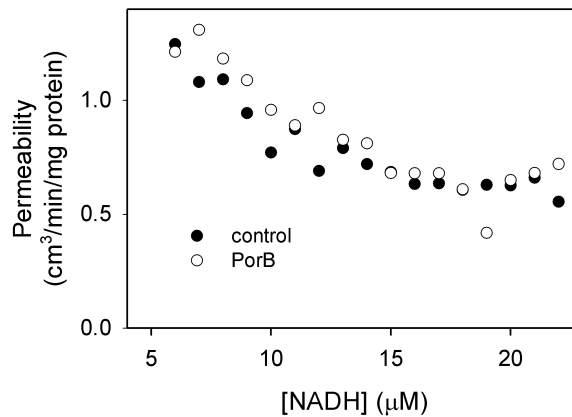
Figure 7.9 NADH Permeability of the outer membrane of mitochondria isolated from empty plasmid (A) or PorB (B) transfected VDAC1⁻ yeast.

Clearly, there is no significant increase of the MOM permeability to NADH after PorB transfection. This lack of increase of permeability is not due to the use of NADH, as there is also no significant increase of ADP/ATP permeability (Fig. 7.9). The ADP/ATP permeability through the mitochondrial outer membrane was estimated by measuring adenylate kinase activity, recorded as the production of NADPH (see methods). In the absence of VDAC, the permeation of ADP/ATP across the intact outer membrane is very slow, resulting a slow production of NADPH. Therefore, there is a huge difference in adenylate kinase activity between the intact and shocked mitochondria. However, the transfection of PorB does not facilitate the permeation of ADP/ATP (Fig. 7.10). The permeability of the MOM to ADP/ATP (cm^3/min/mg protein) is 0.115 in empty plasmid transfected yeast and 0.114 in PorB3 transfected yeast, respectively. Thus in the transfected systems, we failed to obtain any functional PorB channel formation even though it localized in the mitochondrial outer membrane.
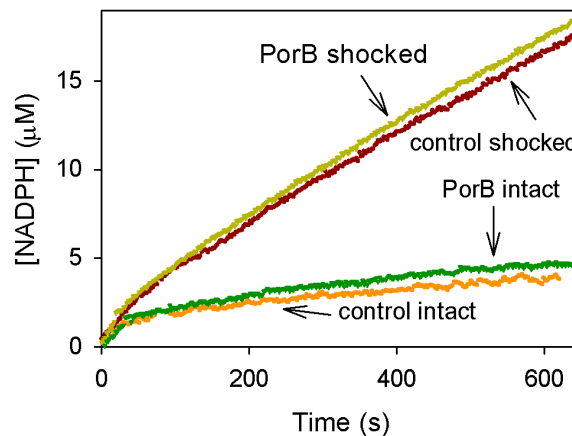
Figure 7.10 NADPH production as an indication of adenylate kinase activity. Concentrations of mitochondrial protein were 108 μg/ml (PorB), 87 μg/ml (control).

Conclusions

For the first hypothesis that PorB may interaction with VDAC, the experiments showed no significant functional interaction in the purified/reconstituted system. The findings that PorB containing liposomes are permeable to ATP lead to the hypothesis that PorB may function as VDAC in the MOM and thus increase metabolite flow and inhibit apoptosis. However, an attempt to test the hypothesis by expressing PorB in VDAC1 knockout yeast was unsuccessful. It is possible that PorB inserted into yeast mitochondria is improperly folded and thus does not form channels. It is also possible that PorB permeability to ADP/ATP is low and undetectable above the background permeability, yet sufficient to inhibit the onset of apoptosis in mammalian cells.

At this point, the mechanism by which PorB inhibits apoptosis, remains elusive. It is possible that the function of PorB or its interaction with VDAC requires some mammalian proteins that is lacking in yeast and is lost after the isolation of mitochondria. It is also possible that PorB inhibits apoptosis in a mechanism that is not related to the MOM permeability to metabolites, as our hypothesis only accounts for part of mitochondria-induced apoptosis. Future studies are needed to understand the significance of the localization of PorB in mitochondria and its mechanism of inhibiting apoptosis.

Chapter 8

Discussion & Future Directions

In this dissertation, I presented my work regarding the relationship between metabolite permeability through the MOM and the onset of apoptosis. The first part of my dissertation deals with the correlation between VDAC closure *in vitro* (in planar membranes), *in vivo* (in MOM) and cytochrome c release from mitochondria (the initiation of apoptosis). The specific mechanism of the interactions between VDAC and the phosphorothioate oligonucleotides was also elucidated. Thus, a hypothetic model of the relationship between the initiation of apoptosis and metabolite permeation through MOM was established.

The second part of my dissertation is further studies on this model. The control of calcium permeability through VDAC gating was demonstrated, which may have implications on mitochondrial swelling and cell apoptosis. In addition, *Neisseria meningitidis* outer membrane protein PorB was found to be similar to VDAC in allowing metabolite flow. Its ability to form channels for metabolite flow in mitochondria was tested but failed.

In this chapter, I indicate some directions for future work and speculate on possible mechanisms.

The immediate effect of VDAC closure

Even though the correlation between VDAC closure and initiation of apoptosis is clear, the immediate effect of VDAC closure and the direct cause of cytochrome c release are still to be determined. The closure of VDAC stops metabolite flow and, in the short

term, the ATP/ADP ratio, phosphocreatine/creatine ratio and the PMF (proton motive force) will increase because of insufficient ADP. These may lead to changes in the enzyme activities in the mitochondria through phosphorylation of the appropriate enzymes. It is possible that the oligomerization of Bax or Bak occurs subsequently, which forms the large protein permeation pores in the outer membrane. Another possible candidate pore is ceramide channel formation, which allows cytochrome c release into the cytosol.

Thus the influence of VDAC closure on metabolite levels, enzyme activities, and apoptotic molecules can be measured to establish the link between MOM permeability to metabolites and initiation of apoptosis.

The open VDAC channels in the MOM

Rostovtseva *et al.* (1998) has found that only 1% of the measured permeability of ADP through the open VDAC channel is needed for the normal mitochondrial respiration. Thus only when the permeability is substantially reduced will the permeation of ADP through the MOM be rate limiting.

Regardless of this estimation, G3139 can easily close VDAC channels to a degree that the respiration is greatly reduced, suggesting the limitation of ADP flow across the MOM. The effect on the mitochondria is actually stronger than what was observed in planar membranes. Thus it is possible that the fraction of VDAC channels that are open is so low that the metabolite flow through VDAC becomes important physiologically.

This is important in understanding the role of PorB in apoptotic regulation. In the experiments, we failed to observe the restoration of function by the expression of PorB in

VDAC knockout yeast. The measured MOM permeability to metabolites such as NADH in PorB transfected yeast is also very low, similar as that of VDAC lacking the MOM. However, the liposome studies showed that PorB is an ATP permeable channel. It is possible that this permeability is so low, compared to that of VDAC, that we cannot detect it. However, in early apoptosis, this low permeability could be enough to increase metabolite flow, as only a few percent of open VDAC is possibly needed. Another issue regarding of function of PorB in the MOM is the amount of insertion. Thus a measurement of the change in total metabolite flux following the expression of PorB needs to be performed to fully understand the problem.

The regulation of Bcl-2 family proteins

The relationship between the onset of apoptosis and MOM permeability needs to be regulated by Bcl-2 family proteins. This regulation could occur at the level of VDAC gating, enzyme activities or apoptotic molecules. It has been observed that the presence of Bax and/or Bak is able to strengthen G3139 inhibition on the MOM permeability. This suggests that G3139 may compete with other anti-apoptotic proteins for binding to VDAC. The presence of pro-apoptotic proteins may bind to those anti-apoptotic proteins and increase the available binding site in VDAC for G3139. However, the specific mechanism is lacking. We know that Bcl-x_L is able to open VDAC channels (Vander Heiden *et al.,* 2001). In addition, any effect of other Bcl-2 family proteins on VDAC needs to be determined. These studies may further the understanding of the regulation of apoptosis by Bcl-2 proteins.

References

Akeson, M., D. Branton, J.J. Kasianowicz, E. Brandin, D.W. Deamer. 1999. Microsecond time-scale discrimination among polycytidylic acid, polyadenylic acid, and polyuridylic acid as homopolymers or as segments within single RNA molecules. *Biophys. J.* 77:3227-3233.

Anderson, E.M., P. Miller, D. Ilsley, W. Marshall, A. Khvorova, C.A. Stein and L. Benimetskaya. 2005. Gene profiling study of G3139- and Bcl-2-targeting siRNAs identifies a unique G3139 molecular signature. *Cancer Gene Ther.* 13:406-414.

Antonsson, B., S. Montessuit, B. Lauper, R. Eskes and J.C. Martinou. 2000. Bax oligomerization is required for channel-forming activity in liposomes and to trigger cytochrome c release from mitochondria. *Biochem. J.* 345:271-278.

Antonsson, B., S. Montessuit, B. Sanchez and J.C. Martinou. 2001. Bax is present as a high molecular weight oligomer/complex in the mitochondrial membrane of apoptotic cells. *J. Biol. Chem.* 276:11615-11623.

Arora, A.S., B.J. Jones, T.C. Patel, S.F. Bronk and G.J. Gores. 1997. Ceramide induces hepatocyte cell death through disruption of mitochondrial function in the rat. *Hepatology* 25:958-963.

Basanez, G., A. Nechushtan, O. Drozhinin, A. Chanturiya, E. Choe, S. Tutt, K.A. Wood, Y.-T. Hsu, J. Zimmerberg and R.J. Youle. 1999. Bax, but not Bcl-X_L, decreases the lifetime of planar phospholipid bilayer membranes at subnanomolar concentrations. *Proc. Natl. Acad. Sci. USA.* 96:5492-5497.

Báthori, G., G. Csordás, C. Garcia-Perez, E. Davies and G. Hajnóczky. 2006. Ca^{2+}-dependent control of the permeability properties of the mitochondrial outer membrane and voltage-dependent anion-selective channel (VDAC). *J Biol Chem.* 281:17347-17358.

Belaud-Rotureau, M.A., N. Leducq, F. Macouillard Poulletier de Ganes, P. Diolez, L. Lacoste, F. Lacombe, P. Bernard and F. Belloc. 2000. Early transitory rise in intracellular pH leads to Bax conformational change during ceramide-induced apoptosis. *Apoptosis.* 5:551-560.

Benimetskaya, L., J. Loike, Z. Khaled, G. Loike, S. Silverstein, L. Cao, J. El-Khoury, T.-Q. Kai and C.A. Stein. Mac-1 (CD11b/CD18) is an oligodeoxynucleotide-binding protein. 1997. *Nat. Med.* **3**, 414-420.

Benimetskaya, L., T. Wittenberger, C.A. Stein, H.-P. Hofmann, C. Weller, J. Lai, P. Miller and V. Gekeler. 2004a. Changes in gene expression induced by phosphorothioate oligodeoxynucleotides (including G3139) in PC3 prostate

carcinoma cells are recapitulated at least in part by treatment with interferon-beta and -gamma. *Clin. Cancer Res.* 10:3678-3688.

Benimetskaya, L., J. Lai, S. Wu, E. Hua, A. Khvorova, P. Miller and C.A. Stein. 2004b. Relative Bcl-2 independence of drug-induced cytotoxicity and resistance in 518A2 melanoma cells. *Clin. Cancer Res.* 10:8371-8379.

Blachly-Dyson, E., S. Peng, M. Colombini, and M. Forte. 1990. Selectivity changes in site-directed mutants of the VDAC ion channel: structural implications. *Science.* 247:1233-1236.

Bossy-Wetzel, E., D. Newmeyer and D. Green. 1998. Mitochondrial cytochrome c release in apoptosis occurs upstream of DEVD-specific caspase activation and independently of mitochondrial transmembrane depolarization. *EMBO J.* 17:37-49.

Brindle, K.M., M.J. Blackledge, R.A. Challiss and G.K. Radda. 1989. ^{31}P NMR magnetization-transfer measurements of ATP turnover during steady-state isometric muscle contraction in the rat hind limb in vivo. *Biochemistry* 28:4887-4893.

Brown, G.C. 1992. Control of respiration and ATP synthesis in mammalian mitochondria and cells. *Biochem. J.* 284:1-13.

Castedo, M., T. Hirsch, S.A. Susin, N. Zamzami, P. Marchetti, A. Macho, A. and G. Kroemer. 1996. Sequential acquisition of mitochondrial and plasma membrane alterations during early lymphocyte apoptosis. *J. Immunol.* 157:512-521.

Cesura, A., E. Pinard, R. Schubenel, V. Goetschy, A. Friedlein, H. Langen, P. Polcic, M. Forte, P. Bernardi and J. Kemp. 2003. The voltage-dependent anion channel is the target for a new class of inhibitors of the mitochondrial permeability transition pore. *J. Biol. Chem.* 278:49812-49818.

Cheng, E.H., T.V. Sheiko, J.K. Flisher, W.J. Craigen and S.J. Korsmeyer. 2003. VDAC2 inhibits BAK activation and mitochondrial apoptosis. *Science* 301:513-517.

Cho, Y., F.C. Zhu, B.A. Luxon and D.G. Gorenstein. 1993. 2D ^{1}H and ^{31}P NMR spectra and distorted A-DNA-like duplex structure of a phosphorodithioate oligonucleotide. *J. Biomol. Struct. Dyn.* 11:685-702.

Clarke, S. 1976. A major polypeptide component of rat liver mitochondria: carbamyl phosphate synthetase. *J. Biol. Chem.* 251**:**950 – 961.

Cescatti, L., C. Pederzolli, and G. Menestrina. 1991. Modification of lysine residues of Staphylococcus aureus alpha-toxin: effects on its channel-forming properties. *J. Membr. Biol.* 119:53-64.

Colombini, M. 1979. A candidate for the permeability pathway of the outer mitochondrial membrane. *Nature.* 279: 643-645.

Colombini, M. 1980a. Structure and mode of action of a voltage-dependent anion-selective channel (VDAC) located in the outer mitochondrial membrane. *Ann. New York Acad. Sci.* 341:552–563.

Colombini, M. 1980b. Pore size and properties of channels from mitochondria isolated from Neurospora crassa. *J. Membr. Biol.* 53:79-84.

Colombini, M. 1986. Voltage gating in VDAC: toward a molecular mechanism, In: C. Miller (Ed.), *Ion Channel Reconstitution* Plenum Press, New York. Section 4, Chapter 10, pp.533-552

Colombini, M. 1987a. Characterization of channels isolated from plant mitochondria. *Methods Enzymol.* 148:465-475.

Colombini, M. 1987b. Regulation of the mitochondrial outer membrane channel, VDAC. *J. Bioenerg. Biomembr*. 19:309–320.

Colombini, M., C.L. Yeung, J. Tung, and T. Konig. 1987. The mitochondrial outer membrane channel, VDAC, is regulated by a synthetic polyanion. *Biochim. Biophys. Acta.* 905:279-286.

Colombini, M. 1989. Voltage gating in the mitochondrial channel, VDAC. *J. Membr. Biol.* 111:103-111.

Colombini, M., E. Blachly-Dyson and M. Forte M. 1996. VDAC, a channel in the outer mitochondrial membrane. *Ion Channels* 4:169-202.

Colombini, M. 2004. VDAC: The channel at the interface between mitochondria and the cytosol. *Mol. Cell Biochem.* 256/257:107-115.

Colombini, M. 2007. Measurement of VDAC permeability in intact mitochondria and reconstituted systems. In: Methods in Cell Biology, "Mitochondria" 2nd edition (Pon, L.A. and Schon. E.A. eds.) Academic Press, San Diego, CA. in press.

Crompton, M., S. Virji and J. Ward. 1998. Cyclophilin-D binds strongly to complexes of the voltage-dependent anion channel and the adenine nucleotide translocase to form the permeability transition pore. *Eur. J. Biochem.* 258:729-735.

Crompton, M. 1999. The mitochondrial permeability transition pore and its role in cell death. *Biochem J* 341:233-249.

Cui, S.T. 2004. Molecular dynamics study of single-stranded DNA in aqueous solution confined in a nanopore. *Mol. Phys.* 102:139-146.

Daum, G., P.C. Bohni and G. Schatz. 1982. Import of proteins into mitochondria. Cytochrome b2 and cytochrome c peroxidase are located in the intermembrane space of yeast mitochondria. *J. Biol. Chem.* 257:13028-13033.

Debatin, K., D. Poncet and G. Kroemer. 2002. Chemotherapy: targeting the mitochondrial cell death pathway. *Oncogene* 21:8786-8803.

De Maria, R., L. Lenti, F. Malisan, F. d'Agostino, B. Tomasini, A. Zeuner, M.R. Rippo and R. Testi. 1997. Requirement for GD3 ganglioside in CD95- and ceramide-induced apoptosis. *Science* 277:1652-1655.

Di Paola, M., T. Cocco and M. Lorusso. 2000. Ceramide interaction with the respiratory chain of heart mitochondria. *Biochemistry* 39:6620-6628.

Douce, R, J. Bourguignon, R. Brouquisse and M. Neuburger. 1987. Isolation of plant mitochondria: general principles and criteria of integrity. *Methods Enzymol* 148:403-412.

Florián, J., M. Štrajbl and A. Warshel. 1998. Conformational Flexibility of Phosphate, Phosphonate, and Phosphorothioate Methyl Esters in Aqueous Solution. *J. Am. Chem. Soc.* 120:7959-7966.

Florke, H., F.P. Thinnes, H. Winkelbach, U. Stadtmuller, G. Paetzold, C. Morys-Wortmann, D. Hesse, H. Sternbach, B. Zimmermann, P. Kaufmann-Kolle, M. Heiden, A. Karabinos, S. Reymann, V.E. Lalk, and N. Hilschmann. 1994. Channel active mammalian porin, purified from crude membrane fractions of human B lymphocytes and bovine skeletal muscle, reversibly binds adenosinetriphosphate (ATP). *Biol.Chem. Hoppe Seyler.* 375:513-520.

Frankel, S.R. 2003. Oblimersen sodium (G3139 Bcl-2 antisense oligonucleotide) therapy in Waldenstrom's macroglobulinemia: a targeted approach to enhance apoptosis. *Semin Oncol.* 30:300-304.

Freitag, H., R. Benz and W. Neupert. 1983. Isolation and properties of the porin of the outer mitochondrial membrane from Neurospora crassa. *Methods Enzymol.* 97:286-294.

Frey, P.A. and R.D. Sammons. 1985. Bond order and charge localization in nucleoside phosphorothioates. *Science* 228:541-5.

Gekeler, V., P. Gimmnich, H.P. Hofmann, C. Grebe, M. Rommele, A. Leja, M. Baudler, L. Benimetskaya, B. Gonser, U. Pieles, T. Maier, T. Wagner, K. Sanders, J.F. Beck, G. Hanauer and C.A. Stein. 2006. G3139 and other CpG-containing immunostimulatory phosphorothioate oligodeoxynucleotides are potent suppressors of the growth of human tumor xenografts in nude mice. *Oligonucleotides* 16:83-93.

Gellerich, F.N., M. Wagner, M. Kapischke, U. Wicker and D. Brdiczka. 1993. Effect of macromolecules on the regulation of the mitochondrial outer membrane pore and the activity of adenylate kinase in the inter-membrane space. *Biochim. Biophys. Acta.* 1142:217-227.

Ghafourifar, P., S.D. Klein, O. Schucht, U. Schenk, M. Pruschy, S. Rocha and C. Richter. 1999. Ceramide induces cytochrome c release from isolated mitochondria. Importance of mitochondrial redox state. *J. Biol. Chem.* 274:6080-6084.

Ghosh, M.K., K. Ghosh K and J.S. Cohen. 1993. Phosphorothioate-phosphodiester oligonucleotide co-polymers: assessment for antisense application. *Anticancer Drug Des.* 8:15-32.

Gietz, R.D. and R.A. Woods. 2002. Transformation of yeast by lithium acetate/single-stranded carrier DNA/polyethylene glycol method. *Methods Enzymol.* 350:87-96.

Gincel, D., H. Zaid and V. Shoshan-Barmatz. 2001. Calcium binding and translocation by the voltage-dependent anion channel: A possible regulatory mechanism in mitochondrial function. *Biochem. J.* 358:147–155.

Guvakova, M.A., L.A. Yakubov, I. Vlodavsky., J.L. Tonkinson and C.A. Stein. 1995. Phosphorothioate oligodeoxynucleotides bind to basic fibroblast growth factor, inhibit its binding to cell surface receptors, and remove it from low affinity binding sites on extracellular matrix. *J. Biol. Chem.* 270**:**2620-2627.

Gross, A., K. Pilcher, E. Blachly-Dyson, E. Basso, J. Jockel, M.C. Bassik, S.J. Korsmeyer and M. Forte. 2000. Biochemical and genetic analysis of the mitochondrial response of yeast to BAX and BCL-X(L). *Mol. Cell Biol.* 20:3125-3136.

Halestrap, A.P. and C. Brennerb. 2003. The adenine nucleotide translocase: a central component of the mitochondrial permeability transition pore and key player in cell death. *Curr Med Chem.* 10:1507-25.

Hall, J.E. 1975. Access resistance of a small circular pole. *J. Gen. Physiol.* 66:531-532.

Hart, S.P., C. Haslett, C. and I. Dransfield 1996. Recognition of apoptotic cells by macrophages. *Experientia* 52:950-956.

He, L. and J.J. Lemasters. 2002. Regulated and unregulated mitochondrial permeability transition pores: a new paradigm of pore structure and function? *FEBS Lett.* 512:1-7.

Henrickson, S.E., M. Misakian, B. Robertson, and J.J. Kasianowicz. 2000. Driven DNA transport into an asymmetric nanometer-scale pore. *Phys. Rev. Lett.* 85:3057-3060.

Holden, M.J. and M. Colombini. 1993. The outer mitochondrial membrane channel, VDAC, is modulated by a protein localized in the intermembrane space. *Biochim. Biophys. Acta* 1144:396-402.

Hodge, T. and M. Colombini. 1997. Regulation of metabolite flux through voltage-gating of VDAC channels. *J. Membr. Biol.* 157:271-279.

Hong, S.J., T.M. Dawson and V.L. Dawson. 2004. Nuclear and mitochondrial conversations in cell death: PARP-1 and AIF signaling. *Trends Pharmacol. Sci.* 25:259-264.

Huang, D.C.S. and A. Strasser. 2000. BH3-only proteins-essential initiators of apoptotic cell death. *Cell* 103:839-842.

Hunter, D.R., R.A. Haworth, J.H. Southard. 1976. Relationship between configuration, function, and permeability in calcium-treated mitochondria. *J. Biol. Chem.* 251:5069-5077.

Jacobson, M.D., J.F. Burne, M.P. King, T. Miyashita, J.C. Reed and M.C. Raff. 1993. Bcl-2 blocks apoptosis in cells lacking mitochondrial DNA. *Nature* 361:365-369.

Jacobson, M.D., J.F. Burne and M.C. Raff. 1994. Programmed cell death and Bcl-2 protection in the absence of nucleus. *EMBO J.* 13:1899-1910.

Jansen, B., H. Schlagbauer-Wadl, B.D. Brown, R.N. Bryan, A. van Elsas, M. Muller, K. Wolff, H.G. Eichler and H. Pehamberger. 1998. Expression of Bcl-2 family members in human melanocytes, in melanoma metastases and in melanoma cell lines. *Nat. Med.* 4:232-234.

Jansen, B., V. Wacheck, E. Heere-Ress, H. Schlagbauer-Wadl, C. Hoeller, T. Lucas, M. Hoermann, U. Hollenstein, K. Wolff, and H. Pehamberger. 2000. Chemosensitisation of malignant melanoma by BCL2 antisense therapy. *Lancet* 356:1728-1733.

Jeans, J. 1925. The Mathematical Theory of Electricity and Magnetism, 5th Ed. Cambridge University Press, Cambridge. pp. 652.

Jordan, T.E. 1954. Vapor pressure of organic compounds, Interscience publishers, Inc., New York.

Kasianowicz, J.J., E. Brandin, D. Branton, and D.W. Deamer. 1996. Characterization of individual polynucleotide molecules using a membrane channel. *Proc. Natl. Acad. Sci. USA*. 93:13770-13773.

Kerr, J.F., A.H. Wyllie and A.R. Currie. 1972. Apoptosis: a basic biological phenomenon with wide-ranging implications in tissue kinetics. *Br. J. Cancer* 26:239-257.

Klasa, R.J., A. Gillum, R.E. Klem, and S.R. Frankel. 2002. Oblimersen Bcl-2 antisense: facilitating apoptosis in anticancer treatment. *Antisense Nucleic Acid Drug Dev.* 12:193-213.

Komarov, A.G., D. Deng, W.J. Craigen, and M. Colombini. 2005. New insights into the mechanism of permeation through large channels. *Biophys. J.* 89:3950-3959.

Krauskopf, A., O. Eriksson, W.J. Craigen, M.A. Forte and P. Bernardi. 2006. Properties of the permeability transition in VDAC1(-/-) mitochondria. *Biochim. Biophys. Acta* 1757:590-595.

Kuwana, T., M.R. Mackey, G. Perkins, M.H. Ellisman, M. Latterich, R. Schneiter, D.R. Green and D.D. Newmeyer. 2002. Bid, bax, and lipids cooperate to form supramolecular openings in the outer mitochondrial membrane. *Cell.* 111:331-342.

Lai, J.C., L. Benimetskaya, A. Khvorova, S. Wu, E. Hua, P. Miller, and C.A. Stein. 2005. Phosphorothioate oligodeoxynucleotides and G3139 induce apoptosis in 518A2 melanoma cells. *Mol. Cancer Ther.* 4:305-315.

Lai, J.C., W. Tan, L. Benimetskaya, P. Miller, M. Colombini and C. A. Stein. 2006. A pharmacologic target of G3139 in melanoma cells may be the mitochondrial VDAC. *Proc. Natl. Acad. Sci. U. S. A.* 103:7494-7499.

Lai, J.C., B.C. Brown, A.M. Voskresenskiy, S. Vonhoff, S. Klussman, W. Tan, M. Colombini, R. Weeratna, P. Miller, L. Benimetskaya and C.A. Stein. 2007. Comparison of d-g3139 and its enantiomer L-g3139 in melanoma cells demonstrates minimal in vitro but dramatic in vivo chiral dependency. *Mol Ther.* 15:270-8.

Lee, A.C., M. Zizi and M. Colombini. 1994. β-NADH decreases the permeability of mitohondrial outer membrane to ADP by a factor of 6. *J. Biol. Chem.* 269:30974-30980.

Lee, A.C., X. Xu, E. Blachly-Dyson, M. Forte and M. Colombini. 1998. The role of yeast VDAC genes on the permeability of the mitochondrial outer membrane. *J. Membr. Biol.* 161:173-181.

Leung, S., H. Miyake, T. Zellweger, A. Tolcher, and M.E. Gleave. 2001. Synergistic chemosensitization and inhibition of progression to androgen independence by antisense Bcl-2 oligodeoxynucleotide and paclitaxel in the LNCaP prostate tumor model. *Int. J. Cancer.* 91:846-850.

Li, P., D. Nijhawan, I. Budihardjo, S.M., M. Srinivasula, M. Ahmad, E.S. Alnemri and X. Wang. 1997. Cytochrome c and dATP-dependent formation of Apaf-1/caspase-9 complex initiates an apoptotic protease cascade. *Cell* 91:479-489.

Li, H, H. Zhu, C.J. Xu, J. Yuan. 1998. Cleavage of BID by caspase 8 mediates the mitochondrial damage in the Fas pathway of apoptosis. *Cell* 94:491-501.

Li, S.K., A.H. Ghanem, C.L. Teng, G.E. Hardee, and W.I. Higuchi. 2001. Iontophoretic transport of oligonucleotides across human epidermal membrane: a study of the Nernst-Plank model. *J. Pharm. Sci.* 90:915-931.

Liberatori, S., B. Canas, C. Tani, L. Bini, G. Buonocore, J. Godovac-Zimmermann, O. Mishra, M. Delivoria-Papadopoulos, R. Bracci and V. Pallini. 2004. Proteomic approach to the identification of voltage-dependent anion channel protein isoforms in guinea pig brain synaptosomes. *Proteomics* 4:1335-1340.

Liu, M.Y. and M. Colombini. 1991. Voltage gating of the mitochondrial outer membrane channel VDAC is regulated by a very conserved protein. *Am. J. physiol.* 260:C371-C374.

Liu, M.Y. and M. Colombini. 1992. A soluble mitochondrial protein increases the voltage dependence of the mitochondrial channel, VDAC. *J. Bioenerg. Biomembr.* 24:41-46.

Liu, M.Y., A. Torgrimson and M. Colombini. 1994. Characterization and partial purification of the VDAC-channel-modulating protein from calf liver mitochondria. *Biochim. Biophys. Acta.* 1185:203-212.

Liu, X., C. Kim, J. Yang, R. Jemmerson and X. Wang. 1996. Induction of apoptotic program in cell-free extracts: requirement for dATP and cytochrome c. *Cell* 86:147-157.

Mangan, P.S., and M. Colombini. 1987. Ultrasteep voltage dependence in a membrane channel. *Proc. Natl. Acad. Sci. USA.* 84:4896-4900.

Mannella, C.A. 1982. Structure of the outer mitochondrial membrane: ordered arrays of porelike subunits in outer-membrane fractions from Neurospora crassa mitochondria. *J. Cell Biol.* 94:680-687.

Mannella, C.A. 1989. Structure of the mitochondrial outer membrane channel derived from electron microscopy of 2D crystals. *J. Bioenerg. Biomembr.* 21:427–437.

Mannella, C.A., M. Forte, and M. Colombini. 1992. Toward the molecular structure of the mitochondrial channel, VDAC. *J. Bioenerg. Biomembr.* 24:7–19.

Marzo, I., C. Brenner, N. Zamzami, S.A. Susin, G. Beutner, D. Brdiczka, R. Remy, Z.-H. Xie, J.C. Reed and G. Kroemer. 1998. The permeability transition pore complex: A target for apoptosis regulation by caspases and bcl-2 related proteins. *J. Exp. Med.* 187:1261-1271.

Massari, P., Y. Ho, L.M. Wetzler. 2000. Neisseria meningitidis porin PorB interacts with mitochondria and protects cells from apoptosis. *Proc. Natl. Acad. Sci. USA* 97:9070-9075.

Massari, P., C.A. King, A.Y. Ho and L.M. Wetzler. 2003. Neisserial PorB is translocated to the mitochondria of HeLa cells infected with Neisseria meningitidis and protects cells from apoptosis. *Cell Microbiol.* 5:99-109.

Montal, M. and P. Mueller. 1972. Formation of bimolecular membranes from lipid monolayers and a study of their electrical properties. *Proc. Natl. Acad. Sci. U. S. A.* 69:3561-3566.

Morikofer-Zwez, S. and P. Walter. 1989. Binding of ADP to rat liver cytosolic proteins and its influence on the ratio of free ATP/free ADP. *Biochem J.* 259:117-24.

Mou T.C., C.W. Gray, T.C. Terwilliger and D.M. Gray. 2001. Ff gene 5 protein has a high binding affinity for single-stranded phosphorothioate DNA. *Biochemistry* 40:2267-2275.

Nicolli, A., E. Basso, V. Petronili, R. Wenger and P. Bernardi. 1996. Interactions of cyclophilin with the mitochondrial inner membrane and regulation of the permeability transition pore, and cyclosporin A-sensitive channel. *J. Biol. Chem.* 271:2185-2192.

Ott, M., J. Robertson, V. Gogvadze, B. Zhivotovsky and S. Orrenius. 2002. Cytochrome c release from mitochondria proceeds by a two-step process. *Proc. Natl. Acad. Sci. USA* 99:1259-1263.

Parsons, D.F., G.R. Williams and B. Chance. 1966. Characteristics of isolated and purified preparations of the outer and inner membranes of mitochondria. *Ann. New York Acad. Sci.* 137:643-666.

Pastorino, J.G., M. Tafani, R.J. Rothman, A. Marcineviciute, J.B. Hoek and J.L. Farber. 1999. Functional consequences of the sustained or transient activation by Bax of the mitochondrial permeability transition pore. *J. Biol. Chem.* 274:31734-31739.

Pavlov, E.V., M. Priault, D. Pietkiewicz, W.H.-Y. Cheng, B. Antonsson, S. Manon, S.J. Korsmeyer, C.A. Mannella and K.W. Kinnally. 2001. A novel, high conductance channel of mitochondria linked to apoptosis in mammalian cells and Bax expression in yeast. *J. Cell Biol.* 155:725-731.

Pavlov, E., S.M. Grigoriev, L.M. Dejean, C.L. Zweihorn, C.A. Mannella and K.W. Kinnally. 2005. The mitochondrial channel VDAC has a cation-selective open state, *Biochim. Biophys. Acta* 1710:96-102.

Peng, S., E. Blachly-Dyson, M. Colombini and M. Forte. 1992. Large scale rearrangement of protein domains is associated with voltage gating of the VDAC channel. *Biophys. J.* 62:123-135.

Porcelli, A.M., A. Ghelli, C. Zanna, P. Pinton, R. Rizzuto and M. Rugolo. 2005. pH difference across the outer mitochondrial membrane measured with a green fluorescent protein mutant, *Biochim. Biophys. Res. Commun.* 326:799-804.

Putcha G.V., M. Deshmukh and E.M. Johnson E.M. 1999. Bax translocation is a critical even in neuronal apoptosis: regulation by neuroprotectants, Bcl-2, and caspases. *J. Neurosci.* 19:7476-85.

Raffo, A., J.C. Lai, P. Miller P, C.A. Stein, and L. Benimetskaya. 2004. Antisense RNA down-regulation of bcl-2 expression in DU145 prostate cancer cells does not diminish the cytostatic effects of G3139 (Oblimersen). *Clin. Cancer Res.* 10:3195-3206.

Rockwell, P., W. O'Connor, K. King, N. Goldstein, L.M. Zhang and C.A. Stein. 1997. Cell-surface perturbations of the epidermal growth factor and vascular endothelial growth factor receptors by phosphorothioate oligodeoxynucleotides. 1997. *Proc. Natl. Acad. Sci. USA* 94:6523-6528.

Rostovtseva, T. and M. Colombini. 1996. ATP flux is controlled by a voltage-gated channel from the mitochondrial outer membrane. *J. Biol. Chem.* 271:28006-28008.

Rostovtseva, T. and M. Colombini. 1997. VDAC channels mediate and gate the flow of ATP: implications for the regulation of mitochondrial function. *Biophys. J.* 72:1954-1962.

Rostovtseva, T.K., A. Komarov, S. M. Bezrukov, M. Colombini. 2002. Dynamics of nucleotides in VDAC channels: structure-specific noise generation. *Biophys. J.* 82:193-205.

Rostovtseva, T.K., B. Antonsson, M. Suzuki, R.J. Youle, M. Colombini and S.M. Benzukov. 2004. Bid, but not Bax, regulates VDAC channels. *J. Biol. Chem.* 279:13573-13583.

Rostovtseva, T.K., W. Tan and M. Colombini. 2005. On the role of VDAC in apoptosis: fact and fiction. *J. Bioenerg. Biomembr.* 37:129-42.

Rostovtseva, T.K., N. Kazemi, M. Weinrich, and S.M. Bezrukov. 2006. Voltage gating of VDAC is regulated by nonlamellar lipids of mitochondrial membranes. *J. Biol. Chem.* 281:37496-37506.

Roth, K. and M.W. Weiner. 1991. Determination of cytosolic ADP and AMP concentrations and the free energy of ATP hydrolysis in human muscle and brain tissues with ^{31}P NMR spectroscopy. *Magn. Reson. Med.* 22:505-511.

Ruffolo S.C. and G.C. Shore. 2003. Bcl-2 selectively interacts with the BID-induced open conformer of BAK, inhibiting BAK auto-oligomerization. *J. Biol. Chem.* 278:25039-25045.

Ruoslahti, E. and J.C. Reed. 1994. Anchorage dependence, intergrins, and apoptosis. *Cell* 77:477-478.

Saenger, W. 1984. *Principles of Nucleic Acid Structure* Modified nucleosides and nucleotides; nucleoside di- and triphosphates; coenzymes and antibiotics. In *Principles of Nucleic Acid Structure*, edited by Cantor CR, New York: Springer-Verlag Inc.

Saito, M., S.J. Korsmeyer and P.H. Schlesinger. 2000. 2BAX-dependent transport of cytochrome c reconstituted in pure liposomes. *Nat. Cell Biol.* 2:553-555.

Salvesen, G.S. and V.M. Dixit. 1997. Caspases: intracellular signaling by proteolysis. *Cell* 91:443-446.

Sampson, J., L. Ross, W. Decker and W. Craigen. 1998. A novel isoform of the mitochondrial outer membrane protein VDAC3 via alternative splicing of a 3-base exon. Functional characteristics and subcellular localization. *J. Biol. Chem.* 273:30482-30486.

Schein, S.J., M. Colombini and A. Finkelstein. 1976. Reconstitution in planar lipid bilayers of a voltage-dependent anion-selective channel obtained from *Paramecium* mitochondria. *J. Membr. Biol.* 30:99–120.

Schulz, G.E. 1996. Porins: General to specific, native to engineered passive pores. *Curr. Opin. Struct. Biol.* 6:485–490.

Schwarzer, C., S. Barnikol-Watanabe, F.P. Thinnes and N. Hilschmann. 2002. Voltage-dependent anion-selective channel (VDAC) interacts with the dynein light chain Tctex1 and the heat-shock protein PBP74. *Int. J. Biochem. Cell Biol.* 34:1059-1070.

Shimizu, S., M. Narita and Y. Tsujimoto. 1999. Bcl-2 family proteins regulate the release of apoptogenic cytochrome c by the mitochondrial channel VDAC. *Nature* 399:483-487.

Shimizu, S., T. Ide, T. Yanagida and Y. Tsujimoto. 2000. Electrophysiological study of a novel large pore formed by Bax and the voltage-dependent anion channel that is permeable to cytochrome c. *J. Biol. Chem.* 275:12321-12325.

Siskind, L. and M. Colombini. 2000. The lipids C2- and C16-ceramide form large stable channels. Implications for apoptosis. *J. Biol. Chem.* 8:38640-38644.

Siskind, L., R. Kolesnick and M. Colombini. 2002. Ceramide channels increase the permeability of the mitochondrial outer membrane to small proteins. *J. Biol. Chem.* 277:26796-26803.

Siskind, L.J, A. Davoody, N. Lewin, S. Marshall and M. Colombini. 2003. Enlargement and contracture of C2-ceramide channels. *Biophys. J.* 85:1560-1575.

Slee, E., S. Keogh and S. Martin. 2000. Cleavage of BID during cytotoxic drug and UV radiation-induced apoptosis occurs downstream of the point of Bcl-2 action and is catalysed by caspase-3: a potential feedback loop for amplification of apoptosis-associated mitochondrial cytochrome c release. *Cell Death Differ.* 7:556-565.

Song, J. and M. Colombini. 1996. Indications of a common folding pattern for VDAC channels from all sources. *J. Bioenerg. Biomembr.* 28:153-161.

Song, J., C. Midson, E. Blachly-Dyson, M. Forte and M. Colombini. 1998a. The topology of VDAC as probed by biotin modification. *J. Biol. Chem.* 273:24406-24413.

Song, J., C. Midson, E. Blachly-Dyson, M. Forte and M. Colombini. 1998b. The sensor regions of VDAC are translocated from within the membrane to the surface during the gating processes. *Biophys. J.* 74:2926-2944.

Song, J., C.A. Minetti, M.S. Blake and M. Colombini. 1998c. Successful recovery of the normal electrophysiological properties of PorB (class 3) porin from Neisseria meningitidis after expression in Escherichia coli and renaturation. *Biochim Biophys Acta.* 1370:289-98.

Song, L., M.R. Hobaugh, C. Shustak, S. Cheley, H. Bayley, and J.E. Gouaux. 1996. Structure of staphylococcal alpha-hemolysin, a heptameric transmembrane pore. *Science* 274:1859-1866.

Sottocasa, G.L., B. Kuylenstierna, L. Ernster and A. Bergstrand. 1967. Separation and some enzymatic properties of the inner and outer membranes of rat liver mitochondria. *Methods Enzymol* 10:448-463.

Staples, B.R. and R.L. Nuttall. 1977. The activity and osmotic coefficients of aqueous calcium chloride at 298.15K. *J. Phys. Chem. Ref. Data* 6:385-407.

Susin, S.A., N. Zamizami, M. Castedo, E. Daugas, E.G. Wang, S. Geley, F. Fassy, J.C. Reed and G. Kroemer. 1997. The central executioner of apoptosis: multiple connections between protease activation and mitochondria in Fas/APO-1/CD95- and ceramide-induced apoptosis. *J. Exp. Med.* 186, 25-37

Szabo, I. and M. Zoratti. 1993. The mitochondrial permeability transition pore may comprise VDAC molecules. I. Binary Structure and voltage dependence of the pore. *FEBS Lett.* 330:201-205.

Szabo, I., V. De Pinto and M. Zoratti. 1993. The mitochondrial permeability transition pore may comprise VDAC molecules. II The electrophysiological properties of VDAC are compatible with those of the mitochondrial megachannel. *FEBS Lett.* 330:206-210.

Tan, W., J.C. Lai, P. Miller, C.A. Stein and M. Colombini. 2007 Phosphorothioate oligonucleotides reduce mitochondrial outer membrane permeability to ADP. *Am. J. Physiol. Cell Physiol.* 292:C1388-C1397.

Thomas, L., E. Blachly-Dyson, M. Colombini, and M. Forte. 1993. Mapping of residues forming the voltage sensor of the VDAC ion channel. *Proc. Natl. Acad. Sci. USA.* 90:5446-5449.

Tuboi, S., T. Suzuki, M. Sato and T. Yoshida. 1990. Rat liver mitochondrial and cytosolic fumarases with identical amino acid sequences are encoded from a single mRNA with two alternative in-phase AUG initiation sites. *Adv. Enzyme Regul.* 30:289-304.

Tyler, D. 1992. The mitochondrion in health & disease. VCH Publisher, Inc. New York.

Vander Heiden, M.G., N.S. Chandel, P.T. Schumacker, C.B. Thompson. 1999. Bcl-xL prevents cell death following growth factor withdrawal by facilitating mitochondrial ATP/ADP exchange. *Mol. Cell* 3:159–167.

Vander Heiden, M.G., N.S. Chandel, X.X. Li, P.T. Schumacker, M. Colombini and C.B. Thompson. 2000. Outer mitochondrial membrane permeability can regulate coupled respiration and cell survival. *Proc. Natl. Acad. Sci. US A* 97:4666-4671.

Vander Heiden, M.G., X.X. Li, E. Gottleib, R.B. Hill, C.B. Thompson and M. Colombini. 2001. Bcl-xL promotes the open configuration of the voltage-dependent anion channel and metabolite passage through the outer mitochondrial membrane. *J. Biol. Chem.* 276:19414-19419.

Waldmeier, P.C., K. Zimmermann, T. Qian, M. Tintelnot-Blomley and J.J. Lemasters. 2003. Cyclophilin D as a drug target. *Curr. Med. Chem.* 10:1485-1506.

Wan, B., C. Doumen, J. Duszysky, G. Salama, T.C. Vary and T.F. LaNoue. 1993. Effects of cardiac work on electrical potential gradient across mitochondrial membrane in perfused rat hearts. *Am. J. Physiol.* 265:H453-H460.

Wang, H.G., N. Pathan, I.M. Ethell, S. Krajewski, Y. Yamaguchi, F. Shibasaki, F. McKeon, T. Bobo, T.F. Franke and J.C. Reed. 1999. Ca2+-induced apoptosis through calcineurin dephosphorylation of BAD. *Science* 284:339-343.

Woodfield, K., A. Ruck, D. Brdiczka and A.P. Halestrap. 1998. Direct demonstration of a specific interaction between cyclophilin-D and the adenine nucleotide translocase confirms their role in the mitochondrial permeability transition. *Biochem J.* 336:287-90.

Wyllie, A.H., J.F.R. Kerr and A.R. Currie. 1980. Cell death: the significance of apoptosis. *Int. Rev. Cytol.* 68:251-306

Xu, X., W. Decker, M. J. Sampson, W. J. Craigen, and M. Colombini. 1999. Mouse VDAC isoforms expressed in yeast: Channel properties and their roles in mitochondrial outer membrane permeability. *J. Membr. Biol.* 170:89-102.

Xu, X., J.G. Forbes, and M. Colombini. 2001. Actin modulates the gating of Neurospora crassa VDAC. *J. Membr. Biol.* 180:73-81.

Yang, J., X. Liu, K. Bhalla, C.N. Kim, A.M. Ibrado, J. Cai, T.I. Peng, D.P. Jones and X. Wang. 1997. Prevention of apoptosis by Bcl-2: release of cytochrome c from mitochondria blocked. *Science*. 275:1129-1132.

Zalk, R., A. Israelson, E.S. Garty, H. Azoulay-Zohar and V. Shoshan-Barmatz. 2005. Oligomeric states of the voltage-dependent anion channel and cytochrome c release from mitochondria. *Biochem. J.* 386:73-83.

Zalman, L.S., H. Nikaido and Y. Kagawa. 1980. Mitochondrial outer membrane contains a protein producing nonspecific diffusion channels. *J. Biol. Chem*. 255:1771-1774.

Zamzami, N., P. Marchetti, M. Castedo, D. Decaudin, A. Macho, T. Hirsh, S.A. Susin, P.X. Petit, B. Mignotte and G. Kroemer. 1995. Sequential reduction of mitochondrial transmembrane potential and generation of reactive oxygen species in early programmed cell death. *J. Exp. Med.* 182, 367-377

Zhang, D.W. and M. Colombini. 1990. Group IIIA-Metal hydroxides indirectly neutralize the voltage sensor of the voltage-dependent mitochondrial channel, VDAC, by interacting with a dynamic binding site. *Biochim. Biophys. Acta* 1025:127-134.

Zimmerberg, J., V.A. Parsegian. 1986. Polymer inaccessible volume changes during opening and closing of a voltage-dependent ionic channel. *Nature* 323:36-39.

Zizi, M., L. Thomas, E. Blachly-Dyson, M. Forte, and M. Colombini. 1995. Oriented channel insertion reveals the motion of a transmembrane beta strand during voltage gating of VDAC. *J. Membr. Biol.* 144:121-129.